

THESIS

Exploration into microscopic nature of spacetimes
by quantum fields and high-energy particles

量子場及び高エネルギー粒子による時空微細構造の探求

Umpei Miyamoto

宮本 雲平

A doctoral dissertation submitted to
Department of Physics,
Waseda University

March, 2005

Contents

1	Introduction	7
1.1	Introduction	7
1.2	Naked singularities (NSs) and quantum effects	8
1.3	High energy cosmic rays and noncommutative geometry	10
2	Particle creation by a collapsing ball	15
2.1	Quantization	15
2.2	Spectrum, luminosity, and energy	18
3	Particle creation in self-similar NS formation	21
3.1	Spherical self-similar spacetimes admitting a NS	21
3.2	Local map	23
3.3	Luminosity and energy	24
3.4	Redshift	27
3.5	Relations among the local map, luminosity, and redshift	28
3.6	Examples	29
3.6.1	Minkowski spacetime	29
3.6.2	Vaidya solution	30
3.6.3	Roberts solution	30
3.6.4	Lemaître-Tolman-Bondi (LTB) solution	31
3.6.5	General relativistic Larson-Penston solution	32
3.7	Summary and Discussion	32
4	Quantum effect and curvature strength of NS	37
4.1	NS in LTB spacetime	37
4.1.1	LTB solutions admitting a NS	37
4.1.2	Curvature strength of the NSs	39
4.2	Map of null rays passing near the naked singularity	40
4.2.1	Local map	40

4.2.2	Outline of the calculation of local map	41
4.2.3	Regime A: $0 \leq r < \eta_A t_0^{1/(1+\mu)}$	42
4.2.4	Regime B: $t_0/\eta_B < r < \eta_A t_0^{1/(1+\mu)}$	43
4.2.5	Regime C: $t/r \ll 1$	44
4.2.6	Matching the approximation regimes	46
4.2.7	Obtaining the local map	47
4.3	Luminosity and energy	48
4.3.1	Non-self-similar LTB spacetimes: $0 < \gamma < 3$	48
4.3.2	Self-similar LTB spacetime: $\gamma = 3$	49
4.4	Summary and discussion	50
5	Mathematics of the doubly special relativity	55
5.1	Hopf algebra	55
5.1.1	Algebra and coalgebra	55
5.1.2	Bialgebra and Hopf algebra	56
5.1.3	Examples of Hopf algebra	57
	Enveloping algebra of a Lie algebra	57
	Function Hopf algebra	58
5.1.4	Dual Hopf algebra	58
5.2	κ -Poincarè algebra and κ -Minkowski spacetime	59
6	Particle velocity in noncommutative spacetime	61
6.1	Modified dispersion relation models	61
6.2	Velocity formula	63
6.3	Arrival time analysis with massive particles	65
6.4	Summary and discussion	67
7	Threshold anomaly in noncommutative spacetime	69
7.1	Finite boost in κ -Minkowski spacetime	69
7.2	Re-consideration of the speed of light	71
7.3	Threshold anomaly	72
7.3.1	Threshold anomaly for TeV γ -rays	74
7.3.2	Threshold anomaly for GZK cutoff	75
7.4	Summary and discussion	76
8	Conclusion	81
8.1	Summary and conclusion	81
8.2	Future prospect	82
A	Cauchy horizon in self-similar collapse	85

<i>CONTENTS</i>	5
B Local map and redshift in diagonal coordinates	87
C Nakedness of the singularity in LTB spacetime	91
D Frequency of naked singularities	93

Chapter 1

Introduction

1.1 Introduction

The general theory of relativity is a classical theory of gravitation, which is based on the coordinate invariance and the equivalence principle [1]. It is believed that general relativity describes the large scale structure of spacetime, and it has indeed revealed the history and present states of our universe [2]. The direct evidence for the validity of general relativity in strong gravitational regime will be obtained by the observations of gravitational waves from inspiral binaries in near future [3]. One of the outstanding features of the general relativity is that spacetime is supposed to be a smooth four dimensional manifold [4]. Gravity is realized as the curvature of the manifold. The picture of curved manifold is the plausible and new concept which Einstein first introduced into the physics. At the same time, it is the fact that such a picture makes physicists confront with the difficulty to quantize the gravitational interaction. It is unlikely that the manifold picture holds even at arbitrarily small scale. From an easy dimensional estimation, one can know that the scales of the curvature radius and the Compton wave length of a massive particle are comparable at the order of l_p , where $l_p \equiv (\hbar G/c^3)^{1/2} \simeq 1.6 \times 10^{-33} \text{cm}$ is the Planck length. The quantum theoretical nature of spacetime would dominate and the smooth manifold picture would break there. Therefore, we believe that there exists a quantum theory of gravity and it saves the situation. There has been many studies on the quantum gravity and the unification of fundamental interactions, such as the loop quantum gravity [5] and string/M theory [6]. These theories gradually have made us know the microscopic nature of spacetimes, although there are many difficulties to provide the satisfactory picture of microscopic spacetime.

We can say with fairly certain that the construction of a quantum gravity theory is one of the most important problems in the theoretical physics. This derives us to the following questions: (i) is there situation or phenomenon in which the quantum gravitational effect of spacetime plays a crucial role in our universe?; (ii) if there is such a phenomenon, is it detectable? As for the former question, it may be sufficient to see that the general relativity generically

predicts *spacetime singularities* under some physically reasonable assumptions, which is proven by Hawking and Penrose [7]. For examples, the black solutions to the Einstein field equation contain the spacetime singularities within their event horizons. Our expanding universe confronts with the big-bang singularity at the beginning of it. Near the spacetime singularities, the curvature radius of spacetimes can be arbitrarily small even below the Planck scale.

The latter question is still an open problem in general relativity. To give an answer to the question is one of the main themes in this thesis. We are concerned with the visibility or detectability of the microscopic nature of spacetime. In the first half of this thesis, we consider the visibility of the spacetime singularities forming in gravitational collapse, i.e., we consider the problem of the *naked singularities* (NSs). In particular, we focus on the role of the *quantum field theory in curved spacetime* [8, 9] in the NS formation. In the latter half of this thesis, we consider the detectability of quantum gravitational effect by the high energy particles such as the *extremely high energy cosmic rays* (EHECRs). In particular, we focus on a model of quantum gravity, which is one of the *noncommutative geometry*. Let us review the previous works on above two directions in order. At the same time, we confirm our motivation.

Through this thesis, we follow the sign conventions of the textbook by Misner, Thorn, and Wheeler about the metric, Riemann, and Einstein tensors [1]. The Greek and the Latin indices run over $0, 1, 2, 3$ and over $1, 2, 3$, respectively. The units of $c = G = \hbar = 1$ are used. This thesis is based on our original papers, Refs. [10], [11], [12] and [13].

1.2 Naked singularities (NSs) and quantum effects

Relativistically important compact objects, such as black holes and neutron stars, form as the consequence of *gravitational collapse*. Apart from the astrophysical interests, the physics of gravitational collapse is related to some fundamental problems in general relativity. In particular, the *cosmic censorship hypothesis* (CCH) presents one of the most important unsolved problems in general relativity [14]. There are two versions of this hypothesis. The weak hypothesis states that all singularities in gravitational collapse are hidden within black holes. This version implies the future predictability of the spacetime outside the event horizon. The strong one asserts that no singularities visible to any observer can exist. This version states that all physically reasonable spacetimes are globally hyperbolic. Despite several attempts neither proof nor precise mathematical formulation of the hypothesis has been available yet. On the contrary, some solutions of the Einstein field equation with regular initial conditions evolving into spacetimes containing NSs have been found [15, 16]. See Figs. 1.1(a) and (b) for schematic diagrams of gravitational collapse ending in black hole and naked singularity formation, respectively.

When a NS forms in gravitational collapse, the Cauchy horizon (CH), which corresponds to the first outgoing null ray, appears in the spacetime. For more mathematically precise definition, see Ref. [4]. Beyond the CH, the NS is exposed to observers. Since we do not know how to impose the boundary condition of any field at the singularity, where all known physics break down,

the physics loses the future predictability in naked-singular spacetimes. For a naked-singular spacetime to be a counterexample against the CCH, it is at least necessary that the CH is stable. Although the CCH was originally stated in the classical context, CHs may be unstable due to the backreaction of quantum effects such as particle creation, i.e., the particle creation would prevent NSs from forming. Research on such a possibility can be traced back to the pioneering works of Ford and Parker [17] and Hiscock, Williams, and Eardley [18]. Ford and Parker considered the particle creation during the formation of a shell-crossing NS to obtain a finite amount of flux [17]. On the other hand, Hiscock *et al.* considered the formation of a shell-focusing NS in the collapse of a null-dust fluid to obtain a diverging amount of flux [18]. Subsequently, such quantum phenomena have been studied in the models of a self-similar dust [19, 20, 21, 10], a self-similar null dust [22, 10], and an analytic dust [23], for which the luminosities are found to diverge as negative powers of the remaining time to the CHs. The analytic model is the spherical dust collapse with an analytic initial density profile with respect to locally Cartesian coordinates. The analyticity of initial density profile and the self-similarity are incompatible in the spherically symmetric dust model. It is argued that the quantum radiation from a strong NS such as a shell-focusing one must diverge as the CH is approached [19, 22], although there is not enough evidence. In addition, such an explosive radiation by naked-singularity formation can be a candidate for a source of the extremely high energy cosmic rays or a central engine of γ -ray burst [24].

As the examples given above show, it is known that generic spherically symmetric self-similar collapse results in strong naked-singularity formation [25, 26]. Among such self-similar models, the general relativistic Larson-Penston (GRLP) solution would be one of the most serious counterexamples against the CCH in the sense that the existence of pressure is taken into account [27, 28]. Moreover, the convergence of more general spherically symmetric collapse to the GRLP solution have been reported both numerically and analytically [29] as a realization of the *self-similarity hypothesis* proposed by Carr [30, 31]. The discovery of the black hole critical behavior also shed light on a self-similar solution as a critical solution (for example, see [32]). We can say with fair certainty that self-similar solutions play important roles near spacetime singularities. Several studies have been done resulting in a complete classification of self-similar solutions so far (see [31] for a review).

Motivated by the above, particle creation during the NS formation in self-similar collapse are investigated in Chap. 3. It is shown that irrespective of the details of the model, a diverging energy flux is emitted from a naked shell-focusing singularity forming in generic spherically symmetric self-similar spacetime. The power and energy of particle creation are calculated on the assumption that the curvature around the singularity causes particle creation, which was proven by [33], at least in the case of self-similar and analytic non-self-similar dust models. Because the collapsing matter is not specified, the results can be applied to several known models of self-similar collapse. This analysis is regarded as a semiclassical counterpart of [34], in which the stability of the CH in self-similar collapse was tested by a classical field.

The results in Chap. 3 reveal that the particle creation in generic self-similar collapse diverges

as the CH is approached. There is another interesting result, leading us to the following study. In a class of self-similar spacetimes, which seem to be non-generic, the luminosity remains finite as the CH is approached. Indeed, it is shown that in the self-similar collapse of a massless scalar field, described by the Roberts solution [35], the luminosity remains finite at the CH. The results of above analysis about the self-similar collapse seems to suggest that curvature strength of the NS along the CH is related to the amount of quantum radiation. Although NSs forming in generic spherically symmetric self-similar spacetimes are known [25] to satisfy the strong curvature condition (SCC) [36] along the CH, the NS appearing in the Roberts solution does not satisfy even the limiting focusing condition (LFC) [37], which is weaker than the SCC.¹ The relation between the curvature strength and quantum effect of NSs has already been suggested in Ref. [23]. It showed the divergence of the quantum radiation in the analytic dust model, in which the forming NS is known to be weak [39, 40], is mild. However, the comprehensive understanding of the relation between the curvature strength and quantum effect of NSs is not available yet. The purpose of Chap. 4 is to show how the amount of quantum radiation during the formation of NSs depends on such a nature of singularities as curvature strength. This analysis will help us obtain knowledge about the instability of CH, which would be predicted by a full semiclassical theory, taking into account the backreaction of quantum fields to gravity. In addition, it is shown how the coupling manner of quantized scalar fields to gravity changes the amount of quantum radiation. The dependence on the coupling manner is important because the CHs will suffer from the semiclassical instability, caused by all fundamental quantum fields.

1.3 High energy cosmic rays and noncommutative geometry

Recently, much attention has been paid to the extremely high energy cosmic rays (EHECRs), which have energies above that attained in any experimental apparatus on Earth [41, 42]. It has been pointed out that these EHECRs provide an opportunity to investigate spacetime properties on very short length scales or very high energy scales. The most striking feature is that some of these detections seem to be inconsistent with existing physics, in which such detections would be restricted by the Greisen-Zatsepin-Kuzmin (GZK) cutoff [43] (see Fig. 1.2 for the spectrum of the EHECRs). That is, if we consider the interaction between the EHECRs and cosmic microwave background, particles with energy $\gtrsim 7 \times 10^{19}$ eV from distant sources cannot reach the Earth. There is also another anomalous phenomenon similar to this. That is the detections of γ -rays above ~ 20 TeV from distant sources ($\gtrsim 100$ Mpc) reported in Refs. [44, 45]. These γ -rays are expected to interact with infrared radio background (IRBG) photons and not to reach the Earth in a standard scenario [46]. In spite of exhaustive research, near sources which can

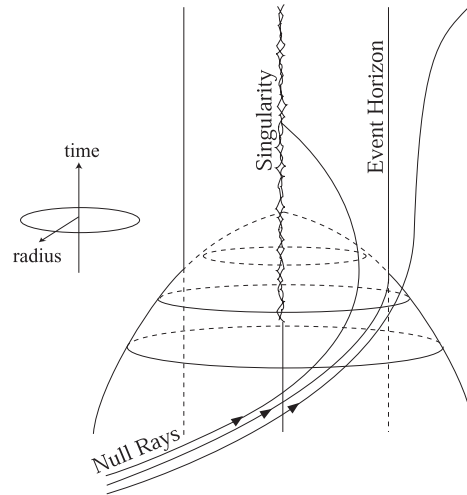
¹Following the work of Clarke and Królak [38], consider a geodesic (N), affinely parameterized by κ , with tangent vector k^μ , and terminating at or emanating from a singularity where $\kappa = 0$. If $\lim_{\kappa \rightarrow 0} \kappa^2 R_{\mu\nu} k^\mu k^\nu \neq 0$ and $\lim_{\kappa \rightarrow 0} \kappa R_{\mu\nu} k^\mu k^\nu \neq 0$, where $R_{\mu\nu}$ is the Ricci tensor, then the SCC and LFC are satisfied along N , respectively. Since the quantity of $R_{\mu\nu} k^\mu k^\nu$ for the Roberts solution indeed vanishes along the CH, the NS satisfies neither the SCC nor LFC.

explain such detections has not been found. Though there are many attempts to explain these anomalous phenomena, there is no absolute solution at present [47].

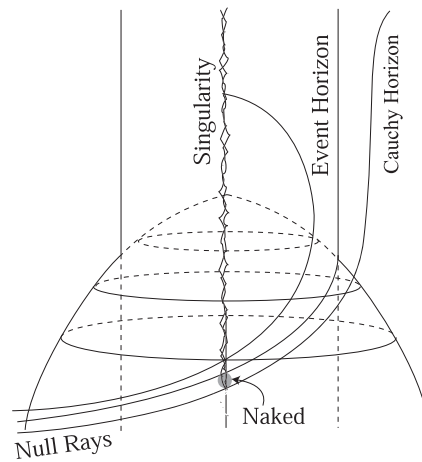
This could imply an encounter with new physics. Some authors argue that the violation of Lorentz invariance (LI) might solve the puzzle of the EHECRs above GZK cutoff [48, 49, 50, 51, 52]. The LI violation might also explain detections of γ -rays above ~ 20 TeV. This possibility has been argued in Refs. [53, 54, 55, 56]. In these models, the LI violation is introduced through the modification of the dispersion relation of particles. We call the theories obtained by this method modified dispersion relation (MDR) models.

One of the ways to modify the dispersion relation is to consider spacetime noncommutativity, which has received attention in recent years since it naturally arises in the contexts of string/M theories [57, 58, 59, 60, 61, 62]. It has also been argued that spacetime uncertainty which comes from a fundamental string scale may be related to spacetime noncommutativity [63]. Apart from string/M theories, spacetime noncommutativity also arises as a result of deformation quantization [64]. Amelino-Camelia *et al.* [65, 66, 67, 68] considered an interesting toy model called κ -Minkowski spacetime where noncommutativity is introduced as $[x^i, t] = i\lambda x^i$, where λ is a free length scale [69, 70, 71, 72]. They obtained a severe constraint on λ through an arrival time analysis of signals from a γ -ray burst [65, 66]. If we accept this scenario, there is no room for detectable symptoms such as anomalous threshold to explain EHECRs [67, 66].

In general, however, it is plausible that not only a dispersion relation but also other relations such as energy-momentum conservation laws might be altered in a Planck scale physics. To investigate these features, we employ the κ -Minkowski spacetime model and compare a group velocity in the κ -Minkowski spacetime with that in the MDR models. The properties of this group velocity were also investigated in Ref. [73]. In Chap. 6, we derive a more realistic velocity formula based on the motion of a wave packet in κ -Minkowski spacetime. With this formula, we find that the spacetime noncommutativity does not affect the velocity of massless particles. Motivated by this observation, we analyze reaction processes which are related to both detections of EHECRs beyond the GZK cutoff and of ~ 20 TeV photons in Chap. 7. In particular, we pay attention to the momentum conservation law which has some ambiguities in this model. We propose to determine the form of the momentum conservation law by deciding whether or not spacetime noncommutativity is consistent with observations. In fact, we *can* exclude some forms of momentum conservation. Though our approach is purely kinematical, our result will provide a strong motivation to consider realistic model of spacetime noncommutativity [74].



(a)



(b)

Figure 1.1: A schematic spacetime diagram representing the formation of (a) a black hole and (b) a naked singularity in spherically symmetric gravitational collapse. Characteristic null rays are depicted. In the black hole formation, the first null ray can escape to infinity. Second null ray forms the event horizon, within which null rays cannot escape to infinity and terminates at the central singularity. In such a black hole formation, the singularity is not visible from observers outside the event horizon. In the naked singularity formation, before the formation of an event horizon, null rays pass through the singularity and carry the information of the singularity to infinity. Such a naked singularity formation violate the weak version of the cosmic censorship hypothesis.

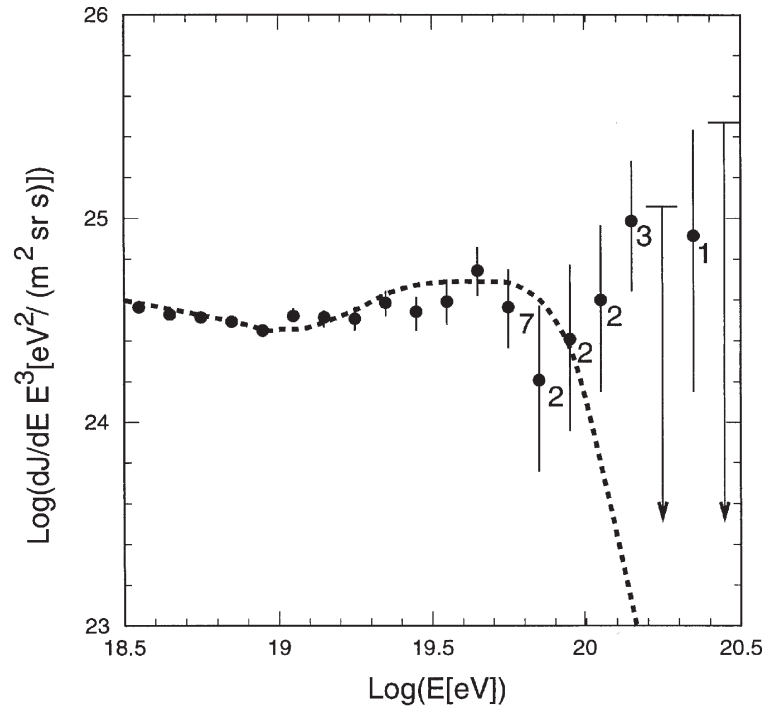


Figure 1.2: The energy spectrum of high energy cosmic rays. The numbers and arrows denotes the count of detected events and the upper bound from the observation, respectively. The dashed curve is a theoretical plot, which assumes uniform sources outside our galaxy. The damping of the theoretical curve around 10^{20}eV corresponds to the GZK cutoff.

Chapter 2

Particle creation by a collapsing ball

2.1 Quantization

The formalism in this section is rather general. Therefore, it can be applied to any spherically symmetric and asymptotically flat spacetimes in which radial null rays define a one-to-one mapping between past null infinity \mathcal{I}^- and future null infinity \mathcal{I}^+ . For example, see Figs. 2.1 and 2.2, which represent the causal structure of a black hole and a NS in gravitational collapse, respectively.

In the asymptotic region, let r, θ, ϕ, t denote the usual quasi-Minkowskian spherical coordinates and time, which are related asymptotically related to null coordinates u and v by $u \simeq t - r$ and $v \simeq t + r$. An ingoing null ray $u = \text{const}$, emanating from \mathcal{I}^- , propagates through the geometry becoming an outgoing null ray $u = \text{const}$, and terminates at \mathcal{I}^+ at $\mathcal{F}(v)$ measured by the coordinate u . Conversely, one can trace a null ray from $u = \text{const}$ on \mathcal{I}^+ to $v = \mathcal{G}(u)$ on \mathcal{I}^- , where the function \mathcal{G} is the inverse of \mathcal{F} .

Let $u_{\omega lm}^{in}$ and $u_{\omega lm}^{out}$ be the solutions of massless Klein-Gordon equation, which are the asymptotical region of the form

$$u_{\omega lm}^{in} \approx \frac{1}{\sqrt{4\pi\omega r}} (e^{-i\omega v} - e^{-i\omega\mathcal{G}(u)}) Y_{lm}(\theta, \phi), \quad (2.1)$$

$$u_{\omega lm}^{out} \approx \frac{1}{\sqrt{4\pi\omega r}} (e^{-i\omega\mathcal{F}(v)} - e^{-i\omega u}) Y_{lm}(\theta, \phi). \quad (2.2)$$

The above asymptotic form is independent of whether the field obeys the minimally coupled equation, $\square\phi = 0$, or non-minimally coupled one, $(\square + \xi R)\phi = 0$, where R and ξ are the Ricci

scalar and arbitral real constant, respectively. These solutions are normalized as follows:

$$\langle u_{\omega lm}, u_{\omega' l' m'} \rangle = \delta(\omega - \omega') \delta_{ll'} \delta_{mm'}, \quad (2.3)$$

$$\langle u_{\omega lm}^*, u_{\omega' l' m'}^* \rangle = -\delta(\omega - \omega') \delta_{ll'} \delta_{mm'}, \quad (2.4)$$

$$\langle u_{\omega lm}, u_{\omega' l' m'}^* \rangle = 0, \quad (2.5)$$

where $\langle \cdot, \cdot \rangle$ is a conserved inner product, defined on a spacelike hypersurface as

$$\langle f_1, f_2 \rangle \equiv -i \int_{\Sigma} (f_1 f_{2,\mu}^* - f_{1,\mu} f_2^*) \sqrt{g_{\Sigma}} d\Sigma^{\mu}. \quad (2.6)$$

This inner product clearly has following properties:

$$\langle \alpha f_1 + \beta f_2, f_3 \rangle = \alpha \langle f_1, f_3 \rangle + \beta \langle f_2, f_3 \rangle, \quad (2.7)$$

$$\langle f_1, \alpha f_2 + \beta f_3 \rangle = \alpha^* \langle f_1, f_2 \rangle + \beta^* \langle f_1, f_3 \rangle, \quad (2.8)$$

$$\langle f_1, f_2 \rangle^* = \langle f_2, f_1 \rangle, \quad \langle f_1^*, f_2 \rangle = -\langle f_2^*, f_1 \rangle, \quad \langle f_1, f_2^* \rangle = -\langle f_2, f_1^* \rangle \quad (2.9)$$

for arbitrary function f_i ($i = 1, 2, 3$), which is smooth and has a suitable support. The normalization of $u_{\omega lm}$, for example, the equation (2.3) can be shown as follows:

$$\begin{aligned} \langle u_{\omega lm}^{in}, u_{\omega' l' m'}^{in} \rangle &\approx \left\langle \frac{e^{-i\omega v}}{\sqrt{4\pi\omega r}} Y_{lm}, \frac{e^{-i\omega' v}}{\sqrt{4\pi\omega' r}} Y_{l'm'} \right\rangle_{\Sigma_{t=-\infty}} \\ &= \frac{-i}{4\pi\sqrt{\omega\omega'}} \int Y_{lm} Y_{l'm'}^* d\Omega \int \left[\frac{e^{-i\omega v}}{r} \frac{\partial}{\partial t} \left(\frac{e^{i\omega' v}}{r} \right) - \frac{\partial}{\partial t} \left(\frac{e^{-i\omega v}}{r} \right) \frac{e^{i\omega' v}}{r} \right] r^2 dr \\ &= \frac{-i\delta_{ll'}\delta_{mm'}}{4\pi\sqrt{\omega\omega'}} \int_{-\infty}^{\infty} dv \left\{ e^{-i\omega v} \partial_v (e^{i\omega' v}) - \partial_v (e^{-i\omega v}) e^{i\omega' v} \right\} \\ &= \frac{-i\delta_{ll'}\delta_{mm'}}{4\pi\sqrt{\omega\omega'}} \left[2\pi i\omega' \delta(\omega - \omega') + 2\pi i\omega \delta(\omega - \omega') \right] \\ &= \delta(\omega - \omega') \delta_{ll'} \delta_{mm'}. \end{aligned}$$

Since both $\{u_{\omega lm}^{in}\}$ and $\{u_{\omega lm}^{out}\}$ constitute complete sets, they can be expanded each other,

$$u_{\omega}^{out} = \int_0^{\infty} d\omega' (\alpha_{\omega\omega'} u_{\omega'}^{in} + \beta_{\omega\omega'} u_{\omega'}^{in*}), \quad (2.10)$$

$$u_{\omega}^{in} = \int_0^{\infty} d\omega' (\gamma_{\omega\omega'} u_{\omega'}^{out} + \sigma_{\omega\omega'} u_{\omega'}^{out*}), \quad (2.11)$$

where same l and m are used in each side of equations. Hereafter, we omit the indices l, m , and the region of the integration with respect to the frequency unless they are not especially needed.

The coefficients, which are called Bogoliubov ones, are computed as follows:

$$\alpha_{\omega\omega'} = \langle u_{\omega}^{out}, u_{\omega'}^{in} \rangle \quad (2.12)$$

$$= \frac{1}{4\pi\sqrt{\omega\omega'}} \int_{-\infty}^{\infty} dv \{ \omega' + \omega\mathcal{F}'(v) \} e^{-i\omega\mathcal{F}(v)+i\omega'v} \quad (2.13)$$

$$= \frac{1}{2\pi} \sqrt{\frac{\omega'}{\omega}} \int_{-\infty}^{\infty} dv e^{-i\omega\mathcal{F}(v)+i\omega'v}, \quad (2.14)$$

$$\beta_{\omega\omega'} = -\langle u_{\omega}^{out}, u_{\omega'}^{in*} \rangle \quad (2.15)$$

$$= \frac{1}{4\pi\sqrt{\omega\omega'}} \int_{-\infty}^{\infty} dv \{ \omega' - \omega\mathcal{F}'(v) \} e^{-i\omega\mathcal{F}(v)-i\omega'v} \quad (2.16)$$

$$= -\frac{1}{2\pi} \sqrt{\frac{\omega'}{\omega}} \int_{-\infty}^{\infty} dv e^{-i\omega\mathcal{F}(v)-i\omega'v}, \quad (2.17)$$

$$\gamma_{\omega\omega'} = \alpha_{\omega'\omega}^*, \quad (2.18)$$

$$\sigma_{\omega\omega'} = -\beta_{\omega'\omega}, \quad (2.19)$$

where we use the integration by parts. One can recognize that the following relation holds,

$$\beta_{\omega\omega'} = -i\alpha_{\omega(-\omega')}. \quad (2.20)$$

Moreover, they are dependent on each other through following relations,

$$\langle u_{\omega}^{out}, u_{\omega'}^{out} \rangle = \delta(\omega - \omega'),$$

$$\langle u_{\omega}^{out}, u_{\omega'}^{out*} \rangle = 0,$$

$$\langle u_{\omega}^{in}, u_{\omega'}^{in} \rangle = \delta(\omega - \omega'),$$

$$\langle u_{\omega}^{in}, u_{\omega'}^{in*} \rangle = 0.$$

Above relations are written as

$$\int d\tilde{\omega} (\alpha_{\omega\tilde{\omega}} \alpha_{\omega'\tilde{\omega}}^* - \beta_{\omega\tilde{\omega}} \beta_{\omega'\tilde{\omega}}^*) = \int d\tilde{\omega} (\gamma_{\tilde{\omega}\omega}^* \gamma_{\tilde{\omega}\omega'} - \sigma_{\tilde{\omega}\omega} \sigma_{\tilde{\omega}\omega'}^*) = \delta(\omega - \omega'), \quad (2.21)$$

$$\int d\tilde{\omega} (\alpha_{\omega\tilde{\omega}} \beta_{\omega'\tilde{\omega}} - \beta_{\omega\tilde{\omega}} \alpha_{\omega'\tilde{\omega}}) = \int d\tilde{\omega} (\sigma_{\tilde{\omega}\omega} \gamma_{\tilde{\omega}\omega'}^* - \gamma_{\tilde{\omega}\omega}^* \sigma_{\tilde{\omega}\omega'}) = 0, \quad (2.22)$$

$$\int d\tilde{\omega} (\gamma_{\omega\tilde{\omega}} \gamma_{\omega'\tilde{\omega}}^* - \sigma_{\omega\tilde{\omega}} \sigma_{\omega'\tilde{\omega}}^*) = \int d\tilde{\omega} (\alpha_{\tilde{\omega}\omega}^* \alpha_{\tilde{\omega}\omega'} - \beta_{\tilde{\omega}\omega} \beta_{\tilde{\omega}\omega'}^*) = \delta(\omega - \omega'), \quad (2.23)$$

$$\int d\tilde{\omega} (\gamma_{\omega\tilde{\omega}} \sigma_{\omega'\tilde{\omega}} - \sigma_{\omega\tilde{\omega}} \gamma_{\omega'\tilde{\omega}}) = \int d\tilde{\omega} (\beta_{\tilde{\omega}\omega} \alpha_{\tilde{\omega}\omega'}^* - \alpha_{\tilde{\omega}\omega}^* \beta_{\tilde{\omega}\omega'}) = 0. \quad (2.24)$$

We can write the Hermitian field operator in the form

$$\phi = \int d\omega (\mathbf{a}_{\omega}^{in} u_{\omega}^{in} + \mathbf{a}_{\omega}^{in\dagger} u_{\omega}^{in*}), \quad (2.25)$$

$$\phi = \int d\omega (\mathbf{a}_{\omega}^{out} u_{\omega}^{out} + \mathbf{a}_{\omega}^{out\dagger} u_{\omega}^{out*}). \quad (2.26)$$

As a consequence of the normalization of $u_{\omega lm}$ and the canonical commutation relations for the field and its conjugate momentum, the creation and annihilation operators satisfy

$$[\mathbf{a}_{\omega lm}, \mathbf{a}_{\omega' l' m'}^\dagger] = \delta(\omega - \omega') \delta_{ll'} \delta_{mm'}, \quad (2.27)$$

$$[\mathbf{a}_{\omega lm}, \mathbf{a}_{\omega' l' m'}] = [\mathbf{a}_{\omega lm}^\dagger, \mathbf{a}_{\omega' l' m'}^\dagger] = 0. \quad (2.28)$$

The creation and annihilation operators for particles defined by u^{in} and u^{out} are related each other as follows:

$$\mathbf{a}_\omega^{in} = \int d\omega' (\alpha_{\omega'\omega} \mathbf{a}_{\omega'}^{out} + \beta_{\omega'\omega}^* \mathbf{a}_{\omega'}^{out\dagger}), \quad (2.29)$$

$$\mathbf{a}_\omega^{out} = \int d\omega' (\gamma_{\omega'\omega} \mathbf{a}_{\omega'}^{in} + \sigma_{\omega'\omega}^* \mathbf{a}_{\omega'}^{in\dagger}). \quad (2.30)$$

We can define vacuum states as the states which can not be annihilated by any annihilated operators as

$$\mathbf{a}_{\omega lm}^{in} |0\rangle_{in} = 0, \quad \mathbf{a}_{\omega lm}^{out} |0\rangle_{out} = 0, \quad (2.31)$$

for all ω , l , and m .

2.2 Spectrum, luminosity, and energy

We assume that the initial state of the quantum field is $|0\rangle_{in}$. Then the expectation value of the particle number of frequency ω on \mathcal{I}^+ is given by

$$N(\omega) \equiv {}_{in}\langle 0 | \mathbf{a}_\omega^{out\dagger} \mathbf{a}_\omega^{out} | 0 \rangle_{in} \quad (2.32)$$

$$= \int d\omega' |\sigma_{\omega'\omega}|^2 \quad (2.33)$$

$$= \int d\omega' |\beta_{\omega\omega'}|^2. \quad (2.34)$$

To evaluate the luminosity and energy of particle creation, we have to specify the coupling manner of scalar fields to gravity. Here, we consider the massless scalar fields coupling to the scalar curvature as

$$(\square - \xi R) \phi = 0, \quad (2.35)$$

where R is the Ricci scalar curvature and ξ is an arbitrary real constant. In particular, the scalar fields with $\xi = 0$ and $\xi = 1/6$ are minimally and conformally coupled ones, respectively. The stress-energy tensor of the scalar field in an asymptotically flat region is given by

$$T_{\mu\nu}^{(\xi)} = \nabla_\mu \phi \nabla_\nu \phi - \frac{1}{2} g_{\mu\nu} \nabla^\alpha \phi \nabla_\alpha \phi - \xi \nabla_\mu \nabla_\nu \phi^2 + \xi g_{\mu\nu} \square \phi^2.$$

The luminosity of the particle creation observed at infinity is obtained by integrating the following component of the stress-energy tensor on a large sphere,

$$T_r^t = -\frac{1}{2}(\phi_{,t}\phi_{,r} + \phi_{,r}\phi_{,t}) + \xi(\phi\phi_{,r} + \phi_{,r}\phi)_{,t}, \quad (2.36)$$

where we symmetrize the each term of the tensor. We need an estimate of the vacuum-expectation value of the above component. A suitable regularization is required in the calculation of vacuum-expectation value because the stress-energy tensor is quadratic in fields at a same point. The regularization for minimally and conformally coupled scalar fields was given in [17] via the point-splitting regularization scheme. We generalize the their scheme to this case,

$$L^{(\xi)} \equiv \int \langle 0|T_r^t|0\rangle r^2 \sin\theta d\theta d\phi \quad (2.37)$$

$$= \sum_{lm} L_{lm}^{(\xi)}, \quad (2.38)$$

where

$$L_{lm}^{(\xi)}(u) = \frac{1}{4\pi} \left[\left(\frac{1}{4} - \xi \right) \left(\frac{\mathcal{G}''}{\mathcal{G}'} \right)^2 + \left(\xi - \frac{1}{6} \right) \frac{\mathcal{G}'''}{\mathcal{G}'} \right]. \quad (2.39)$$

The luminosity of quantum emission is the sum of all these modes, but it diverges because the above luminosity (2.39) is independent of (l, m) . Such divergence is due to the neglect of the back-scattering by the potential barrier in strong gravitational fields, which will reduce the emission for highly rotational modes. Hereafter, we shall omit the quantum numbers (l, m) and one should keep in mind that the above expression holds only for small l . The total energy of emitted particles is estimated by integrating the luminosity with respect to u ,

$$E^{(\xi)}(u) \equiv \int_{-\infty}^u L^{(\xi)}(u') du'.$$

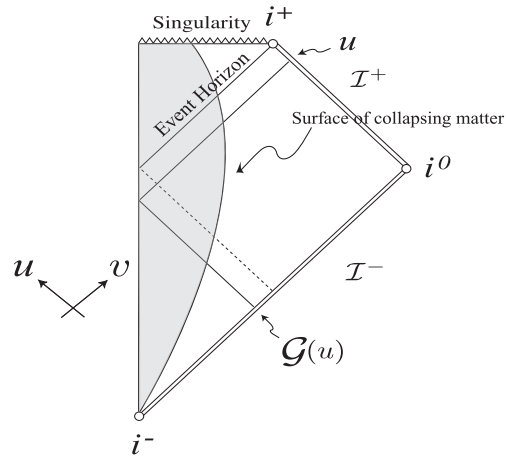


Figure 2.1: A possible causal structure of the black hole formation in gravitational collapse. The singularity is totally spacelike and covered by the event horizon. An ingoing null ray $u = \text{const}$ can be traced backward in time from \mathcal{I}^+ to \mathcal{I}^- , which turns out to be an ingoing null ray $v = \mathcal{G}(u)$.

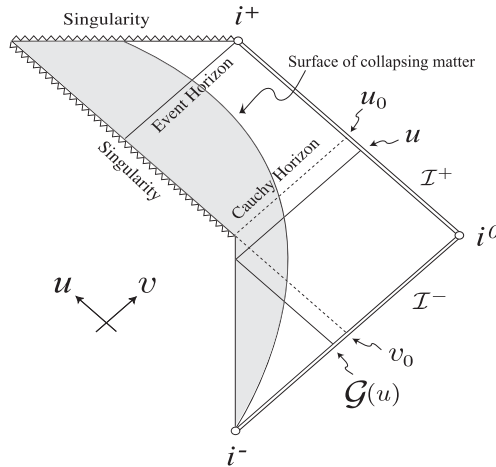


Figure 2.2: A possible causal structure of the naked-singular spacetime considered in this thesis. A singularity occurs at the spacetime point (u_0, v_0) and is visible from \mathcal{I}^+ , where (u, v) are suitable null coordinates. An ingoing null ray $u = \text{const}$ can be traced backward in time from \mathcal{I}^+ to \mathcal{I}^- , which turns out to be an ingoing null ray $v = \mathcal{G}(u)$. The outgoing null ray $u = u_0$ and ingoing null ray $v = v_0$ represent the CH and the null ray that terminates at the NS.

Chapter 3

Particle creation in self-similar NS formation

Generic spherically symmetric self-similar collapse results in strong naked-singularity formation. In this chapter we are concerned with particle creation during a naked-singularity formation in spherically symmetric self-similar collapse without specifying the collapsing matter. In the generic case, the luminosity of particle emission is found to be proportional to the inverse square of the remaining time to the CH. The constant of proportion can be arbitrarily large in the limit to a marginally naked singularity. Therefore, the unbounded luminosity is especially striking in the case that an event horizon is very close to the CH because the emitted energy can be arbitrarily large in spite of a cutoff expected from quantum gravity. The divergence of redshifts and blueshifts of emitted particles is found to cause the divergence of luminosity to positive or negative infinity, depending on the coupling manner of scalar fields to gravity. On the other hand, it is found that there is a special class of self-similar spacetimes in which the semiclassical instability of the CH is not efficient.

3.1 Spherical self-similar spacetimes admitting a NS

In this chapter a class of spacetimes which are spherically symmetric and admitting a homothetic Killing vector field ξ , which satisfies $\mathcal{L}_\xi g_{\mu\nu} = 2g_{\mu\nu}$, is considered. The line element of this class of spacetime in an advanced null coordinate system is written as

$$ds^2 = g_{vv}(x)dv^2 + 2g_{vR}(x)dv dR + R^2 d\Omega^2, \quad (3.1)$$

where $x \equiv v/R$, $d\Omega^2$ is the line element of a unit two dimensional sphere, and the homothetic Killing vector field is of the form $\xi = v\partial_v + R\partial_R$. In this spacetime, the geodesic equation for

an outgoing null ray is written as

$$\frac{dv}{dR} = -\frac{2g_{vR}}{g_{vv}} = xf(x), \quad (3.2)$$

where

$$f(x) \equiv -\frac{2g_{vR}}{xg_{vv}}. \quad (3.3)$$

Equation (3.2) can be written also as

$$\frac{dx}{dR} = \frac{x(f(x) - 1)}{R}, \quad (3.4)$$

which is integrated to give

$$\frac{R}{R_0} = \exp \left[\int_{x_0}^x F(x') dx' \right], \quad F(x) \equiv \frac{1}{x(f(x) - 1)}, \quad (3.5)$$

where x_0 and R_0 are constants which are related as $R_0 = R(x = x_0)$. The constant x_0 is chosen as $x_0 < x^+$ and $x_0 \neq 0$.

What we have to do first is to extract features of $f(x)$, which determines the spacetime structure. The Misner-Sharp mass in this spacetime is given by

$$m(v, R) \equiv \frac{R}{2} (1 - \nabla_\mu R \nabla^\mu R) = \frac{R}{2} \left(1 + \frac{4}{x^2 f^2 g_{vv}} \right).$$

The regularity of the center $R = 0$ in the region $v < 0$ and the absence of a trapped or a marginally trapped surface for $0 < R$ and $v \leq 0$ are assumed. The latter condition is $\nabla_\mu R \nabla^\mu R > 0$ for all $x \in (-\infty, 0]$, which is written as $g_{vv} < 0$ for all $x \in (-\infty, 0]$ in the present case. The inevitability of a curvature singularity at the origin $v = R = 0$ can be shown except for a flat spacetime [34]. In this article we consider self-similar spacetimes with a globally naked singularity, of which existence breaks the weak version of the cosmic censorship hypothesis. One of the possible causal structures of the naked-singular spacetimes is depicted in Fig. 2.2. The coordinate v is set to be the proper time along the regular center to remove a gauge freedom $v \rightarrow V(v)$, so that $\lim_{x \rightarrow -\infty} g_{vv} = -1$. When m/R^3 is required to be finite at the regular center, the function $f(x)$ behaves as

$$f \simeq 2/x \quad \text{as } x \rightarrow -\infty. \quad (3.6)$$

The quantity m/R^3 must be finite also in the limit $v \rightarrow 0$ for fixed $R (> 0)$ so that

$$f = O(|x|^\beta) \quad \text{as } x \rightarrow 0, \quad (3.7)$$

where $\beta \leq -1$. When there are positive roots of the algebraic equation $f(x) = 1$, it can be shown that the curve $x = x^+$ is a CH, as we will see in Appendix A, where x^+ is the smallest root. The differentiability of the metric function f is assumed to be as follows:

$$\frac{1}{f} \in C^0((-\infty, x^+)), \quad f \in C^{2-} \quad \text{at } x = x^+. \quad (3.8)$$

The former condition guarantees the existence and uniqueness of geodesics in this system. It is also assumed¹ that

$$f'(x^+) < 0. \quad (3.9)$$

The schematic plot of the function $f(x)$ is shown in Fig. 3.1(a).

3.2 Local map

To estimate the luminosity of particle creation just before the singularity occurs, the pole at $x = x^+$ should be extracted from the integrand in Eq. (3.5) as follows:

$$\begin{aligned} \frac{R}{R_0} &= \exp \left[\int_{x_0}^x \left\{ F(x') - \frac{1}{\gamma(x' - x^+)} \right\} dx' \right] \exp \left[\int_{x_0}^x \frac{dx'}{\gamma(x' - x^+)} \right] \\ &= \exp \left[\int_{x_0}^x F^*(x') dx' \right] \left(\frac{x^+ - x}{x^+ - x_0} \right)^{1/\gamma}, \end{aligned} \quad (3.10)$$

where

$$\begin{aligned} \gamma &\equiv x^+ f'(x^+), \\ F^*(x) &\equiv F(x) - \frac{1}{\gamma(x - x^+)}. \end{aligned} \quad (3.11)$$

The constant R_0 in Eq. (3.5), which parameterizes solutions, is related to the time $v_c \equiv v(R = 0) < 0$ when the outgoing null ray emanates from the regular center as follows:

$$\begin{aligned} \frac{R}{R_0} &= \exp \left[- \int_{x_0}^x \frac{dx'}{x'} \right] \exp \left[\int_{x_0}^x \left\{ F(x') + \frac{1}{x'} \right\} dx' \right] \\ &= \left| \frac{Rx_0}{v} \right| \exp \left[\int_{x_0}^x \frac{f(x')}{x' (f(x') - 1)} dx' \right]. \end{aligned}$$

Taking the limit of $R \rightarrow 0$ ($v < 0$), following relation is obtained:

$$R_0 = - \frac{v_c}{|x_0| I}, \quad I \equiv \exp \left[\int_{x_0}^{-\infty} \frac{f(x')}{x' (f(x') - 1)} dx' \right], \quad (3.12)$$

¹One can prove $f'(x^+) \leq 0$ with the dominant energy condition on collapsing matter and the equality is excluded by a physically reasonable requirement on the collapsing matter at the CH [34].

where condition (3.6) ensures the convergence of the integral in Eq. (3.12).

Combination of Eqs. (3.10) and (3.12) yields

$$R = C(R, x) (v^+(R) - v)^{1/\gamma} v_c, \quad (3.13)$$

where

$$\begin{aligned} v^+(R) &\equiv x^+ R, \\ C(R, x) &\equiv -|x_0|^{-1} I^{-1} [(x^+ - x_0)R]^{-1/\gamma} \exp \left[\int_{x_0}^x F^*(x') dx' \right]. \end{aligned}$$

Before turning to the derivation of the local map, a few remarks should be made concerning the function $C(R, x)$. Due to condition (3.8), $C(R, x)$ converges to some finite constant in the limit $x \rightarrow x^+$ for fixed R . The dependence of $C(R, x)$ on x_0 is only an apparent one as

$$\frac{\partial C}{\partial x_0} = 0, \quad (3.14)$$

which we use in Sec. 3.5.

Now let us consider a pair of ingoing and outgoing null rays such that the latter is the reflection of the former at the regular center. An observer who rests at $R = \mathfrak{R}$ will encounter the null ray twice so that we denote the time of first encounter by v_1 and that of the second by v_2 . The relation between v_1 and v_2 , which we call the local map, is obtained from Eq. (3.13):

$$v_1 = \frac{\mathfrak{R}}{C(\mathfrak{R}, x_2)} (v^+(\mathfrak{R}) - v_2)^{\alpha_1}, \quad (3.15)$$

where

$$\begin{aligned} x_2 &\equiv v_2/\mathfrak{R}, \\ \alpha_1 &\equiv -1/\gamma. \end{aligned} \quad (3.16)$$

The time intervals $-v_1 (> 0)$ and $v^+(\mathfrak{R}) - v_2$ are depicted schematically in Fig. 3.1(b). It is noted that the result does not change even if we choose a small value of \mathfrak{R} . Namely, the nature of the local map is determined by the behavior of null rays near the singularity.

3.3 Luminosity and energy

A global map $v = \mathcal{G}(u)$ is defined to be a relation between the moments when one null ray leaves \mathcal{I}^- and terminates at \mathcal{I}^+ after passing through the regular center (see Fig. 2.2). Assuming the geometric optics approximation, one can obtain the luminosity of emission as the vacuum

expectation value of a stress-energy tensor by the point-splitting regularization from the global map [17],

$$L = \frac{1}{24\pi} \left[\frac{3}{2} \left(\frac{\mathcal{G}''}{\mathcal{G}'} \right)^2 - \frac{\mathcal{G}'''}{\mathcal{G}'} \right]$$

for a minimally coupled scalar field, and

$$\hat{L} = \frac{1}{48\pi} \left(\frac{\mathcal{G}''}{\mathcal{G}'} \right)^2$$

for a conformally coupled scalar field.

Spherically symmetric self-similar spacetimes are not asymptotically flat in general. They therefore should be matched with an outer asymptotically flat region via a proper non-self-similar region. This matching procedure is quite straightforward for dust collapse [19]. Although it seems to be necessary to solve null geodesic equations in such a “patched-up” spacetime, the main properties of the global map must be determined by the behavior of null rays passing near the point where the singularity occurs. This expectation has been confirmed in [33], at least for the self-similar and analytic dust models. Therefore, one can safely assume that the global map inherits the main properties of the local map, such as the value of the exponent and differentiability. This means that from Eq. (3.15), the asymptotic form of the global map would take the form

$$\mathcal{G}(u) = v_0 - (u_0 - u)^\alpha \mathcal{G}_*(u),$$

where the null rays $u = u_0$ and $v = v_0$ are the CH and the ingoing null ray that terminates at the NS, respectively. The function $\mathcal{G}_*(u)$ is a regular function which does not vanish at the CH and α is the exponent of the local map, α_1 in Eq. (3.15).

In the case of $\alpha = 1$, the leading contribution to the luminosity of particle creation is calculated as

$$L = \frac{2\mathcal{G}'^2(u_0) - \mathcal{G}_*(u_0)\mathcal{G}_*''(u_0)}{8\pi\mathcal{G}_*^2(u_0)}, \quad (3.17)$$

$$\hat{L} = \frac{1}{12\pi} \left(\frac{\mathcal{G}'_*(u_0)}{\mathcal{G}_*(u_0)} \right)^2, \quad (3.18)$$

so that the luminosity remains finite at the CH. Unfortunately $\mathcal{G}_*(u_0)$ and its derivatives cannot be known until the null geodesic equation is solved globally, so that one could not know the luminosity of emission from only the information contained in the local map. In terms of redshift, $\alpha = 1$ corresponds to the case that the redshift of a particle remains finite at the CH, as we will see in Sec. 3.4.

On the other hand, in the case of $\alpha \neq 1$ the leading contribution is obtained as

$$L = \frac{\alpha^2 - 1}{48\pi(u_0 - u)^2}, \quad (3.19)$$

for a minimally coupled scalar field. For a conformally coupled one, the luminosity of emission is obtained by replacing the factor $(\alpha^2 - 1)$ in Eq. (3.19) for $(\alpha - 1)^2$. The luminosity is proportional to the inverse square of the remaining time to the CH. If $\alpha > 1$, the luminosity diverges to positive infinity for both minimally and conformally coupled scalar fields, while if $0 < \alpha < 1$, the luminosity diverges to negative and positive infinity for minimally and conformally coupled scalar fields, respectively. In terms of the redshift of particles, the case that $\alpha > 1$ ($0 < \alpha < 1$) corresponds to infinite redshift (blueshift) at the CH, as we will see in Sec. 3.4. The emitted energy can be estimated as

$$E = \int_{-\infty}^u L(u') du' = \frac{\alpha^2 - 1}{48\pi(u_0 - u)}. \quad (3.20)$$

Although the emitted energy diverges when the CH is approached, this divergence needs to be regarded carefully. The semiclassical approximation would cease to be valid when the curvature radius at some spacetime point inside star reaches the Planck scale. Here we make a natural assumption that such a situation happens at the center of a star at $v = -t_{\text{QG}}$ ². In the case of $\alpha > 1$, it can be expected that for a ray emanating from the center at $v = -t_{\text{QG}}$, the time difference $u_0 - u$ would be greater than the order of t_{QG} due to redshift, i.e., $\Delta u \equiv u_0 - u > t_{\text{QG}}$. Then energy emitted by the time $u_0 - \Delta u$ is

$$E = \frac{\alpha^2 - 1}{48\pi\Delta u} < \frac{\alpha^2 - 1}{48\pi} E_{\text{QG}}, \quad (3.21)$$

where $E_{\text{QG}} \equiv 1/t_{\text{QG}}$. If the factor $(\alpha^2 - 1)/(48\pi)$ is on the order of unity, the total radiated energy within the semiclassical phase is less than the order of E_{QG} , which would be of course much less than the mass of ordinary astrophysical stars. It would be better to say that a collapsing star would enter the phase of quantum gravity with most of its mass intact. Therefore, one could not predict whether a star which collapses to a NS evaporates away or ceases to radiate at its final epoch. This has been pointed out in [75] after careful investigation. We should not overlook that this feature is much different from that of black hole evaporation, in which quantum gravitational effects appear after a black hole loses almost all its mass.

One can recognize, however, that if $\alpha \gg 1$ the radiated energy could be large. This situation is realized in the limit to marginally NS, in which the CH and event horizon coincide³. To

²The time t_{QG} can be regarded as the Planck time t_{pl} ; at least this is the case for self-similar dust model.

³When the CH and event horizon exactly coincide, radiation reduces to the Hawking one [17, 18]. This fact cannot be derived with the method making use of the local map since in this case, $\gamma = 0$ in Eq. (3.10). It is not surprising since an event horizon, which plays a central role in the Hawking radiation, is not a local object but a global one [76].

illustrate the unbounded increase of α in this limit, we have to look deeper into the causal structure, which is determined by the function f . We order the positive roots of the equation $f(x) = 1$ as $0 < x_1 = x^+ < x_2 < \dots < x_n$, where we count multiple roots as one root. The existence of x_a satisfying $\lim_{x \rightarrow x_a} f(x) = +\infty$ with $x_n < x_a$ and the continuity of f in the region $x_1 < x < x_a$ are assumed. In the region $x \in (x_n, x_a)$, $dR/dv > 0$ along the null geodesics and $\lim_{x \rightarrow x_a} dR/dv = 0$ from Eq. (3.2). This implies that outgoing null rays in this region are to turn back in the direction of the singularity at $x = x_a$ and that the curve $x = x_n$ is the last outgoing null ray which can escape to infinity. That is to say, $x = x_a$ and $x = x_n \equiv x_e$ are the apparent horizon and event horizon, respectively. Hereafter, we shall concentrate on the case of $n = 2$. The function $f(x)$ would be written as

$$f(x) - 1 = f_*(x)(x - x^+)(x_e - x)^m, \quad 0 < x < x_a, \quad (3.22)$$

where $f_*(x)$ is a function which satisfies $f_*(x^+) < 0$ and m is some positive integer. The exponent of the factor $(x - x^+)$ is restricted to unity because of the condition $f'(x^+) < 0$ and the differentiability $f \in C^{2-}$ at $x = x^+$. With Eq. (3.22), the exponent of the local map is calculated as

$$\alpha_1 \equiv -\frac{1}{x^+ f'(x^+)} = -\frac{1}{x^+ f'_*(x^+) (x_e - x^+)^m}, \quad (3.23)$$

to show that α_1 can be arbitrarily large in the limit $x^+ \rightarrow x_e$.

3.4 Redshift

The estimation of redshift of the radial null ray would help us understand the behavior of the luminosity and would be necessary for discussing the validity of geometric optics and semiclassical approximations. Hereafter the tangent vector of the null ray is denoted by $k^\mu \equiv dx^\mu/d\lambda$, where λ is an affine parameter.

With the null condition $k^\mu k_\mu = 0$, the v -component of the geodesic equation $k^\mu \nabla_\mu k^\nu = 0$ leads to

$$\frac{dk^v}{d\lambda} + \frac{(k^v)^2}{R} \left(\frac{1}{g_{vR}} \frac{dg_{vR}}{dx} + \frac{x}{2} \frac{1}{g_{vR}} \frac{dg_{vv}}{dx} \right) = 0.$$

Furthermore by using the relation

$$\frac{d}{d\lambda} = \frac{k^v}{R} \left(1 + \frac{xg_{vv}}{2g_{vR}} \right) \frac{d}{dx},$$

$k^v(x)$ is integrated to give

$$\frac{k^v(x)}{k_0^v} = \exp \left[\int_{\tilde{x}_0}^x \tilde{F}(x') dx' \right] = \exp \left[\int_{\tilde{x}_0}^x \tilde{F}^*(x') dx' \right] \left(\frac{x^+ - x}{x^+ - \tilde{x}_0} \right)^{-(1+\gamma)/\gamma}, \quad (3.24)$$

where

$$\begin{aligned}\tilde{F}(x) &\equiv -\frac{1}{g_{vR}} \frac{dg_{vR}}{dx} + \frac{1}{1-f} \left(\frac{1}{x} + \frac{1}{f} \frac{df}{dx} \right), \\ \tilde{F}^*(x) &\equiv \tilde{F}(x) + \frac{1+\gamma}{\gamma} \frac{1}{x-x^+}.\end{aligned}$$

The constant \tilde{x}_0 , which is set as $\tilde{x}_0 < x^+$, and the constant k_0^v are related as $k_0^v = k^v(\tilde{x}_0)$.

The constant k_0^v is related to $k_c^v \equiv k^v(R=0)$ as

$$k_0^v = \frac{k_c^v}{\tilde{I}}, \quad \tilde{I} \equiv \exp \left[\int_{\tilde{x}_0}^{-\infty} \tilde{F}(x') dx' \right]. \quad (3.25)$$

Combination of Eqs. (3.24) and (3.25) yields

$$k^v(x) = \tilde{C}(R, x) (v^+(R) - v)^{\alpha_1 - 1} k_c^v, \quad (3.26)$$

where

$$\tilde{C}(R, x) \equiv \tilde{I}^{-1} [(x^+ - \tilde{x}_0)R]^{(1+\gamma)/\gamma} \exp \left[\int_{\tilde{x}_0}^x \tilde{F}^*(x') dx' \right].$$

Now, let us consider time-like observers who rest at $R=0$ and $R=\mathfrak{R}$ ($d\theta = d\phi = 0$). The observed frequency is given by $\hat{\omega} \equiv -u_\mu k^\mu = \sqrt{|g_{vv}(x)|} k^v(x)$, where u_μ is the four-velocity of observer. When $\hat{\omega}_1 \equiv \lim_{x \rightarrow -\infty} \hat{\omega}(x)$ and $\hat{\omega}_2 \equiv \lim_{x \rightarrow x^+} \hat{\omega}(x)$ are defined, Eq. (3.26) yields

$$\frac{\hat{\omega}_2}{\hat{\omega}_1} = \sqrt{\left| \frac{g_{vv}(x^+)}{g_{vv}(-\infty)} \right|} \tilde{C}(\mathfrak{R}, x_2) (v^+(\mathfrak{R}) - v_2)^{\alpha_1 - 1}. \quad (3.27)$$

Thus we see that if $\alpha_1 > 1$ ($0 < \alpha_1 < 1$) the redshift (blueshift) of emitted particle diverges at the CH, while it remains finite if $\alpha_1 = 1$. The relation between the redshift derived above and the local map will be presented in the next section.

3.5 Relations among the local map, luminosity, and redshift

There would be a relation between the local map and redshift because the local map describes a kind of time delay. Since the asymptotic behavior of the local map and redshift in the limit $x \rightarrow x^+$ is considered here, the time dependence is omitted as $C(R, x) \rightarrow C(R)$. From Eq. (3.15), the relation

$$\frac{dv_2}{dv_1} = \frac{\gamma C(\mathfrak{R})}{\mathfrak{R}} (v^+(\mathfrak{R}) - v_2)^{(1+\gamma)/\gamma} \quad (3.28)$$

holds to give an alternative definition of redshift. Indeed, the time dependence in Eq. (3.28) can be replaced with the ratio of k^v by Eq. (3.26) as

$$\frac{dv_2}{dv_1} = \left| \frac{g_{vv}(-\infty)}{g_{vv}(x^+)} \right| \frac{k_c^v}{k^v(x_2)}, \quad (3.29)$$

where we set $x_0 = \tilde{x}_0$ in the evaluation of the integral in C to derive Eq. (3.29) since C does not depend on x_0 from Eq. (3.14). Equation (3.29) can be written as

$$\frac{d\tau_2}{d\tau_1} = \frac{\hat{\omega}_1}{\hat{\omega}_2}, \quad (3.30)$$

where $d\tau_i \equiv \sqrt{|g_{vv}|} dv_i$ ($i = 1, 2$) is the proper time measured by the observer. This relates the time delay and redshift to reveal that the redshift essentially corresponds to the local map and also to confirm the consistency of the analyses in Secs. 3.2 and 3.4.

There exists a plausible relation also between the luminosity of emission and the redshift of particles as mentioned in Sec. 3.3. In the case of $\alpha > 1$ ($0 < \alpha < 1$), the luminosity and redshift (blueshift) diverge at the CH from Eqs. (3.19) and (3.27), while the luminosity and redshift remain finite at the CH in the case of $\alpha = 1$. We may, therefore, reasonably conclude that the divergence of the redshift or blueshift at the CH causes that of the luminosity.

3.6 Examples

In this section, we will take examples to illustrate how the features obtained in the previous sections are realized in concrete models. Since several models are written in the diagonal form of a metric tensor, the formulation and notations for the diagonal form of a metric tensor are developed in Appendix B.

3.6.1 Minkowski spacetime

Although neither singularity nor horizon exists in Minkowski spacetime, one can test the formalism by applying it to this trivial spacetime. The line element is written as

$$ds^2 = -dv^2 + 2dv dR + R^2 d\Omega^2,$$

or

$$ds^2 = -dt^2 + dr^2 + r^2 d\Omega^2.$$

From definitions (3.3) and (B.2), one obtains

$$f(x) = \frac{2}{x}, \quad w_{\pm}(z) = \pm \frac{1}{z}.$$

The roots of the algebraic equations $f(x) = 1$ and $w_{\pm}(z) = 1$ are given as $x^+ = 2$ and $z^{\pm} = \pm 1$, respectively. It must be noted that the function $f(x)$ satisfies conditions (3.6)-(3.9), which have been assumed to derive the local map. According to Eqs. (3.11), (3.16), (B.4), and (B.8), one can easily check that the exponents of local maps, α_1 and α_2 , are unity. This fact just tells us that the redshift and luminosity remain finite in a flat spacetime.

3.6.2 Vaidya solution

The Vaidya solution describes the collapse of a null-dust fluid [77]. The global map for the self-similar Vaidya collapse was derived in [22].

The line element in the self-similar Vaidya spacetime is written as

$$ds^2 = -(1 - m(x)) dv^2 + 2dv dR + R^2 d\Omega^2,$$

where $m(x) = 0$ for $x < 0$ and $m(x) = 2\mu x$ for $x \geq 0$. The constant μ is restricted as $0 < \mu < 1/16$ for the nakedness, so that the spacetime with $\mu = 1/16$ corresponds to a marginally naked-singular one. The function $f(x)$ is written as

$$f(x) = \frac{2}{x(1 - m(x))}.$$

The roots of algebraic equation $f(x) = 1$ are given as

$$x^+ = \frac{1 - \sqrt{1 - 16\mu}}{4\mu} \quad \text{and} \quad x_e = \frac{1 + \sqrt{1 - 16\mu}}{4\mu}.$$

What has to be noticed is that f satisfies conditions (3.6)-(3.9). The exponent is calculated as

$$\alpha_1 \equiv -\frac{1}{x^+ f'(x^+)} = \frac{1 + \sqrt{1 - 16\mu}}{2\sqrt{1 - 16\mu}}.$$

This exponent coincides with that of the global map which was obtained in [22]. One can see that $\lim_{\mu \rightarrow 0} \alpha_1 = 1$ and $\lim_{\mu \rightarrow 1/16} \alpha_1 = \infty$, where the former and latter correspond to the limits of Minkowski and marginally naked-singular spacetime. This example is a good illustration of the efficiency of the local map and the divergence of α_1 in the limit to marginally NS.

3.6.3 Roberts solution

The Roberts solution describes the self-similar collapse of a massless scalar field [35]. The line element is given as

$$ds^2 = -\left(1 - \frac{2h(x)h'(x)}{\sqrt{1 + h^2(x)}}\right) dv^2 + \frac{2}{\sqrt{1 + h^2(x)}} dv dR + R^2 d\Omega^2, \quad (3.31)$$

where $h(x) = 0$ for $x < 0$ and $h(x) = \sigma x$ for $x \geq 0$, so that the region with negative v is flat. The constant σ is restricted here as $|\sigma| < 1/2$ for the causal structure such that the spacetime has a time-like NS as in Fig. 3.2. The function $f(x)$ is written as

$$f(x) = \frac{2}{x(\sqrt{1+h^2} - 2hh')}.$$

The conditions on $f(x)$ are again satisfied. The algebraic equation $f(x) = 1$ has a positive root $x^+ = 2/\sqrt{1-4\sigma^2}$ so that the exponent of local map is calculated as

$$\alpha_1 \equiv -\frac{1}{x^+ f'(x^+)} = 1$$

for $|\sigma| < 1/2$. Thus we see that the Roberts solution provides a non-trivial example of spacetime in which the luminosity of particle creation remains finite at the CH in self-similar collapse.

3.6.4 Lemaître-Tolman-Bondi (LTB) solution

The Lemaître-Tolman-Bondi (LTB) solution describes the collapse of a dust fluid [78]. Although both global and local maps were derived in [19] and [33] respectively for self-similar LTB collapse, the exponent in [19] is reproduced from the formalism in Sec. 3.2.

The line element of self-similar LTB spacetime (for example, see [19]) is

$$ds^2 = -dt^2 + \left[\frac{1 - az/3}{(1 - az)^{1/3}} \right]^2 dr^2 + r^2(1 - az)^{4/3} d\Omega^2,$$

where the constant a is related to a ‘‘mass parameter’’ λ as $a = \frac{3}{2}\sqrt{\lambda}$. The constant λ is restricted to the range $0 < \lambda < 6(26 - 15\sqrt{3}) \equiv \lambda_m$, where the latter inequality is imposed by the nakedness of the singularity [15], so that the spacetime with $\lambda = \lambda_m$ corresponds to marginally naked-singular one. One obtains the function $w_{\pm}(z)$ according to definition (B.2) as

$$w_{\pm}(z) = \pm \frac{1 - az/3}{z(1 - az)^{1/3}}. \quad (3.32)$$

The required conditions on w_{\pm} in calculating the local map are satisfied. When a new variable $y \equiv (1 - az)^{1/3}$ introduced, Eq. (3.32) can be written as

$$w_{\pm}^2(z) = 1 - \frac{4g_+(y)g_-(y)}{[g_+(y) + g_-(y)]^2},$$

where $g_{\pm}(y) \equiv 3y^4 \mp ay^3 - 3y \mp 2a$, so that the roots of algebraic equations $w_{\pm}(z) = 1$ correspond to those of $g_{\mp}(y) = 0$. Using the chain rule $d/dz = (dy/dz)d/dy$, one obtains

$$z^{\pm} w'_{\pm}(z^{\pm}) = \frac{2(1 - 3\alpha_{\mp}^3)g'_{\mp}(\alpha_{\mp})}{3\alpha_{\pm}g_{\pm}(\alpha_{\mp})},$$

where $\alpha_{\pm} \equiv (1 - az^{\mp})^{1/3}$ and the prime denotes differentiation with respect to the argument of the function. The exponent of local map is calculated as

$$\alpha_2 \equiv \frac{z^- w'_-(z^-)}{z^+ w'_+(z^+)} = \frac{\alpha_-^3 g'_+(\alpha_+)}{\alpha_+^3 g'_-(\alpha_-)}$$

to coincide with the one derived in [19, 33]. This exponent becomes close to unity as $\lambda \rightarrow 0$ and increases monotonically with λ to diverge to infinity as $\lambda \rightarrow \lambda_m$.

3.6.5 General relativistic Larson-Penston solution

As the last example the general relativistic Larson-Penston (GRLP) solution, which describes the self-similar collapse of a perfect fluid [27, 28], is considered. For the present, it may be useful to review the GRLP solution and its importance, although we have mentioned them in the Introduction. The equation of state must have the form of $P = k\rho$ from the requirement of self-similarity, where k is a constant. The GRLP solution represents a naked-singularity formation in the range $0 < k \lesssim 0.0105$, where the upper bound is imposed by the nakedness of the singularity. This solution is interesting because it provides the first example in which the pressure does not prevent the formation of a NS. Moreover, the convergence to the GRLP solution of more general solutions near the central region of stars have been strongly suggested numerically and supported by a mode analysis [29] as a realization of the self-similarity hypothesis [30]. From the above, the GRLP solution will be a strongest known counterexample against the cosmic censorship hypothesis.

Because the GRLP solution is a numerical one, an explicit expression of the exponent of local map could not be obtained analytically, although it is unlikely that α is equal to unity. To show rigorously that the luminosity of emission is proportional to the inverse square of the remaining time to the CH and that the constant of proportion diverges in the limit to marginally NS, the dependence of exponent α on k should be clarified numerically.

3.7 Summary and Discussion

We have been concerned with a quantum mechanical particle creation during the naked-singularity formation in spherically symmetric self-similar collapse. The luminosity, energy, and redshift of emitted particles are analytically calculated on the assumption that the curvature around the singularity causes particle creation and the metric function f is C^{2-} around the CH. As a result, in the generic case in which the exponent of the local map $\alpha \neq 1$, the luminosity has been found to diverge as $L \propto (t_{ch} - t)^{-2}$, where $(t_{ch} - t)$ is the remaining time until a distant observer would receive a first light ray from the NS. It is worth pointing out that the weaker differentiability of the CH leads to a different result, i.e., the luminosity of emission has a different time dependence, although we have not looked deeper into such a possibility in this paper. The

square inverse proportion of the luminosity to the remaining time is due to the scale invariance of self-similar spacetimes. The constant of proportion has been found to be arbitrarily large in the limit to marginally NS. Therefore, this explosive radiation is especially striking in the case that the event horizon is very close to the CH because the emitted energy can be arbitrarily large in spite of a cutoff expected from quantum gravity. We go on from this to the conclusion that if the back reaction to a gravitational field is taken into account, the semiclassical effect would cause the instability of the CH and might recover the cosmic censor in this limiting case. On the other hand, in the non-generic case in which $\alpha = 1$ the luminosity remains finite at the CH, so that the semiclassical instability of the CH seems not to be efficient for this special class of self-similar solutions. The collapse of a massless scalar field described by the Roberts solution indeed does correspond to this case. In addition, it has been found that the diverging redshift and blueshift cause the divergence of the luminosity to positive or negative infinity, depending on the manner of the coupling of scalar fields to gravity. The divergence will be a criterion for the stability/instability of a CH in a gravitational collapse.

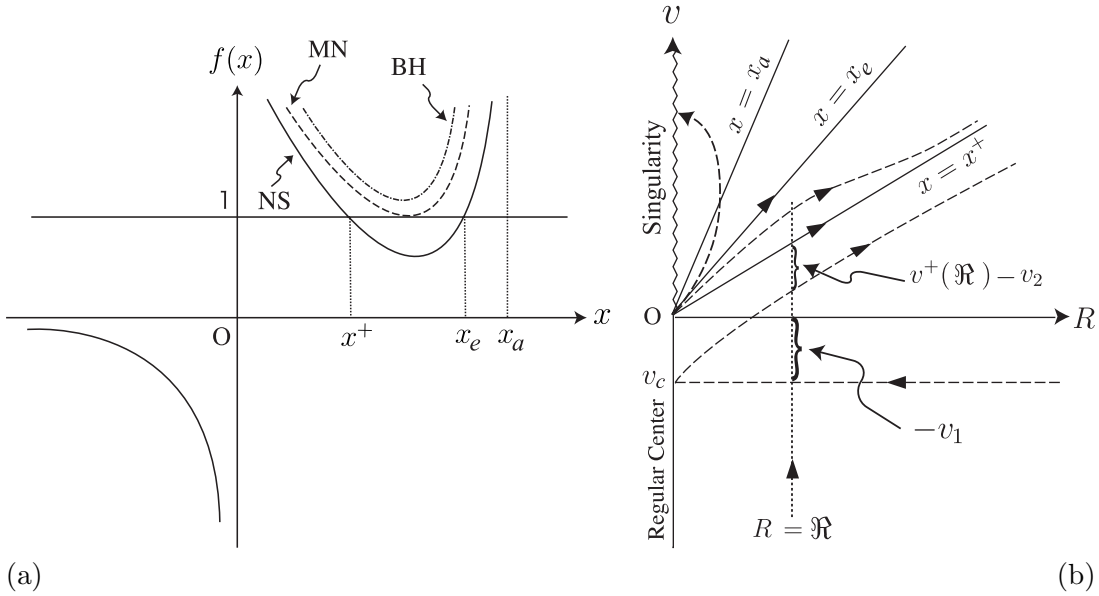


Figure 3.1: (a) Schematic plots of $f(x)$ defined by Eq. (3.3) for typical collapsing spacetimes which end in a NS or a black hole. Depending on the number of roots of $f(x) = 1$, which we denote by j , the causal structure of spacetime changes. The cases of $j = 0, 1$, and 2 are depicted. (i) The case of $j = 2$: $f(x) (x > 0)$ is depicted by a solid line. The two roots are denoted by x^+ and x_e ($x^+ < x_e$). The geodesics $x = x^+$ and $x = x_e$ represent the CH and event horizon, respectively. This kind of spacetime admits a NS. (ii) The case of $j = 1$: $f(x) (x > 0)$ is depicted by a dashed line. In this case, $x^+ = x_e$ holds, i.e., the CH and event horizon coincide. This type of singularity is called marginally naked (MN). (iii) The case of $j = 0$: $f(x) (x > 0)$ is depicted by a dot-dashed line. In this case the collapse ends in a black hole (BH). (b) A typical spacetime diagram of a collapsing body which ends in a naked singularity in (v, R) coordinates. A null ray which is reflected at the regular center and characteristic null rays in respective regions divided by horizons are depicted. The time intervals $v^+(\mathfrak{R}) - v_2$ and $-v_1$ in Eq. (3.15) are depicted. The dotted line is the world line of an observer at $R = \mathfrak{R}$.

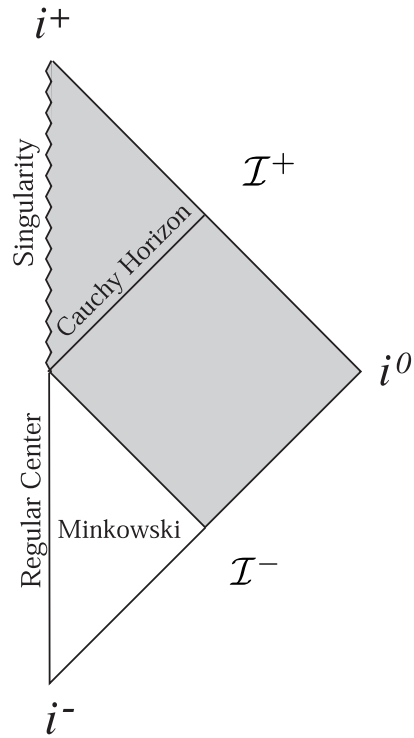


Figure 3.2: The conformal diagram of the Roberts solution Eq. (3.31) with $|\sigma| < 1/2$. The region $v < 0$ is flat and the shading region is filled with a collapsing massless scalar field. A time-like NS occurs at $v = 0$.

Chapter 4

Quantum effect and curvature strength of NS

The aim of this chapter is to examine the relation between the curvature strength of NSs and the number of created particles. To reach this aim, we analytically estimate the luminosity and total energy of emitted particles during the formation of shell-focusing NSs in a wide class of spherical dust collapse. It is found that if the NS satisfies the strong curvature condition (SCC), the quantum radiation diverges as the Cauchy horizon is approached, whereas, if the NS does not satisfy the limiting focusing condition (LFC), the radiation remains finite. If the NS does not satisfy the SCC but does the LFC, the radiation may be either divergent or finite. From the viewpoint of the cosmic censorship, the finite amount of quantum emission is crucial because the CHs will be free from the instability expected from the backreaction of quantum fields. In addition, it is also discussed how the coupling manner of quantum fields to gravity affects the amount of radiation.

4.1 NS in LTB spacetime

4.1.1 LTB solutions admitting a NS

The LTB solution [78], which describes the collapse of a dust ball, in a comoving coordinate system is written as

$$\begin{aligned} ds^2 &= -dt^2 + \frac{R'^2}{1+f(r)} dr^2 + R^2(t,r) d\Omega^2, \\ \dot{R}^2 &= \frac{F(r)}{R} + f(r), \\ \rho &= \frac{F'}{8\pi R^2 R'} \end{aligned} \tag{4.1}$$

where ρ is the energy density, $d\Omega^2$ is the line element of a unit two-dimensional sphere, and the prime and dot denote the partial derivatives with respect to r and t , respectively. Since we are concerned with the collapse of a dust fluid, we require $\dot{R} < 0$. Arbitrary functions $F(r)$ and $1 + f(r) > 0$ are twice the conserved Misner-Sharp mass and the specific energy, respectively. Hereafter we concentrate on the marginally bound case for simplicity, which is defined by $f = 0$. In such a case, Eq. (4.1) is integrated to give

$$R^3 = \frac{9}{4}F(r)[t - t_s(r)]^2, \quad (4.2)$$

where $t_s(r)$ is an arbitrary function of r . The time $t = t_s(r)$ corresponds to one when a dust shell at r meets the shell-focusing singularity, which is defined by $R = 0$. It is possible to choose as $t_s(r) = r$ by the scaling of r . LTB solutions can describe the formation of a shell-focusing NS from regular spacetimes. It has been shown that the shell-focusing singularity occurring at $R = 0$ with $r > 0$ is totally spacelike [79], and therefore our discussion will be confined to the singularity at $(t, r) = (0, 0)$.

Here, we introduce a class of marginally bound LTB solutions in which the leading term of mass function F near the regular center takes the form of

$$F(r) = \frac{4\lambda^3}{9(\mu + 1)^3}r^{3\mu+1} + o(r^{3\mu+1}), \quad (4.3)$$

where $\mu (\geq 0)$ and $\lambda (> 0)$ are constants. The nontrivial form of factor and power in Eq. (4.3) is just for later convenience. In Appendix C, it is shown that this class of LTB spacetimes results in the formation of a shell-focusing NS, which could be globally naked and could violate the weak version of CCH. Radial null geodesics are described near the center by

$$\frac{dt}{dr} = \pm R' \simeq \pm \lambda r^\mu \mathcal{F}(t/r), \quad (4.4)$$

where

$$\mathcal{F}(z) \equiv \left[1 - \frac{3\mu + 1}{3(\mu + 1)}z \right] (1 - z)^{-1/3}.$$

Here, the upper and lower signs correspond to outgoing and ingoing null geodesics, respectively.

It will be helpful for later discussion to look into the initial regular density profile of the dust fluid near the regular center. The initial density profile at an initial time slice of $t = t_{in} < 0$ is written as,

$$\rho(t_{in}, r) = \frac{1}{6\pi t_{in}^2} \left[1 + 2 \left(1 + \frac{F}{rF'} \right) \frac{r}{t_{in}} + O((r/t_{in})^2) \right].$$

Therefore, in the present case, the initial density profile in terms of physical radius $R \propto r^{\mu+1/3}$ takes the form of

$$\rho_{\text{in}}(R) = \rho_0 + \rho_1 R^\gamma + \dots, \quad (4.5)$$

where

$$\gamma \equiv \frac{3}{3\mu + 1}, \quad \rho_0 \equiv \frac{1}{6\pi t_{\text{in}}^2}, \quad \rho_1 \equiv -\frac{(3\mu + 2)(\mu + 1)^{3/(3\mu+1)}}{3(3\mu + 1)\pi\lambda^{3/(3\mu+1)}(-t_{\text{in}})^{(9\mu+5)/(3\mu+1)}}. \quad (4.6)$$

Note that the parameter γ is in the region of $0 < \gamma \leq 3$ for $\mu \geq 0$. In particular, the analytic and self-similar LTB models are the cases with $\gamma = 2$ ($\mu = 1/6$) and $\gamma = 3$ ($\mu = 0$), respectively.

4.1.2 Curvature strength of the NSs

The curvature strength of spacetime singularities is defined in a hope that weak convergence would imply the extendibility of the spacetime in a distributional sense. In this context, Tipler defined the *strong curvature condition* (SCC) [36], while Królak defined a weaker condition, which we call the *limiting focusing condition* (LFC) [37]. The sufficient and necessary conditions for the singularities in spherically symmetric spacetimes with vanishing radial pressure satisfying the LFC or SCC are given in simple forms [40]. Here, we explain the results obtained in [40]. If a singularity is naked, the relation between the circumferential radius R and the Misner-Sharp mass m is given by

$$R \simeq 2y_0 m^\beta \quad (4.7)$$

near the singularity along the null geodesics terminating at or emanating from the NS. The constant β is in the region of

$$1/3 < \beta \leq 1. \quad (4.8)$$

The constants y_0 and β are determined by requiring that there exist a positive finite limit of $y_0 \equiv \lim_{m \rightarrow 0} R/(2m^\beta)$ along the null geodesics terminating at or emanating from the NS. If the geodesic satisfies the ‘‘gravity-dominance condition’’ [40], which the null geodesic terminating at or emanating from the shell-focusing NS in LTB spacetime satisfies, the sufficient and necessary conditions are summarized as the following theorem [40]: *if and only if $1/3 < \beta < 1/2$ is satisfied, neither the SCC nor the LFC holds; if and only if $1/2 \leq \beta < 1$ is satisfied, not the SCC but only the LFC holds; and if and only if $\beta = 1$, both the SCC and the LFC hold, for the radial null geodesic terminating at or emanating from the NS.*

In the case of the LTB spacetimes we consider, from Eq. (C.2), $R \propto r^{\mu+1}$ holds along the outgoing null geodesic emanating from the NS, i.e., along the CH ¹

$$\beta = \frac{\mu + 1}{3\mu + 1} = \frac{2\gamma + 3}{9}. \quad (4.9)$$

With the above theorem by Harada *et al.*, the NS for $0 < \gamma < 3/4$ satisfy neither the LFC nor the SCC along the outgoing null geodesic emanating from the NS. The NS for $3/4 \leq \gamma < 3$ does not satisfy the SCC but does the LFC. The NS for $\gamma = 3$ satisfies both the LFC and the SCC. See also the Table 4.1 for the relation among γ , β , and the curvature strength of NSs.

4.2 Map of null rays passing near the naked singularity

4.2.1 Local map

The *global map*, $v = \mathcal{G}(u)$, is defined as the relation between the moments when a null ray leaves \mathcal{I}^- and when it terminates at \mathcal{I}^+ after passing through the regular center (see Fig. 2.2). The global map plays crucial roles in the estimate of quantum radiation in the geometrical-optics approximation. The global map cannot be obtained without solving the null geodesic equation from \mathcal{I}^- to \mathcal{I}^+ globally.

However, the main properties of the global map for NS formation will be determined by the behavior of null rays near the singularities, since the particle creation will be caused by the curvature around singularities. From this point of view, Tanaka and Singh proposed an alternative map, which we call the *local map* [33]. They considered an observer on a comoving shell who sends ingoing null rays. These null rays are reflected at the regular center, and come back to the same comoving observer. A radial null geodesic crosses a comoving shell located at a fixed comoving radius r before and after the reflection at the center. Thus these null rays define a map between the sending time and the receiving time measured by the proper time for the comoving observer. See Fig. 4.1 for a schematic illustration of the local map. The local map is expected to have the same structure as the global map because there are no singular features in the map between the proper time on a comoving shell at a finite distance and those measured by the null coordinates naturally defined at infinity.

This expectation has been confirmed for the self-similar dust [33, 10] and the analytic dust [33] models. Two of the present authors generalized the local map to a general class of self-similar spacetimes without specifying the collapsing matter, and the validity of such a local map was confirmed for the self-similar Vaidya model [10]. Therefore, one can safely assume that the local map has the same structure as the global map in the LTB spacetimes dealt with in this paper.

¹The null ray given by Eq. (C.2) is a asymptotic solution of the null geodesic equation with the boundary condition of $t(0) = 0$. In fact, Eq. (C.2) is the *earliest* null ray which emanates from the singularity. This was proved by Christodoulou [79] and this proof can be easily generalized to other cases.

In this section, we calculate the local map by solving the radial null geodesic equation for the non-self-similar LTB spacetimes ($\mu > 0$). The local map for the self-similar LTB spacetime ($\mu = 0$) was obtained in Refs. [33] and [10].

4.2.2 Outline of the calculation of local map

To make the notation simple, we change the coordinates as

$$\begin{aligned} r' &= \lambda^{1/\mu} r, \\ t' &= \lambda^{1/\mu} t, \end{aligned}$$

and we abbreviate r' and t' as r and t , respectively, hereafter in this section. Then, the null geodesic equation (4.4) becomes

$$\frac{dt}{dr} = \pm r^\mu \mathcal{F}(t/r). \quad (4.10)$$

Before getting into a substantial calculation, it is convenient to summarize the calculation scheme for obtaining the local map, which we will implement in the following subsections. To obtain the local map, we have to obtain solutions of Eq. (4.10) near $r = 0$, which correspond to radial null rays passing through the center at $t = t(0) = -t_0$ ($t_0 > 0$) and then take the limit $t_0 \rightarrow 0$. We cannot expect, however, to have general exact solutions to this equation. Hence, here we adopt the following scheme to obtain the local map. First, we apply three different approximation regimes A, B and C, and find three kinds of expressions, $t = t^A(r)$, $t = t^B(r)$ and $t = t^C(r)$, respectively. Next we show that these three regimes have an overlapping region, where all three approximations are valid and the obtained approximate solutions can be matched with each other. Finally, we calculate the local map, that is, we calculate the relation between the sending time and the receiving time of the null ray at a comoving observer near the center.

In Sec. 4.2.3, we apply approximation regime A, where $0 \leq r < \eta_A t_0^{1/(1+\mu)}$ is satisfied. Here, $\eta_A (\ll 1)$ is a positive constant independent of t_0 . In this regime, we can deal with the center and then we can relate the ingoing and outgoing null rays, which reach the center at the same time $t = -t_0$. In Sec. 4.2.4, we apply approximation regime B, where $t_0/\eta_B < r < \eta_A t_0^{1/(1+\mu)}$ is satisfied. Here, $\eta_B (\ll 1)$ is a positive constant. This regime is possible only when $t_0 < (\eta_A \eta_B)^{(1+\mu)/\mu}$. Although regime B is completely included in regime A, regime B enables us to have an explicit expression for solutions and is therefore essential to obtain the local map. In Sec. 4.2.5, we apply approximation regime C, where $t/r \ll 1$ is assumed. When we put $t/r = O(\eta_C)$, where $\eta_C (\ll 1)$ is a sufficiently small constant, it turns out that the approximation is valid for $t_0/\eta_C \lesssim r \lesssim \eta_C^{1/\mu}$. Regimes A and B trivially have an overlapping region. When we take the limit $t_0 \rightarrow 0$, regime B and regime C have an overlapping region and regime C is still valid at a finite radius. See also Fig. 4.2 for the illustration of regions, where each regime is valid. In Sec. 4.2.6, we implement the matching between the approximate solutions $t = t^B(r)$ and $t = t^C(r)$ in the overlapping

region. In Sec. 4.2.7, the local map is finally obtained for a comoving observer at a finite radius in the region for regime C. This is the generalization of Tanaka and Singh [33].

4.2.3 Regime A: $0 \leq r < \eta_A t_0^{1/(1+\mu)}$

To find a null geodesic for $0 \leq r < \eta_A t_0^{1/(1+\mu)}$, we put

$$\frac{r}{t_0^{1/(\mu+1)}} = \epsilon \zeta, \quad (4.11)$$

$$\frac{r}{t_0} = \frac{\zeta}{\delta}, \quad (4.12)$$

where ϵ and δ are constants, and ζ is variable for r . $\epsilon < \eta_A$ and $\zeta = O(1)$ is assumed. δ is introduced for later convenience and not necessarily small in regime A. From Eqs. (4.11) and (4.12), the following relations hold:

$$t_0 = \epsilon^{(\mu+1)/\mu} \delta^{(\mu+1)/\mu}, \quad (4.13)$$

$$r = \epsilon^{(\mu+1)/\mu} \delta^{1/\mu} \zeta. \quad (4.14)$$

The null geodesic $t = t^A(r)$ can be expanded by ϵ as follows:

$$t^A(r) = -t_0 + \sum_{n=1}^{\infty} \epsilon^{(\mu+1)(n\mu+1)/\mu} t_n^A(\zeta), \quad (4.15)$$

where $t_n^A(\zeta)$ ($n = 1, 2, \dots$) are the functions of ζ of order unity. Substituting Eq. (4.15) into Eq. (4.10), the following differential equations are obtained,

$$\frac{dt_1^A}{d\zeta}(\zeta) = \pm \delta^{(\mu+1)/\mu} \zeta^\mu \mathcal{F}(-\delta/\zeta), \quad (4.16)$$

$$\frac{dt_2^A}{d\zeta}(\zeta) = \pm \delta \zeta^{\mu-1} \mathcal{F}'(-\delta/\zeta) t_1^A(\zeta), \quad (4.17)$$

$$\frac{dt_3^A}{d\zeta}(\zeta) = \pm \frac{1}{2} \delta^{(\mu-1)/\mu} \zeta^{\mu-2} \mathcal{F}''(-\delta/\zeta) (t_1^A)^2(\zeta) \pm \delta \zeta^{\mu-1} \mathcal{F}'(-\delta/\zeta) t_2^A(\zeta), \quad (4.18)$$

and so on, where \mathcal{F}' and \mathcal{F}'' denote the derivatives of \mathcal{F} with respect to its argument. Since $t^A(0) = -t_0$, $t_n^A(0) = 0$ must be satisfied for $n \geq 1$. Equation (4.16) can be integrated immediately to give

$$t_1^A(\zeta) = \pm \frac{1}{\mu+1} \delta^{(\mu+1)/\mu} \zeta^{\mu+1} (1 + \delta/\zeta)^{2/3}. \quad (4.19)$$

With $t_1^A(\zeta)$ obtained above, Eq. (4.17) is integrated to give

$$t_2^A(\zeta) = \frac{1}{\mu+1} \delta^{(2\mu+1)/\mu} \int_0^\zeta \hat{\zeta}^{2\mu} \mathcal{F}'(-\delta/\hat{\zeta})(1+\delta/\hat{\zeta})^{2/3} d\hat{\zeta} \quad (4.20)$$

$$= \delta^{(\mu+1)(2\mu+1)/\mu} I_2(\zeta/\delta), \quad (4.21)$$

where

$$I_2(y) \equiv \frac{1}{\mu+1} \int_0^y x^{2\mu} \mathcal{F}'(-1/x)(1+1/x)^{2/3} dx. \quad (4.22)$$

This integration cannot be expressed in terms of elementary functions. In a similar way, one can write $t_3^A(\zeta)$ in an integral form,

$$\begin{aligned} t_3^A(\zeta) &= \pm \int_0^\zeta \left[\frac{1}{2(\mu+1)^2} \delta^{(3\mu+1)/\mu} \hat{\zeta}^{3\mu} \mathcal{F}''(-\delta/\hat{\zeta})(1+\delta/\hat{\zeta})^{4/3} \right. \\ &\quad \left. + \delta^{(2\mu^2+4\mu+1)/\mu} \hat{\zeta}^{\mu-1} \mathcal{F}'(-\delta/\hat{\zeta}) I_2(\hat{\zeta}/\delta) \right] d\hat{\zeta} \\ &= \pm \delta^{(\mu+1)(3\mu+1)/\mu} I_3(\zeta/\delta), \end{aligned}$$

where

$$I_3(y) \equiv \int_0^y \left[\frac{1}{2(\mu+1)^2} x^{3\mu} \mathcal{F}''(-1/x)(1+1/x)^{4/3} + x^{\mu-1} \mathcal{F}'(-1/x) I_2(x) \right] dx. \quad (4.23)$$

It should be noted that we can safely take the limit $r \rightarrow 0$ in this regime because we do not assume δ is small.

4.2.4 Regime B: $t_0/\eta_B < r < \eta_A t_0^{1/(1+\mu)}$

For the approximation regime B, we will additionally assume that $\delta < \eta_B$. This also requires that $t_0 \ll 1$ from Eq. (4.13). The approximate solution $t = t^B(r)$ can be obtained by approximating $t = t^A(r)$ with $\delta \ll 1$. Hence, we define $t_n^B(\zeta)$ as the function which is obtained by approximating $t_n^A(\zeta)$ with $\delta \ll 1$. Thus, we have

$$t_1^B = \pm \frac{1}{\mu+1} \delta^{(\mu+1)/\mu} \zeta^{\mu+1} \left[1 + \frac{2}{3} \zeta^{-1} \delta + O(\delta^2) \right]. \quad (4.24)$$

The approximate form of t_2^A for $\delta \ll 1$ can be obtained by using the asymptotic form of $I_2(y)$ for large y in Eq. (4.22) given by

$$I_2(y) = C_2 - \frac{2\mu}{3(\mu+1)^2(2\mu+1)} y^{2\mu+1} [1 + O(1/y)],$$

where C_2 is a constant. Except for the term of C_2 , all other terms are completely determined by integrating the expanded integrand. Therefore, $t_2^B(\zeta)$ is obtained as

$$t_2^B(\zeta) = C_2 \delta^{(\mu+1)(2\mu+1)/\mu} - \frac{2\mu}{3(\mu+1)^2(2\mu+1)} \delta^{(2\mu+1)/\mu} \zeta^{2\mu+1} [1 + O(\delta)]. \quad (4.25)$$

Similarly, the asymptotic form of I_3 is given by

$$I_3(y) = C_3 + \left[\frac{2\mu^2 + \mu + 1}{9(\mu+1)^3(2\mu+1)(3\mu+1)} y^{3\mu+1} - \frac{2C_2}{3(\mu+1)} y^\mu \right] [1 + O(1/y)].$$

and hence $t_3^B(\zeta)$ is

$$t_3^B(\zeta) = \pm C_3 \delta^{(\mu+1)(3\mu+1)/\mu} \pm \frac{2\mu^2 + \mu + 1}{9(\mu+1)^3(2\mu+1)(3\mu+1)} \delta^{(3\mu+1)/\mu} \zeta^{3\mu+1} [1 + O(\delta)] \\ \mp \frac{2C_2}{3(\mu+1)} \delta^{(2\mu^2+4\mu+1)/\mu} \zeta^\mu [1 + O(\delta)]. \quad (4.26)$$

Then, an approximate solution is obtained by Eqs. (4.13)-(4.15) and (4.24)-(4.26) as

$$t^B(r) = -t_0 + C_2 t_0^{2\mu+1} \pm C_3 t_0^{3\mu+1} \\ + \left[\pm \frac{1}{\mu+1} r^{\mu+1} - \frac{2\mu}{3(\mu+1)^2(2\mu+1)} r^{2\mu+1} \pm \frac{2\mu^2 + \mu + 1}{9(\mu+1)^3(2\mu+1)(3\mu+1)} r^{3\mu+1} \right] \\ \times [1 + O(\delta)]. \quad (4.27)$$

For later use, we have obtained the explicit expression up to the third order. It is straightforward to compute higher orders. It should be noted that we cannot take the limit $r \rightarrow 0$ in this expression (4.27).

4.2.5 Regime C: $t/r \ll 1$

Suppose $t/r \ll 1$. Here, we introduce $\eta \ll 1$, which controls Suppose $t/r \ll 1$. Here, we introduce $\eta_C \ll 1$, which controls the order of t/r , i.e., $t/r = O(\eta_C)$. In this approximation regime, we can expand f by t/r on the right hand side of Eq. (4.10) and obtain the expanded form of solutions.

Let us consider the critical outgoing and ingoing null geodesics $t = t_\pm^{\text{crit}}(r)$, which emanate from and terminate at the NS, i.e., $t = r = 0$. $t = t_+^{\text{crit}}(r)$ gives the CH by definition. If we assume $t/r = O(\eta_C)$, they are obtained by expanding the null geodesic equation (4.10) with power series of r with the boundary condition of $t(0) = 0$,

$$t_\pm^{\text{crit}}(r) = \pm \frac{1}{\mu+1} r^{\mu+1} - \frac{2\mu}{3(\mu+1)^2(2\mu+1)} r^{2\mu+1} \\ \pm \frac{2\mu^2 + \mu + 1}{9(\mu+1)^3(2\mu+1)(3\mu+1)} r^{3\mu+1} + O(\eta_C^4), \quad (4.28)$$

where the upper (lower) sign corresponds to emanating (terminating) null ray. For $0 < r \lesssim \eta_C^{1/\mu}$, $t/r = O(\eta_C)$ is satisfied on the critical null rays and this approximation is justified. That is, approximation regime C is valid for $0 < r \lesssim \eta_C^{1/\mu}$ on the critical null rays.

However, we are interested in null rays which are slightly earlier than these critical null rays. We expand the solution as follows:

$$t = t^C(r) = \sum_{n=1}^{\infty} t_n^C(r), \quad (4.29)$$

where we assume $t_n^C(r)/r = O(\eta_C^n)$. Substituting Eq. (4.29) into Eq. (4.10) and expanding the right hand side, the following differential equations are obtained:

$$\frac{dt_1^C}{dr} = \pm r^\mu, \quad (4.30)$$

$$\frac{dt_2^C}{dr} = \mp \frac{2\mu}{3(\mu+1)} r^{\mu-1} t_1^C(r), \quad (4.31)$$

$$\frac{dt_3^C}{dr} = \mp \frac{2\mu}{3(\mu+1)} r^{\mu-1} t_2^C(r) \mp \frac{\mu-1}{9(\mu+1)} r^{\mu-2} (t_1^C)^2(r). \quad (4.32)$$

These equations are integrated to yield

$$t_1^C(r) = D_\pm \pm \frac{1}{\mu+1} r^{\mu+1}, \quad (4.33)$$

$$t_2^C(r) = \mp \frac{2}{3(\mu+1)} D_\pm r^\mu - \frac{2\mu}{3(\mu+1)^2(2\mu+1)} r^{2\mu+1}, \quad (4.34)$$

$$t_3^C(r) = \mp \frac{1}{9(\mu+1)} D_\pm^2 r^{\mu-1} + \frac{1}{9\mu(\mu+1)} D_\pm r^{2\mu} \pm \frac{2\mu^2 + \mu + 1}{9(\mu+1)^3(2\mu+1)(3\mu+1)} r^{3\mu+1}, \quad (4.35)$$

where D_\pm is an integration constant which appears in the integration of Eq. (4.30). Integration constants for Eqs. (4.31) and (4.32) are set to be zero. From Eqs. (4.29), (4.33)-(4.35), the solution takes the following form:

$$\begin{aligned} t^C(r) &= D_\pm \\ &\pm \frac{1}{\mu+1} r^{\mu+1} \\ &\mp \frac{2}{3(\mu+1)} D_\pm r^\mu - \frac{2\mu}{3(\mu+1)^2(2\mu+1)} r^{2\mu+1} \\ &\mp \frac{1}{9(\mu+1)} D_\pm^2 r^{\mu-1} + \frac{1}{9\mu(\mu+1)} D_\pm r^{2\mu} \pm \frac{2\mu^2 + \mu + 1}{9(\mu+1)^3(2\mu+1)(3\mu+1)} r^{3\mu+1} \\ &+ O(\eta_C^4). \end{aligned} \quad (4.36)$$

Now, we can examine in what region the solution (4.36) is valid. To justify the expansion (4.29), $t_n^C(r)/r = O(\eta_C^n)$ must be satisfied. This is the case if

$$\max\left(r^\mu, \frac{D_\pm}{r}\right) = O(\eta_C).$$

If D_\pm is sufficiently small, the above condition implies

$$D_\pm/\eta_C \lesssim r \lesssim \eta_C^{1/\mu}.$$

This is the region where approximation regime C is valid for the null geodesic passing through the center at $t(0) = -t_0 < 0$. The relation between D_\pm and t_0 is shown in the following subsection.

4.2.6 Matching the approximation regimes

Since we are interested in the null rays which are close to the critical null geodesics, we take the limit $t_0 \rightarrow 0$. The region for approximation regime B is completely included in that for regime A and the matching is trivially implemented. If we assume $D_\pm = O(t_0)$, the region where regime C is valid must have an overlap with the region for regime B if $t_0 \lesssim (\eta_A \eta_C)^{(\mu+1)/\mu}$. This means that we can relate the integration constants D_\pm which appear in the regime C solution $t = t^C(r)$ to t_0 which appear in the regime B solution $t = t^B(r)$ by matching these two solutions in the overlapping region.

Different expressions $t = t^B(r)$ and $t = t^C(r)$ for the null geodesic are obtained independently in Secs. 4.2.4 and 4.2.5. We can see the solution $t = t^B(r)$ given by Eq. (4.27) coincide with the solution $t = t^C(r)$ given by Eq. (4.36) in several lowest orders if the constant terms satisfy the following relation:

$$D_\pm \simeq -t_0 + C_2 t_0^{2\mu+1} \pm C_3 t_0^{3\mu+1}. \quad (4.37)$$

This justifies the assumption that D_\pm is sufficiently small and $D_\pm = O(t_0)$ in the limit $t_0 \rightarrow 0$. This also implies that approximation regime C is valid for $t_0/\eta_C \lesssim r \lesssim \eta_C^{1/\mu}$. Here, let us see the condition on t_0 which must be satisfied for the matching. t_0 has to satisfy

$$t_0 < \min\left((\eta_A \eta_B)^{(\mu+1)/\mu}, (\eta_A \eta_C)^{(\mu+1)/\mu}\right), \quad (4.38)$$

so that the region for the regime B and the overlapping region for the regime B and C can exist. It is possible to take such a small t_0 because we are interested in the limit $t_0 \rightarrow 0$. See also Fig. 4.2.

4.2.7 Obtaining the local map

To obtain the local map for this spacetime, we consider a comoving observer at $r = r_0$, where r_0 satisfies $r_0 \lesssim \eta_C^{1/\mu}$. As time proceeds, this observer approaches the ingoing critical null ray $t = t_-^{\text{crit}}(r)$ and therefore enters the region $t_0/\eta_C \lesssim r \lesssim \eta_C^{1/\mu}$, where approximation regime C is valid. Then, $t_{\pm}(r_0) = t_{\pm}^{\text{C}}(r_0)$ are regarded as the sending time and receiving time of the null geodesic, where the sign \pm is introduced to distinguish the outgoing and ingoing null rays. From Eq. (4.36), the constant D_{\pm} is specified as

$$-D_{\pm} = t_{\pm}^{\text{crit}}(r_0) - t_{\pm}(r_0) + O(t_0\eta_C),$$

where $t_{\pm}^{\text{crit}}(r_0)$ is the moment when the observer crosses the null geodesic (4.28). Therefore, if we take η_C to be sufficiently small, D_- (D_+) is interpreted as the time difference between the moments when the observer emits (receives) the null ray and crosses the null ray terminating at (emanating from) the NS. See also Fig. 4.1.

Since we consider a set of an ingoing null ray which reaches the center at $t = -t_0$ and an outgoing null ray which can be regarded as a reflected ray of the former at $t = -t_0$, we pick up both the ingoing and outgoing null rays with the common value for t_0 . When we eliminate t_0 from Eq. (4.37) for both signs, we have the relation between D_+ and D_- as

$$D_- \simeq D_+ - 2C_3(-D_+)^{3\mu+1},$$

which can be rewritten in terms of the sending and receiving times $t_{\pm}(r_0)$ at $r = r_0$ for sufficiently small r_0 as

$$t_-^{\text{C}}(r_0) \simeq t_-^{\text{crit}}(r_0) - [t_+^{\text{crit}}(r_0) - t_+^{\text{C}}(r_0)] - 2C_3 [t_+^{\text{crit}}(r_0) - t_+^{\text{C}}(r_0)]^{3\mu+1}. \quad (4.39)$$

Equation (4.39) is the very local map, relating the moments when the comoving observer locating at $r = r_0$ sends the ingoing null ray and receives the reflected outgoing null rays. If we revive λ , the final result becomes

$$t_-^{\text{C}}(r_0) \simeq t_-^{\text{crit}}(r_0) - [t_+^{\text{crit}}(r_0) - t_+^{\text{C}}(r_0)] - 2C_3\lambda^3 [t_+^{\text{crit}}(r_0) - t_+^{\text{C}}(r_0)]^{3\mu+1}. \quad (4.40)$$

Now, notice that the comoving observer must be in the region $t_0/\eta_C \lesssim r_0 \lesssim \eta_C^{1/\mu}\lambda^{-1/\mu}$. It means that the asymptotic structure of the local map in the limit $t_0 \rightarrow 0$, therefore the main feature of the global map, is determined only by the behavior of the null rays in the small but *finite* region $0 < r \lesssim \eta_C^{1/\mu}\lambda^{-1/\mu}$.

4.3 Luminosity and energy

4.3.1 Non-self-similar LTB spacetimes: $0 < \gamma < 3$

As described in Sec. 4.2, we assume that the local map and the global map have same structure. It means that from Eq. (4.40), the asymptotic form of the global map will take the form of

$$\mathcal{G}(u) \simeq v_0 - A(u_0 - u) - Ag\lambda^3(u_0 - u)^{3\mu+1},$$

where $u = u_0$ and $v = v_0$ are the CH and the ingoing null ray that terminates at the NS, respectively. A and g are constants. Noting that $\mu = (3 - \gamma)/(3\gamma)$, one can calculate the luminosity of particle creation as

$$L^{(\xi)} \simeq \left(\xi - \frac{1}{6} \right) \frac{3(3 - \gamma)(3 - 2\gamma)}{4\pi\gamma^3} g\omega_s^{(3-\gamma)/\gamma} (u_0 - u)^{-3+3/\gamma} \quad (4.41)$$

$$+ \left[\xi - \frac{7\gamma - 15}{36(\gamma - 2)} \right] \frac{27(\gamma - 2)(3 - \gamma)}{4\pi\gamma^4} g^2\omega_s^{2(3-\gamma)/\gamma} (u_0 - u)^{-4+6/\gamma} \quad (4.42)$$

$$+ O\left((u_0 - u)^{-5+9/\gamma}\right), \quad (4.43)$$

where we have defined the ‘‘frequency’’ of the NSs as

$$\omega_s \equiv \lambda^{1/\mu} = \lambda^{3\gamma/(3-\gamma)}. \quad (4.44)$$

In Appendix D, we show the frequency (4.44) is equivalent to one defined in Ref. [23]. One can easily recognize that depending on whether the scalar field couples to the scalar curvature conformally ($\xi = 1/6$) or not ($\xi \neq 1/6$), the leading term of the luminosity changes. Let us examine the time dependence of the luminosity and total energy of emitted particles into detail for the cases of $\xi \neq 1/6$ and $\xi = 1/6$ in order.

In the case of $\xi \neq 1/6$, the first term in Eq. (4.43) dominates except for the special case of $\gamma = 3/2$. In the case of $0 < \gamma \leq 1$, the leading term vanishes as $u \rightarrow u_0$ as the CH is approached. On the other hand, in the case of $1 < \gamma < 3$ and $\gamma \neq 3/2$, the luminosity diverges as the CH is approached as a negative power of the remaining time until the CH. The special case of $\gamma = 3/2$, in which the factor of the first term in Eq. (4.43) vanishes, is divided to two sub-cases depending on whether $\xi \neq 1/4$ or $\xi = 1/4$. If $\xi \neq 1/4$, the second term in Eq. (4.43) survives to be a finite constant. On the other hand, if $\xi = 1/4$, the factor of the second term also vanishes. Therefore, higher order terms contribute to the luminosity, which turn out to be finite at most. Therefore, in the both sub-cases of $\gamma = 3/2$, the luminosity remains finite at the CH. Now, let us examine the total energy of emitted particles. In the case of $3/2 < \gamma < 3$, the leading term in the energy is

$$E^{(\xi)} \simeq - \left(\xi - \frac{1}{6} \right) \frac{3(3 - \gamma)}{4\pi\gamma^2} g\omega_s^{(3-\gamma)/\gamma} (u_0 - u)^{-2+3/\gamma}, \quad (4.45)$$

so that the total energy of emitted particles diverges as the CH is approached. In particular, in the case of analytic LTB solution ($\gamma = 2$), the energy diverges as $(u_0 - u)^{-1/2}$, which coincides with the result in [23]. In the case of $0 < \gamma < 3/2$, the total energy remains finite as the CH is approached. In the special case of $\gamma = 3/2$, the energy also remains finite. See also Table 4.1(a).

In the case of the conformally coupled scalar field, which is defined by Eq. (2.35) with $\xi = 1/6$, the second term in Eq. (4.43) dominates. It is found that in the case of $0 < \gamma \leq 3/2$, the luminosity remains finite at most. While, in the case of $3/2 < \gamma < 3$, the luminosity diverges as the negative power of the remaining time until the CH. Let us examine the total energy of the emitted particles. In the case of $2 < \gamma < 3$,

$$E^{(1/6)} \simeq \frac{(3 - \gamma)^2}{16\pi\gamma^3(\gamma - 2)} g^2 \omega_s^{2(3-\gamma)/\gamma} (u_0 - u)^{-3+6/\gamma}, \quad (4.46)$$

which diverges as the CH is approached. In the case of $\gamma = 2$,

$$E^{(1/6)} \simeq \frac{3}{256\pi} g^2 \omega_s \ln \omega_s^{-1} (u_0 - u)^{-1}, \quad (4.47)$$

so that the energy diverges logarithmically, which coincides with the result in [23] again. On the other hand, if $0 < \gamma < 2$ the energy remains finite at most. See also Table 4.1(b).

It follows from what has been seen that the radiation by the conformally coupled scalar field is milder than that of the non-conformally coupled scalar fields for a given value of γ . Such a consequence would result from the fact that the coupling of the conformal scalar field to gravity is weaker than that of the other scalar fields. It has been known that a conformally coupled scalar field must have non-zero and finite mass to be created in the early universe, while non-conformally coupled scalar particles are created regardless of their mass [8, 80].

4.3.2 Self-similar LTB spacetime: $\gamma = 3$

The global map for the self-similar LTB spacetime ending in NS formation was derived analytically in [19]. Then, its main property was re-produced with the local-map method [33] and chapter 3 in this thesis. The global map for the null rays passing near the CH is given by

$$\mathcal{G}(u) \simeq v_0 - B(u_0 - u)^\alpha [1 + q(u_0 - u) + O((u_0 - u)^2)], \quad (4.48)$$

where α , B , and q are constants. The terms in the square brackets in Eq. (4.48) is an analytic function of $(u_0 - u)^2$. The constant α depends only on the parameter λ in Eq. (4.3) and is

²In previous works on particle creation during NS formation in the self-similar LTB spacetime, only the constant term in the square bracket in Eq. (4.48) was considered [19, 10, 33], which was sufficient to obtaining results. It is easy to calculate the higher order terms by the local-map method and to show that they constitute an analytic function near the CH. It is possible, however, that the emergence of the scale, q , in Eq. (4.48) from such a scale invariant spacetime as self-similar LTB solution indicates the breakdown of the local-map method. What extent the local-map method is valid leaves room for discussion.

shown to be greater than unity for the region of λ in which the singularity is naked [19]. Using the global map (4.48), we can compute the luminosity and energy of the particle creation as

$$L^{(\xi)} \simeq \frac{(\alpha - 1)(\alpha + 1 - 12\xi)}{48\pi}(u_0 - u)^{-2} + \frac{\alpha^2 - 1}{24\pi\alpha}q(u_0 - u)^{-1}, \quad (4.49)$$

$$E^{(\xi)} \simeq \frac{(\alpha - 1)(\alpha + 1 - 12\xi)}{48\pi}(u_0 - u)^{-1} + \frac{\alpha^2 - 1}{24\pi\alpha}q \ln q^{-1}(u_0 - u)^{-1}. \quad (4.50)$$

Each first term in Eqs. (4.49) and (4.50) dominates except for the special case of $\xi = (\alpha + 1)/12$. Therefore, the luminosity and energy generically diverge as the inverse square and the inverse of the remaining time to the CH, respectively. On the other hand, in the special case of $\xi = (\alpha + 1)/12$, each second term in Eqs. (4.49) and (4.50) dominates so that the power and energy diverge inversely and logarithmically, respectively. This case, however, should be regarded as a non-realistic case in the sense that the coupling constant ξ is fine-tuned as to be a special value, determined by the detail of the collapse, α . See also Tables 4.1(a) and 4.1(b).

4.4 Summary and discussion

In this chapter we have considered particle creation during the formation of shell-focusing NSs in the wide class of spherical dust collapse, which is described by the marginally bound LTB solutions. Each solution has different initial density profile, and the resulting NSs have a variety of curvature strength along the CHs. The luminosity and energy of particle creation have been estimated for each LTB solution and each scalar field that couples to scalar curvature in the linear form. The results are summarized in Tables 4.1(a) and 4.1(b).

We first mention the validity of the approximations which have been assumed in this article. After that, we discuss the relations between the quantum radiation and the curvature strength of the NSs and also the coupling manner of scalar fields. Last, we discuss the implications of the present result to the CCH.

The analysis has been based on three assumptions: the validity of the local-map method, the geometrical-optics approximation, and the quantum field theory in curved spacetime. The validity of each approximation seems to leave room for discussion. See Ref. [23] for the discussion on the geometric optics approximation and Refs. [75] and [10] for the quantum field theory in curved spacetime, respectively. Here, we focus on the local-map method, on which our analysis is totally based. The point is that the crucial factor of particle creation, the redshift of particles, must be determined by the geometry near the NS, while in the Hawking radiation the redshift is determined by the event horizon, which is a global object. It is unlikely that the global map has a different structure from that of the local map, since there is no singular feature in the map between the moments on the comoving observer at a finite distance and that of the null coordinates naturally defined at infinity. Indeed, in the models of the self-similar LTB [33, 10], the analytic LTB [33] and the self-similar Vaidya [10], the local-map method provides the correct

results, which are obtained with the global map. Therefore, we have assumed the validity of the local-map method.

From the results, it is found that following statements hold for the generic naked-singular LTB spacetimes: *the SCC along the CH is a sufficient condition for the luminosity and energy of the created scalar particles to diverge as the CH is approached; while, not to satisfy the LFC is a sufficient condition for the luminosity and energy to be finite at the CH; if the NS does not satisfy the SCC but does the LFC, the luminosity and energy can be either divergent or finite.* We only consider the dust collapse for simplicity; however, the above statements as to the curvature strength and the quantum radiation would be independent of the collapsing matter because the particle creation is a purely kinematic phenomenon and not directly related to the Einstein field equations. Therefore, we conjecture that the above statements hold for spherically symmetric collapsing spacetimes with *any kinds of collapsing matter*. Of course, its validity should be verified or examined with known solutions ending in NS formation. The self-similar models which have ever been examined, the collapse of a null-dust fluid [77, 22, 10], a massless scalar field [35, 10], and a perfect fluid [27, 28, 10], support this conjecture. There are many examples to be investigated: the NS formation in the counter-rotating particles [81, 40], non-self-similar null dust [77], null strange quark matter [82], various matter fields in the critical collapse [32] and so on. Here, we also mention the coupling manner of scalar fields to gravity. Although the quantum radiation due to the conformally coupled scalar field is less than that of other scalar fields, including the minimally coupled scalar field, the dependence of the amount of radiation on the coupling manner is not so drastic as to modify the above statements.

Next, we move on to the implication of the results to the CCH. The diverging radiation from strong NSs corresponds to an instability of the strong NS formation. The system will enter into a phase where the backreaction from the quantum field to spacetime plays an important role. While, the finite radiation from the weak NSs corresponds to a stability of the weak NS formation. It is striking because the weak NSs seem to need another mechanism if they are to hide behind horizons. Of course, we cannot dismiss the possibility that the effect of backreaction suppresses the quantum radiation and the strong NSs appear, all things considered.

In the present analysis, we do not find a necessary and sufficient condition on the curvature strength of NSs for the quantum radiation to be divergent or finite. We believe that a new definition of strength of (naked) singularities should be proposed from the viewpoint of the behavior of quantum fields on spacetimes rather than the viewpoint of the behavior of classical particles. Such a philosophy can be seen also in the wave-probe approach to NSs [83, 84, 85], which is based on the theory of dynamics in non-globally hyperbolic spacetimes developed first by Wald [86]. On this point, there is room for further investigation.

Table 4.1: The relation among the curvature strength of naked singularities, the luminosity, and the energy of scalar fields near the Cauchy horizons (a) for the non-conformally coupled scalar fields ($\xi \neq 1/6$) and (b) for the conformally coupled scalar field ($\xi = 1/6$). The constant γ parameterizes the initial density profile of a dust fluid. SCC implies LFC.

(a)

γ	0		3/4		1		3/2		3
Strength	–	Weak	LFC						SCC
Luminosity	–	Finite			Divergent	Finite	Divergent		
Energy	–	Finite					Divergent		

(b)

γ	0		3/4		3/2		2		3
Strength	–	Weak	LFC						SCC
Luminosity	–	Finite			Divergent				
Energy	–	Finite					Divergent		

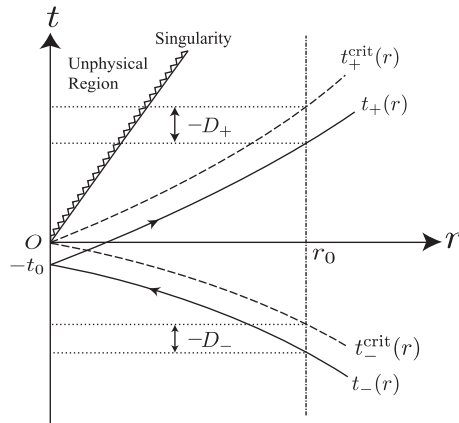


Figure 4.1: A schematic spacetime diagram of the dust-filled region with the illustration of the local map defined in Sec. 4.2. A pair of an ingoing null ray $t_-(r)$ and an outgoing null ray $t_+(r)$ is depicted (solid line), which passes near the NS, locating at $(t, r) = (0, 0)$. Null rays terminating at and emanating from the NS, $t_-^{\text{crit}}(r)$ and $t_+^{\text{crit}}(r)$, are also depicted (dashed lines), where the latter is the CH. A comoving observer is locating at $r = r_0 = \text{constant}$. The local map is defined as the relation between $t_-(r_0)$ and $t_+(r_0)$.

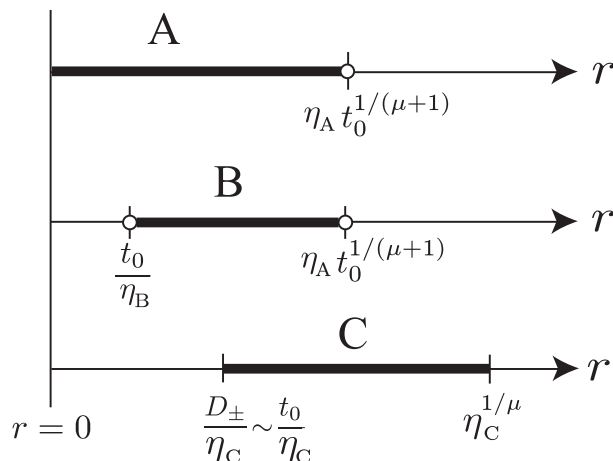


Figure 4.2: A schematic illustration of the regions, where regimes A, B and C are valid. The regions for regimes A, B and C are $0 \leq r < \eta_A t_0^{1/(\mu+1)}$, $t_0/\eta_B < r < \eta_A t_0^{1/(\mu+1)}$ and $D_{\pm}/\eta_C \sim t_0/\eta_C \lesssim r \lesssim \eta_C^{1/\mu}$, respectively, where $\eta_X \ll 1$ ($X = A, B, C$) is a constant independent of t_0 . The region for B is included in that for A. The regions for B and C exist if $t_0 < (\eta_A \eta_B)^{(\mu+1)/\mu}$ and $t_0 < \eta_C^{(\mu+1)/\mu}$ are satisfied, respectively. The regions for B and C overlap if $t_0 < (\eta_A \eta_C)^{(\mu+1)/\mu}$. All these conditions are satisfied for $t_0 < \min[(\eta_A \eta_B)^{(\mu+1)/\mu}, (\eta_A \eta_C)^{(\mu+1)/\mu}]$. In the limit $t_0 \rightarrow 0$, the regions for A and B shrink to zero but the region for C, where the comoving observer should locate, remains finite.

Chapter 5

Mathematics of the doubly special relativity

The Lorentz invariance violation which we consider in this thesis is due to the existence of a scale in the fundamental transformation of the frame in flat spacetimes. Usually, the transformation between the Galileian frames is given by the Poincarè algebra, which intrinsically the physical parameter c (speed of light). On the other hand, the “ κ -Poincarè algebra” intrinsically has a more fundamental scale κ , which corresponds to the “minimum” scale of the spacetime. We see that the dispersion relation of particles under such a spacetime symmetry is modified. We see also that the spacetime noncommutativity appears as a “dual” property of the modified symmetry. We review the mathematical structure of Hopf algebras (for example, see [87]), which are regarded as a generalization of Lie algebras. Then, we introduce the κ -Poincarè algebra as a Hopf algebra and the κ -Minkowski noncommutative spacetime as its dual.

5.1 Hopf algebra

Firs, let us see the definition of an algebra and a coalgebra, the latter is a dual structure of the former.

5.1.1 Algebra and coalgebra

Definition 5.1.1 (Algebra) *An algebra¹ (A, m, u) over \mathbf{C} is a linear space A and linear maps,*

$$\begin{aligned} m : A \otimes A &\longrightarrow A, & (\text{product}) \\ u : \mathbf{C} &\longrightarrow A, & (\text{unit map}) \end{aligned}$$

¹Here, we define the algebra with an unit element. Usually, an algebra does not have to contain an unit element.

such that

$$\begin{aligned} m \cdot (m \otimes id) &= m \cdot (id \otimes m), & (\text{associative law}) \\ m \cdot (id \otimes u) &= m \cdot (u \otimes id) = id. & (\text{unitive law}) \end{aligned}$$

Definition 5.1.2 (Coalgebra) A coalgebra (C, Δ, ϵ) over \mathbf{C} is a vector space C and linear maps,

$$\begin{aligned} \Delta : C &\longrightarrow C \otimes C, & (\text{coproduct}) \\ \epsilon : C &\longrightarrow \mathbf{C}, & (\text{counit}) \end{aligned}$$

such that

$$\begin{aligned} (id \otimes \Delta) \cdot \Delta &= (\Delta \otimes id) \cdot \Delta, & (\text{coassociative law}) \\ (id \otimes \epsilon) \cdot \Delta &= (\epsilon \otimes id) \cdot \Delta. & (\text{counitive law}) \end{aligned}$$

For algebras A and B , $f \in \text{Hom}_{\mathbf{C}}(A, B)$ ² is called an *algebra map* when for $a_1, a_2 \in A$ the following is satisfies,

$$f(a_1 a_2) = f(a_1) f(a_2), \quad f(1_A) = 1_B,$$

where 1_A and 1_B is an unit element in A and B , respectively. On the other hand, f is called a *anti-algebra map* when the following is satisfies,

$$f(a_1 a_2) = f(a_2) f(a_1), \quad f(1_A) = 1_B.$$

For coalgebras C and D , $f \in \text{Hom}_{\mathbf{C}}(C, D)$ is called a *coalgebra map* when the following is satisfied,

$$\Delta_D(f(c)) = (f \otimes f) \Delta_C(c), \quad \epsilon_D(f(c)) = \epsilon_C(c), \quad \forall c \in C.$$

On the other hand, f is called an *anti-coalgebra map* when the following is satisfied,

$$\Delta_D(f(c)) = (f \otimes f) \Delta'_C(c), \quad \epsilon_D(f(c)) = \epsilon_C(c), \quad \forall c \in C,$$

where $\Delta' \equiv \tau \cdot \Delta$ and $\tau(c \otimes c') \equiv c' \otimes c$.

5.1.2 Bialgebra and Hopf algebra

Definition 5.1.3 (Bialgebra) Now, we are the position that we can define bialgebra algebras and Hopf algebras as a bialgebra with a antipode as follows. Suppose that B has the structures as an algebra (B, m, u) and a coalgebra (B, Δ, ϵ) . $(B, m, u, \Delta, \epsilon)$ is said to be a bialgebra if it satisfies one of the following conditions, which are equivalent each other,

²The set of homeomorphism between the linear spaces, A and B , over the field \mathbf{C} .

- $\Delta : B \longrightarrow B \otimes B$ and $\epsilon : B \longrightarrow \mathbf{C}$ are both algebra maps
- $m : B \otimes B \longrightarrow B$ and $u : B \longrightarrow \mathbf{C}$ are both coalgebra maps

Definition 5.1.4 (Antipode) Suppose $(H, m, u, \Delta, \epsilon)$ to be a bialgebra. If a linear map $S : H \longrightarrow H \otimes H$ satisfies

$$m(S \otimes id)\Delta = u \cdot \epsilon = m(id \otimes S)\Delta,$$

S is called an antipode.

Definition 5.1.5 (Hopf algebra (quantum group)) A bialgebra which has a antipode, $(H, m, u, \Delta, \epsilon, S)$, is called a Hopf algebra.

For bialgebras the folloing proposition, which ensures the uniqueness of the Hopf algebra, holds,

Theorem 5.1.1 The antipode S for a bialgebra is unique, if any. Then, S is a anti-algebra map and a anti-coalgebra map.

A bialgebra or a Hopf algebra is said to be *commutative* if it is commutative as an algebra. On the other hand, a coalgebra, bialgebra, or a Hopf algebra is said to be *cocommutative* if $\Delta' = \Delta$ holds.

5.1.3 Examples of Hopf algebra

It will be helpful to introduce some examples of Hopf algebra. Especially, we will introduce the κ -Poincarè algebra in the following section as a deformed enveloping algebra of the Poincarè one.

Enveloping algebra of a Lie algebra

A Lie algebra over \mathbf{C} is a vector space over \mathbf{C} and has a bilinear map,

$$[\cdot, \cdot] : g \times g \longrightarrow g,$$

such that, for $\xi, \eta, \zeta \in g$,

$$[\xi, \eta] = -[\eta, \xi], \quad (\text{anti-symmetry})$$

$$[\xi, [\eta, \zeta]] + [\eta, [\zeta, \xi]] + [\zeta, [\xi, \eta]] = 0. \quad (\text{Jacobi's identity})$$

For a Lie algebra g , if a tensor algebra and a bilinear map $[\cdot, \cdot]$ are difined as

$$T(g) = \bigoplus_{k=0}^{\infty} T^k(g),$$

$$T^0(g) = \mathbf{C}, \quad T^k(g) = \overbrace{g \otimes \cdots \otimes g}^k,$$

$$[\xi, \eta] = \xi \otimes \eta - \eta \otimes \xi, \quad \forall \xi, \eta \in g,$$

then, g is said to be an *universal enveloping algebra* $U(g)$. Furthermore, for generators $\xi \in g$, if a coproduct, a counit, and an antipode are defined as

$$\begin{aligned}\Delta(\xi) &= \xi \otimes 1 + 1 \otimes \xi, \\ \epsilon(\xi) &= 0, \\ S(\xi) &= -\xi,\end{aligned}\tag{5.1}$$

and for other elements in $U(g)$, if Δ and ϵ are extended as algebra maps and S are extended as an antialgebra map, then $U(g)$ becomes a Hopf algebra.

Function Hopf algebra

Suppose a group G and the set of functions on G , $Fun(G)$, that is

$$Fun(G) : G \longrightarrow \mathbf{C}.\tag{5.2}$$

$Fun(G)$ becomes a linear space if the sum and scalar multiplication are defined as

$$(\phi + \psi)(g) = \phi(g) + \psi(g),\tag{5.3}$$

$$(\alpha\phi)(g) = \alpha(\phi(g)).\tag{5.4}$$

Furthermore, a product, unit element, counit map, and antipode can be defined as

$$(\phi\psi)(g) = \phi(g)\psi(g),\tag{5.5}$$

$$1_F(g) = 1,\tag{5.6}$$

$$\Delta\phi(g_1, g_2) = \phi(g_1g_2),\tag{5.7}$$

$$\epsilon\phi = \phi(e),\tag{5.8}$$

$$(S\phi)(g) = \phi(g^{-1}).\tag{5.9}$$

Then, $(Fun(G), \cdot, 1, \Delta, \epsilon, S)$ becomes a Hopf algebra. Clearly, such a Hopf algebra is commutative from Eq. (5.5). On the other hand, such a Hopf algebra is not cocommutative if the group G is not commutative from Eq. (5.7).

5.1.4 Dual Hopf algebra

In general, one can define a dual space V^* of V , which is a linear space over \mathbf{C} . Therefore, one can define a *dual Hopf algebra* H^* of a Hopf algebra H as

$$H^* : H \longrightarrow \mathbf{C}.\tag{5.10}$$

Reflecting the structure of H as a Hopf algebra to the structure of H^* , one can make H^* be a Hopf algebra. For $t \in H$ and $x \in H^*$, let us denote $x(t) = \langle x, t \rangle$. The dual space H^* is a Hopf algebra if the product, unit element, and so on in H^* are defined as follows:

$$\langle xy, t \rangle = \langle x \otimes y, \Delta t \rangle, \quad (5.11)$$

$$\langle 1, t \rangle = \epsilon(t), \quad (5.12)$$

$$\langle \Delta x, s \otimes t \rangle = \langle x, st \rangle, \quad (5.13)$$

$$\epsilon(x) = \langle x, 1 \rangle, \quad (5.14)$$

$$\langle Sx, t \rangle = \langle x, St \rangle. \quad (5.15)$$

One can see that the structure of H as an algebra and a coalgebra is reflected to the structure of H^* as a coalgebra and an algebra, respectively.

5.2 κ -Poincaré algebra and κ -Minkowski spacetime

Now we can introduce the κ -Poincaré algebra as a Hopf algebra and the κ -Minkowski spacetime as the dual space of the κ -Poincaré algebra. Furthermore, one will see the each mathematical structure of Hopf algebra has a corresponding physical meaning.

The generators of the κ -Poincaré algebra \mathcal{P}_κ satisfy the following commutation relations:

$$[M_{\mu\nu}, M_{\rho\sigma}] = i(\eta_{\mu\sigma}M_{\nu\rho} - \eta_{\mu\rho}M_{\nu\sigma} + \eta_{\nu\rho}M_{\mu\sigma} - \eta_{\nu\sigma}M_{\mu\rho}), \quad (5.16)$$

$$[M_i, p_0] = 0, \quad (5.17)$$

$$[M_i, p_j] = i\epsilon_{ijk}p_k, \quad (5.18)$$

$$[N_i, p_0] = ip_i, \quad (5.19)$$

$$[N_i, p_j] = -i\delta_{ij} \left[\frac{1}{2\lambda} (1 - e^{2p_0\lambda}) + \frac{\lambda}{2} \mathbf{p}^2 \right] + i\lambda p_i p_j, \quad (5.20)$$

$$[p_\mu, p_\nu] = 0, \quad (5.21)$$

where $M_i \equiv \frac{1}{2}\epsilon_{ijk}M_{jk}$, $N_i \equiv M_{0i}$ and p_μ are generators of rotation, boost and translation, respectively. We abbreviate $\sum_i p_i^2$ as \mathbf{p}^2 . We can recover the ordinary commutation relations of the Poincaré algebra in the limit $\lambda \rightarrow 0$. The dispersion relation is determined by the eigenvalue of the Casimir operator, that commutes with all elements in \mathcal{P}_κ ,

$$\frac{2 \cosh(\lambda p_0)}{\lambda^2} - \mathbf{p}^2 e^{-\lambda p_0} = \frac{2 \cosh(\lambda m)}{\lambda^2}, \quad (5.22)$$

where the rest mass m is defined as the energy with $p_i = 0$. The coproducts $\Delta : \mathcal{P}_\kappa \rightarrow \mathcal{P}_\kappa \otimes \mathcal{P}_\kappa$

of the basic generators are

$$\Delta(M_i) = M_i \otimes 1 + 1 \otimes M_i, \quad (5.23)$$

$$\Delta(N_i) = N_i \otimes 1 + e^{p_0 \lambda} \otimes N_i - \lambda \epsilon_{ijk} p_j \otimes M_k, \quad (5.24)$$

$$\Delta(p_0) = p_0 \otimes 1 + 1 \otimes p_0, \quad (5.25)$$

$$\Delta(p_i) = p_i \otimes 1 + e^{p_0 \lambda} \otimes p_i. \quad (5.26)$$

The above coproducts of p_μ , (5.25) and (5.26), are interpreted as the non-Abelian addition law of energy-momenta for particles 1 and 2 as

$$(E_1, \mathbf{p}_1) \hat{+} (E_2, \mathbf{p}_2) := \left(E_1 + E_2, \mathbf{p}_1 + e^{\lambda E_1} \mathbf{p}_2 \right), \quad (5.27)$$

where we identify p_0 with energy E . Note that the associativity of the addition law is given by the coassociativity $(\Delta \otimes id) \circ \Delta = (id \otimes \Delta) \circ \Delta$. The coproducts of other elements in \mathcal{P}_κ are extended as $\Delta(1) = 1 \otimes 1$ and $\Delta(MM') = \Delta(M)\Delta(M')$, $\forall M, M' \in \mathcal{P}_\kappa$. We can check the consistency between this extension of the coproducts as an algebra homomorphism and the commutation relation, i.e., $\Delta[M, M'] = [\Delta M, \Delta M']$. This consistency guarantees that the κ -Poincaré algebra is form-invariant for multi-particle systems.

The asymmetry of the coproducts for the permutation of particles is called noncocommutativity. The noncocommutativity of the coproducts for the translation sector $T \subset \mathcal{P}_\kappa$ has two important meanings. One is that the noncocommutativity of the κ -Minkowski spacetime is a direct consequence of the noncocommutativity. Elements in the κ -Minkowski spacetime are defined as linear functionals on the translation sector, $T^* : T \rightarrow \mathbf{C}$. The products in T^* is defined in terms of coproducts in T , i.e., $\forall x, y \in T^*$ and $\forall p \in T$,

$$\langle xy, p \rangle := \langle x \otimes y, \Delta p \rangle \quad (5.28)$$

$$= \sum_a \langle x, p_{a(1)} \rangle \langle y, p_{a(2)} \rangle, \quad (5.29)$$

where we write the coproducts as $\Delta(p) = \sum_a p_{a(1)} \otimes p_{a(2)}$. With the duality relations $\langle x^\mu, p_\nu \rangle = -i\delta_\nu^\mu$, this leads to the following commutation relations [72]:

$$[x^i, x^0] = i\lambda x^i, \quad (5.30)$$

$$[x^0, x^0] = 0, \quad (5.31)$$

$$[x^i, x^j] = 0. \quad (5.32)$$

The other is that the noncocommutativity leads to a deformed group velocity formula [12], which is different from the usual velocity formula $dE/d\mathbf{p}$ as will be shown in the next chapter.

Chapter 6

Particle velocity in noncommutative spacetime

In this chapter, we investigate a particle velocity in the κ -Minkowski spacetime, which is one of the realization of a noncommutative spacetime. We emphasize that arrival time analyses by high-energy γ -rays or neutrinos, which have been considered as powerful tools to restrict the violation of Lorentz invariance, are not effective to detect spacetime noncommutativity. In contrast with these examples, we point out a possibility that *low-energy massive particles* play an important role to detect it. In Sec. 6.1, we review the previous discussion in the MDR models. After that, we derive the particle velocity formula in Sec. 6.2. In Sec. 6.3, we consider the observational possibilities of time delay by comparing a particle velocity in the usual Minkowski spacetime with that in the κ -Minkowski spacetime and MDR models. We show that the spacetime noncommutativity does *not* affect the velocity of massless particles, which implies that the arrival time analysis by γ -rays is *not* useful to detect the spacetime noncommutativity. We also discuss a possibility that the spacetime noncommutativity might be detected by using low-energy massive particles. Section 6.4 is devoted to summary and discussion.

6.1 Modified dispersion relation models

Although there are various ways to modify the dispersion relation, we consider here the form in Ref. [65] as $p^2 + m^2 = E^2[1 + f(E/E_{QG})]$, where f is a model-dependent function and E_{QG} is the effective energy scale of quantum gravity. For simplicity, we assume that f is an analytic function. Although in general, f and E_{QG} may depend on the species and properties of the particles [88, 52], we do not consider this possibility, which implies that the effects of quantum gravity originate from the spacetime structure. In the low-energy limit, $E \ll E_{QG}$, the above

dispersion relation becomes

$$p^2 + m^2 = E^2 + \frac{\xi E^n}{E_{QG}^{n-2}}, \quad (6.1)$$

up to the lowest correction. We have chosen $\xi = \pm 1$ and $n \geq 3$ is the integer, which is determined by the form of the function f . Note that $E < m$ for $\xi = 1$ in the low-momentum limit. This type of dispersion relation also appears in the Liouville string approach to quantum gravity [89].

The velocity v_{MDR} in this model is obtained by differentiating the dispersion relation (6.1) with respect to p ,

$$v_{MDR} := \frac{dE}{dp} = \frac{2\sqrt{E^2 - m^2 + \xi E^n/E_{QG}^{n-2}}}{2E + n\xi E^{n-1}/E_{QG}^{n-2}}. \quad (6.2)$$

It should be noted that v_{MDR} depends on the energy even for massless particles because of the correction term. We can make use of the energy dependence to restrict E_{QG} .

Let us consider a γ -ray from the distant source. We approximate the velocity of the γ -ray by expanding Eq. (6.2) by E/E_{QG} to

$$v_{MDR} \approx 1 - \frac{\xi(n-1)}{2} \left(\frac{E}{E_{QG}} \right)^{n-2}. \quad (6.3)$$

Although the correction term may be very small, the difference of arrival time depending on the energy of the photons may become large enough to measure if the γ -rays travel a very long distance [90, 65, 91, 66]. The time delay is evaluated as

$$\begin{aligned} \delta t &= \frac{L}{v_{MDR}(E_1)} - \frac{L}{v_{MDR}(E_2)} \\ &\approx \frac{(n-1)\xi L}{2E_{QG}^{n-2}} (E_1^{n-2} - E_2^{n-2}), \end{aligned} \quad (6.4)$$

where L , E_1 and E_2 are the distance from the source to the Earth, amounts of the energy of particles 1 and 2, respectively.

One of the examples of this kind of analyses is the arrival time analysis by γ -rays from Mk 421 (~ 150 Mpc from the Earth). It was reported that γ -rays in the energy range between 1 and 2 TeV arrived at the Earth within the time difference ~ 200 seconds [90]. Then, E_{QG} is constrained to $E_{QG} \gtrsim [3.6 \times (n-1)(n-2) \times 10^{13}]^{1/(n-2)} \times 10^3$ GeV. Since the value of n has been assumed to be 3 in most of the previous works, it has been concluded that $E_{QG} \gtrsim 7.2 \times 10^{16}$ GeV. We should note, however, that n may be 4 or larger. In this case, the constraint becomes $E_{QG} \gtrsim 1.5 \times 10^{10}$ GeV for $n = 4$ and $E_{QG} \gtrsim 7.6 \times 10^7$ GeV for $n = 5$. Hence the constraint may become quite loose compared with the previous reports.

6.2 Velocity formula

We can define differentiation, integration and Fourier transformation [69, 70] in κ -Minkowski spacetime. The plane wave $\psi_{(E,\mathbf{p})} = e^{i\mathbf{p}\cdot\mathbf{x}} e^{iEt}$ in the κ -Minkowski spacetime introduced in [92, 93] respects the non-Abelian addition law of energy-momenta in the sense

$$\psi_{(E_1,\mathbf{p}_1)}\psi_{(E_2,\mathbf{p}_2)} = e^{i\mathbf{p}_1\cdot\mathbf{x}} e^{iE_1t} e^{i\mathbf{p}_2\cdot\mathbf{x}} e^{iE_2t} \quad (6.5)$$

$$= \psi_{(E_1+E_2,\mathbf{p}_1+e^{\lambda E_1}\mathbf{p}_2)}. \quad (6.6)$$

From the properties of the plane wave and the κ -Minkowski spacetime introduced in Sec 5.2, we can establish group velocity formulae. For this purpose, we consider infinitesimal changes ΔE and $\Delta\mathbf{p}$ in E and \mathbf{p} , respectively, as a result of adding $(\Delta E', \Delta\mathbf{p}')$ as

$$(E, \mathbf{p}) \hat{+} (\Delta E', \Delta\mathbf{p}') = (E + \Delta E, \mathbf{p} + \Delta\mathbf{p}). \quad (6.7)$$

By the addition law (5.27), we have

$$(\Delta E', \Delta\mathbf{p}') = (\Delta E, \frac{\Delta\mathbf{p}}{e^{\lambda E}}). \quad (6.8)$$

Next, we construct a wave packet by superposing plane waves. Here we only consider two waves for simplicity, whose momenta and amounts of energy are different infinitesimally from each other ¹.

$$\begin{aligned} I &= \psi_{(E-\Delta E, \mathbf{p}-\Delta\mathbf{p})} + \psi_{(E+\Delta E, \mathbf{p}+\Delta\mathbf{p})} \\ &\cong 2e^{i\mathbf{p}\cdot\mathbf{x}} e^{iEt} \cos \left[\frac{\Delta\mathbf{p}}{e^{\lambda E}} \cdot \left(\mathbf{x} + \frac{e^{\lambda E} \Delta E t}{\Delta\mathbf{p}} \right) \right], \end{aligned} \quad (6.9)$$

where we neglected the terms that vanish in the limit $\Delta\mathbf{p} \rightarrow 0$. The group velocity \mathbf{v}_l of this wave packet can be written as

$$\mathbf{v}_l := e^{\lambda E} \frac{dE}{d\mathbf{p}}. \quad (6.10)$$

There remains ambiguity in constructing the wave packet because of the noncommutativity of the spacetime. Another possibility is

$$(\Delta E', \Delta\mathbf{p}') \hat{+} (E, \mathbf{p}) = (E + \Delta E, \mathbf{p} + \Delta\mathbf{p}). \quad (6.11)$$

In this case, the corresponding group velocity \mathbf{v}_r is

$$\mathbf{v}_r := \left(1 - \lambda\mathbf{p} \cdot \frac{dE}{d\mathbf{p}} \right)^{-1} \frac{dE}{d\mathbf{p}}. \quad (6.12)$$

¹Strictly speaking, this is not a Gaussian wave packet. However, it is sufficient to obtain a group velocity.

These velocities can be expressed explicitly in terms of the functions of E and m by using the dispersion relation. By the definitions of \mathbf{v}_l and \mathbf{v}_r , we find

$$\mathbf{v}_l = \frac{e^{\lambda E/2} \sqrt{2[\cosh(\lambda E) - \cosh(\lambda m)]}}{|e^{\lambda E} - \cosh(\lambda m)|} \mathbf{e}, \quad (6.13)$$

$$\mathbf{v}_r = \frac{e^{-\lambda E/2} \sqrt{2[\cosh(\lambda E) - \cosh(\lambda m)]}}{|e^{-\lambda E} - \cosh(\lambda m)|} \mathbf{e}, \quad (6.14)$$

where $\mathbf{e} := \mathbf{p}/|\mathbf{p}|$. We find that the velocities have the same direction as that of the momenta. Note also that there is a correspondence between the transformations $\lambda \rightarrow -\lambda$ and $\mathbf{v}_l \rightarrow \mathbf{v}_r$.

These velocities were also investigated by Lukierski and Nowicki and the following facts were pointed out in Ref. [73]: (i) $v_l := |\mathbf{v}_l|$, $v_r := |\mathbf{v}_r| \leq 1$ for all energies, (ii) $dv_l/dE > 0$, $dv_r/dE > 0$, and (iii) v_r has a classical velocity addition law, i.e., the addition of parallel velocities v_{r1} and v_{r2} becomes

$$v_{r12} = \frac{v_{r1} + v_{r2}}{1 + v_{r1}v_{r2}}. \quad (6.15)$$

If the boost generator N_i was an even function for λ , this addition law would hold even for v_l because of the correspondence mentioned above. However, this is not the case. We postpone the interpretation of this asymmetry as future work.

Next, we discuss the application of the above velocity formulae. In the MDR models, since the energy scale of quantum gravity E_{QG} is introduced perturbatively (see Eq (6.3)), it is reasonable to apply the velocity formulae under the condition on $E \ll E_{QG}$. While if we apply the velocity formulae in the κ -Minkowski spacetime, the energy range is not restricted.

Let us examine the case beyond the quantum gravity scale, i.e., $|\lambda E| \gg 1$. Since we can obtain the information about v_r by using the transformation $\lambda \rightarrow -\lambda$ to v_l , we only examine v_l below. We evaluate the velocity v_l in the following limits (see Table 6.1.). When $\lambda > 0$ and $E/m \gg 1$, we can find that the velocity of massive particles approaches 1 much faster than that in the Minkowski spacetime as the energy of the particle increases. However, for $\lambda < 0$ and $E/m \gg 1$, the difference of the velocity from 1 becomes large as the mass of the particle increases. Note that if $|\lambda(E - m)| \ll 1$, we obtain $|\lambda m| \gg 1$ by using the condition $|\lambda E| \gg 1$. Since $E - m$ is written as $m(1/\sqrt{1 - v_M^2} - 1)$ in the Minkowski spacetime, where v_M is the velocity in the Minkowski spacetime, we can rewrite the condition $|\lambda(E - m)| \ll 1$ as $|\lambda m(1/\sqrt{1 - v_M^2} - 1)| \ll 1$, which leads to $v_M \ll 1$ because of $|\lambda m| \gg 1$. Then, we find $v_l \simeq v_M \sqrt{2\lambda m}$ and $v_l \simeq e^{\lambda m} v_M \sqrt{-2\lambda m}$ for $\lambda > 0$ and for $\lambda < 0$, respectively. Thus, we find that v_l for the case $|\lambda m| \gg 1$ is quite different from v_M , which is a good approximation for describing a velocity of macroscopic bodies in our world under the conditions we are considering. To describe a velocity of macroscopic bodies in the κ -Minkowski spacetime, we must consider carefully what are the energy and the momentum, since these quantities are obtained by a total

sum of those of elementary particles according to the addition law (5.27). The above discrepancy may be explained in this reason. Below, we only consider elementary particles and restrict the discussion to the case $|\lambda m| \ll 1$.

Table 6.1: Approximation of the velocity v_l in the case $|\lambda E| \gg 1$

	$E/m \gg 1$	$ \lambda(E - m) \ll 1$
$\lambda > 0$	$1 + e^{-2\lambda E} \left[\frac{1}{2} - \cosh^2(\lambda m) \right]$	$2\sqrt{\lambda(E - m)}$
$\lambda < 0$	$1/\cosh(\lambda m)$	$2e^{\lambda m} \sqrt{\lambda(m - E)}$

6.3 Arrival time analysis with massive particles

In this section, we compare v_l with v_{MDR} and discuss the possibility of detection of effective scale of quantum gravity by observations and experiments. The behavior of the velocities is quite different depending on the mass and energy of the particle. Hence, we consider two limiting cases: (i) the ‘‘relativistic’’ case ($m \ll E$) and (ii) ‘‘non-relativistic’’ case ($m \approx E$)².

In the relativistic case, $m \ll E$, and under the assumptions, $E \ll E_{QG}$ and $E \ll |\lambda^{-1}|$, v_{MDR} and v_l are

$$v_{MDR} \approx 1 - \frac{1}{2} \left(\frac{m}{E} \right)^2 - \frac{\xi(n-1)}{2} \left(\frac{E}{E_{QG}} \right)^{n-2}, \quad (6.16)$$

$$v_l \approx 1 - \frac{1}{2} \left(\frac{m}{E} \right)^2 + \frac{\lambda m^2}{2E}, \quad (6.17)$$

at the lowest order of m/E and E/E_{QG} in the MDR models and λE in the κ -Minkowski spacetime, respectively. When $m = 0$ in the MDR models, E_{QG} can be constrained by the γ -rays from the Mk 421 as mentioned in Sec. II. However, since $v_l = 1$ for massless particles, (we can confirm this is also true for all order of λm and λE), λ is not constrained by massless particles. This is an important result since the result notices us that there are a wide variety of candidates for the theory of quantum gravity, some of which the scale of quantum gravity is not constrained by present observations. The situation changes for massive particles since the lowest order correction appears in the coupled form with the mass of the particle in the κ -Minkowski spacetime, while that of the MDR models does not depend on the mass of the particle.

First, we consider neutrinos from supernovae with energy $E_\nu \sim 10^{10}$ eV to detect spacetime noncommutativity. We assume that the mass of an electron neutrino and all the parameters necessary to describe neutrino physics are determined by other experiments and observations,

²In the MDR models and in the κ -Minkowski spacetime, it is possible that the particle moves very slowly (fast) even if the condition $m \ll E$ ($m \approx E$) is satisfied.

and use the delay of the arrival time between the neutrinos and gravitational waves to evaluate the scale of quantum gravity. In this case, the delay of the arrival time is

$$\delta t \approx \frac{Lm_\nu^2}{2E_\nu} \left(\frac{1}{E_\nu} + \lambda \right). \quad (6.18)$$

Since neutrinos are emitted continuously during about 10 s, it is impossible to determine the time when the neutrino is emitted more accurate than that time scale. For this reason, $\delta t \gtrsim 10$ s is necessary to detect the effect of quantum gravity. As for λ , since there is no restriction from the arrival time analysis of γ -rays, λ may take a large value. However, by considering reaction processes by collider experiments, we can restrict $|\lambda| \lesssim 10^{-12} \text{ eV}^{-1}$ since the threshold of the reaction will change drastically for $|\lambda| > 1/E_{th}$, where E_{th} is the threshold energy in the Minkowski spacetime [12]. Then, L becomes far longer than the horizon scale in the present universe even if $|\lambda| = 10^{-12} \text{ eV}^{-1}$. Thus, it is difficult to detect this effect in this phenomena.

Neutrinos from γ -ray bursts in fireball models have a different energy scale. In the bursts, neutrinos with energy $\sim 10^{14} \text{ eV}$ and γ -rays are expected to be radiated away in $\sim 1 \text{ s}$ [94]. We show that we cannot detect spacetime noncommutativity even if we neglect the dissipation of the γ -ray. In the $E \gg 1/|\lambda|$ case, we can evaluate the delay of the arrival time of neutrinos compared with the γ -rays from Table 6.1 as

$$\delta t \approx \frac{L}{2} e^{-2\lambda E} [1 + 2(\lambda m_\nu)^2] \quad \text{for } \lambda > 0, \quad (6.19)$$

$$\delta t \approx \frac{L}{2} (\lambda m_\nu)^2 \quad \text{for } \lambda < 0, \quad (6.20)$$

where we have used the conditions $E/m \gg 1$ and $|\lambda m| \ll 1$. If we assume $\delta t \sim 1 \text{ s}$ and $|\lambda| = 10^{-12} \text{ eV}^{-1}$, the path of the particle's travel becomes far longer than the horizon scale in the present universe. In the $E \sim 1/|\lambda|$ case, the arrival time delay cannot be described in a simple way. There is, however, no qualitative difference from the above case. Hence, it is difficult to detect spacetime noncommutativity by this method.

Next, we examine the non-relativistic case, $m \sim E \ll E_{QG}$ (or $|\lambda^{-1}|$). The velocity in each model are

$$v_{MDR} \approx \sqrt{1 - \left(\frac{m}{E}\right)^2} \times \left[1 + \frac{\xi E^2(1-n) + nm^2}{2(E^2 - m^2)} \left(\frac{E}{E_{QG}}\right)^{n-2} \right], \quad (6.21)$$

$$v_l \approx \sqrt{1 - \left(\frac{m}{E}\right)^2} \left(1 + \frac{\lambda m^2}{2E} \right). \quad (6.22)$$

Note that the absolute value of the correction for the velocity in the κ -Minkowski spacetime decreases with the energy, while that in the MDR model increases. Although, in the low-energy

limit, the dispersion relation in the κ -Minkowski spacetime has the same form as that in the MDR models, the correction for the velocity is quite different.

Because of the above difference in the correction terms, there is a possibility that the evidence for spacetime noncommutativity can be detected in use of the low-energy massive particles. Here, we consider the ultra-cold neutrons with energy $E_n - m_n \sim 10^{-2}$ eV [95]. Since the mass of a neutron m_n is measured with high accuracy, we can estimate the time interval in which the neutron travels the interval L in the Minkowski spacetime. If a time lag is obtained in an experiment, it can be interpreted as the effect of spacetime noncommutativity. This time lag is calculated in the κ -Minkowski spacetime as

$$\delta t = \frac{L}{v_l} - \frac{L}{v_M} \approx \frac{L}{v_M} \frac{\lambda m_n^2}{2E_n}. \quad (6.23)$$

By substituting the value of the apparatus [96], $L \sim 100$ m, we have

$$\delta t \sim 10^{-1} \lambda m_n. \quad (6.24)$$

If the resolution for the measurement of the time lag is $\sim 10^{-10}$ s and $|\lambda| \gtrsim 10^{-18}$ eV $^{-1}$, we can detect spacetime noncommutativity.

6.4 Summary and discussion

We have investigated what are the qualitative differences of the velocity formula in the κ -Minkowski spacetime from that in the MDR models. Most of the previous papers had adopted the MDR models since the MDR models are among the simplest ones of quantum gravity. However, many of the MDR models do not have physical foundation in how the correction terms of naturally arise in the dispersion relation. For example, since the usual Lorentz transformation had been used in the previous work, one could not have avoided the existence of a preferred frame as a result. Since we have taken the standpoint that the existence of a preferred frame is not favorable, we have considered the κ -Minkowski spacetime where the deformed Lorentz transformation and the deformed dispersion relation arise as a result of the deformation quantization.

We have found that since massless particles move in a constant speed in the κ -Minkowski spacetime, the arrival time analyses by γ -rays are not capable to detect the difference from the Minkowski spacetime. This example shows that it is difficult to constrain all kinds of Lorentz invariance by a single experiment. Therefore, we need to investigate specific models individually. We have also considered the possibility to detect spacetime noncommutativity by low-energy massive particles. In our model, if the resolution for the measurement of the time lag is given by $\sim 10^{-10}$ s, it is possible to constrain λ to $|\lambda| \gtrsim 10^{-18}$ eV $^{-1}$. Although these features had not been investigated so far, it may be important.

Chapter 7

Threshold anomaly in noncommutative spacetime

In this chapter, we discuss the astrophysical implications of κ -Minkowski spacetime, in which spacetime noncommutativity exists. We first re-consider the velocity formula for particles based on the motion of a wave packet. The result is that a massless particle moves at a constant speed as in the usual Minkowski spacetime, which implies that an arrival time analysis by γ -rays from Markarian (Mk) 421 *does not* exclude spacetime noncommutativity. Based on this observation, we analyze reaction processes in κ -Minkowski spacetime which are related to the puzzling detections of extremely high energy cosmic rays above the Greisen-Zatsepin-Kuzmin cutoff and of high-energy (~ 20 TeV) γ -rays from Mk 501. In these analyses, we take into account the ambiguity of the momentum conservation law which can not be determined uniquely from a mathematical viewpoint. We find that peculiar types of momentum conservation law with some length scale of noncommutativity above a critical length scale can explain such puzzling detections. We also obtain stringent constraints on the length scale of noncommutativity and the freedom of momentum conservation law.

7.1 Finite boost in κ -Minkowski spacetime

We briefly review κ -Minkowski spacetime. The basic commutation relations are

$$[x^i, t] = i\lambda x^i, \quad [x^i, x^j] = 0. \quad (7.1)$$

We can define differentiation, integration [69] and Fourier transformation in this spacetime [70]. In order to define Fourier transformation consistently, the energy E and the momentum $\mathbf{p} =$

(p_1, p_2, p_3) of a particle form a non-Abelian group G which can be written in a matrix form as,

$$(E, \mathbf{p}) := \begin{pmatrix} e^{\lambda E} & p_1 & p_2 & p_3 \\ 0 & 1 & 0 & 0 \\ 0 & 0 & 1 & 0 \\ 0 & 0 & 0 & 1 \end{pmatrix}. \quad (7.2)$$

Thus, if we denote the additive operator in κ -Minkowski spacetime by $\hat{+}$ to distinguish from the conventional one, we can write as

$$\begin{aligned} (E_1 \hat{+} E_2, \mathbf{p}_1 \hat{+} \mathbf{p}_2) &:= (E_1, \mathbf{p}_1)(E_2, \mathbf{p}_2) \\ &= (E_1 + E_2, \mathbf{p}_1 + e^{\lambda E_1} \mathbf{p}_2). \end{aligned} \quad (7.3)$$

Following Ref. [66], we describe a plane wave as

$$\psi_{(E, \mathbf{p})} = e^{i\mathbf{p} \cdot \mathbf{x}} e^{iEt}, \quad (7.4)$$

and place the t generator to the right of x generator, i.e., $\psi_{(E, \mathbf{p})} \neq e^{iEt} e^{i\mathbf{p} \cdot \mathbf{x}}$. Then, the property

$$\psi_{(E_1, \mathbf{p}_1)(E_2, \mathbf{p}_2)} = \psi_{\mathbf{p}_1, E_1} \psi_{\mathbf{p}_2, E_2}, \quad (7.5)$$

is found. We can also define the wave in the reverse direction as

$$\psi_{(E, \mathbf{p})^{-1}} := e^{-i\mathbf{p} e^{-\lambda E} \cdot \mathbf{x}} e^{-iEt} = e^{-iEt} e^{-i\mathbf{p} \cdot \mathbf{x}}, \quad (7.6)$$

which implies that $(E, \mathbf{p})^{-1}$ is an inversion of (E, \mathbf{p}) .

Because of these noncommutative structures, modification of Poincaré invariance is required to describe physics in a covariant way [71]. The rotation and boost generators can be written as

$$M_i = -\epsilon_{imn} p_m \frac{\partial}{\partial p_n}, \quad (7.7)$$

$$N_i = p_i \frac{\partial}{\partial E} - \left(\frac{\lambda}{2} \mathbf{p}^2 + \frac{1 - e^{2\lambda E}}{2\lambda} \right) \frac{\partial}{\partial p_i} + \lambda p_i p_j \frac{\partial}{\partial p_j}. \quad (7.8)$$

Using (7.8), a finite boost transformation for the $i = 1$ direction can be obtained as [97]

$$p_1 = \frac{\tanh(\lambda m) \sinh \xi}{\lambda [1 - \tanh(\lambda m) \cosh \xi]}, \quad (7.9)$$

$$p_2 = p_3 = 0, \quad (7.10)$$

$$E = m + \frac{1}{\lambda} \ln \left[\frac{1 - \tanh(\lambda m)}{1 - \tanh(\lambda m) \cosh \xi} \right], \quad (7.11)$$

where ξ is a boost parameter and we choose $\mathbf{p} = 0$ and $E = m$, i.e., m is a rest mass of the particle, for $\xi = 0$.

Because of (7.8), the dispersion relation is altered as

$$\lambda^{-2}(e^{\lambda E} + e^{-\lambda E} - 2) - \mathbf{p}^2 e^{-\lambda E} = K^2, \quad (7.12)$$

where K is a constant with the dimension of mass. If we take a rest frame, this can be expressed as

$$\lambda^{-2}(e^{\lambda m} + e^{-\lambda m} - 2) = K^2. \quad (7.13)$$

7.2 Re-consideration of the speed of light

Here, we derive a new velocity formula which is one of the main results of this paper. The velocity of the particle in the usual Minkowski spacetime is

$$\mathbf{v} = \frac{dE}{d\mathbf{p}}. \quad (7.14)$$

If we apply this in κ -Minkowski spacetime, $|\mathbf{v}| = e^{-\lambda E}$ is obtained for a massless particle, where we used Eq. (7.12). This formula, together with the data on γ -rays associated with Markarian (Mk) 421 in Ref. [90] leads to the constraint $|\lambda| \lesssim 10^{-33}$ meter [65, 66, 90]. Since this discussion depends crucially on the form of Eq. (7.14), i.e., on what is the velocity, we reexamine the group velocity formula by forming a wave packet in κ -Minkowski spacetime as a more realistic situation. For this purpose, we consider infinitesimal changes ΔE and $\Delta \mathbf{p}$ in E and \mathbf{p} , respectively, as a result of adding $(\Delta E', \Delta \mathbf{p}')$ as

$$(E \hat{+} \Delta E', \mathbf{p} \hat{+} \Delta \mathbf{p}') = (E + \Delta E, \mathbf{p} + \Delta \mathbf{p}). \quad (7.15)$$

In this case, we can express $(\Delta E', \Delta \mathbf{p}')$ as

$$(\Delta E', \Delta \mathbf{p}') \cong (\Delta E, \frac{\Delta \mathbf{p}}{e^{\lambda E}}), \quad (7.16)$$

where we keep only terms in first order in ΔE and $\Delta \mathbf{p}$. By using Eqs. (7.5) and (7.16), we make a wave packet as follows¹

$$\begin{aligned} I &= \psi_{(E-\Delta E, \mathbf{p}-\Delta \mathbf{p})} + \psi_{(E+\Delta E, \mathbf{p}+\Delta \mathbf{p})} \\ &= \psi_{(E, \mathbf{p})(-\Delta E', -\Delta \mathbf{p}')} + \psi_{(E, \mathbf{p})(\Delta E', \Delta \mathbf{p}')} \\ &= \psi_{(E, \mathbf{p})} \psi_{(-\Delta E', -\Delta \mathbf{p}')} + \psi_{(E, \mathbf{p})} \psi_{(\Delta E', \Delta \mathbf{p}')} \\ &= \psi_{(E, \mathbf{p})} [e^{-i\Delta \mathbf{p}' \cdot \mathbf{x}} e^{-i\Delta E' t} + e^{i\Delta \mathbf{p}' \cdot \mathbf{x}} e^{i\Delta E' t}] \\ &\cong 2e^{i\mathbf{p} \cdot \mathbf{x}} e^{iEt} \cos \left[\frac{\Delta \mathbf{p}}{e^{\lambda E}} \cdot \left(\mathbf{x} + \frac{e^{\lambda E} \Delta E t}{\Delta \mathbf{p}} \right) \right]. \end{aligned} \quad (7.17)$$

¹This is not a Gaussian wave packet. However, it is sufficient to obtain a group velocity. The extension for more general wave packet will be straight forward.

By considering $|I|^2$, the group velocity \mathbf{v}_l can be written as

$$\mathbf{v}_l := e^{\lambda E} \frac{dE}{d\mathbf{p}}. \quad (7.18)$$

We also consider a similar relation

$$(\Delta E' \hat{+} E, \Delta \mathbf{p}' \hat{+} \mathbf{p}) = (E + \Delta E, \mathbf{p} + \Delta \mathbf{p}), \quad (7.19)$$

which is different from Eq. (7.15) due to noncommutativity. In this case, the corresponding group velocity \mathbf{v}_r is

$$\mathbf{v}_r := \frac{\frac{dE}{d\mathbf{p}}}{1 - \lambda \mathbf{p} \cdot \frac{dE}{d\mathbf{p}}}. \quad (7.20)$$

Using (7.12) and (7.13), we obtain the important conclusion that *massless particles move in a constant speed* $|\mathbf{v}_l| = |\mathbf{v}_r| = 1$ *as in the usual Minkowski spacetime for arbitrary* λ ². Therefore, the argument in Ref. [65, 91, 66, 93, 90] does not apply. In this case, there appears the possibility that the large value of λ ($\gtrsim 10^{-33}\text{m}$) may solve the puzzling problems of EHECRs above GZK cutoff and of ~ 20 TeV photons simultaneously. We investigate this possibility next. However, we emphasize on the importance of the result *not* because κ -Minkowski spacetime can avoid the constraint *but* because our result provides an opportunity to reconsider LI deformation models in general.

7.3 Threshold anomaly

We first consider the two-body head-on collision of particles and subsequent creation of two particles $1 + 2 \rightarrow 3 + 4$. We define the energy E_i and momentum \mathbf{p}_i of the i -th particle as those in the laboratory frame. We denote the rest mass of the i -th particle as m_i . We also assume that $m_2 = 0$, $m_3 \neq 0$, $m_4 \neq 0$ and $\mathbf{p}_i = (p_i, 0, 0)$. In the usual Minkowski spacetime, we use the dispersion relation

$$E_i^2 - p_i^2 = m_i^2, \quad (7.21)$$

and the energy momentum conservation law,

$$p_1 + p_2 = p_3 + p_4, \quad (7.22)$$

$$E_1 + E_2 = E_3 + E_4, \quad (7.23)$$

²Recently, a particle velocity was also discussed in Ref. [98] which gives the same answer as ours for massless particles.

to obtain the threshold value of E_1 , which we denote by $E_{th,0}$. We assume that the resultant particles are at rest in the center-of-mass frame in the threshold reaction. In the laboratory frame, this means that the resultant particles move in the same speed, that is

$$\frac{p_3}{m_3} = \frac{p_4}{m_4}. \quad (7.24)$$

We also assume that p_2 has an opposite sign against that of p_1 . If we neglect higher order terms in E_2 , then

$$E_{th,0} = \frac{(m_3 + m_4)^2 - m_1^2}{4E_2}. \quad (7.25)$$

We also define the threshold value of p_1 as $p_{th,0}$ which can be approximated as $p_{th,0} \sim E_{th,0}$.

Next, we consider the same reaction in κ -Minkowski spacetime. Eq. (7.21) is replaced by

$$\begin{aligned} & \lambda^{-2}(e^{\lambda E_i} + e^{-\lambda E_i} - 2) - (p_i)^2 e^{-\lambda E_i} \\ &= \lambda^{-2}(e^{\lambda m_i} + e^{-\lambda m_i} - 2). \end{aligned} \quad (7.26)$$

If we interpret the algebra in κ -Minkowski spacetime faithfully, the energy momentum conservation law is expressed as

$$(E_1, p_1)(E_2, p_2) = (E_3, p_3)(E_4, p_4). \quad (7.27)$$

Even if it holds, one should note that we need a rule to distinguish two particles. If we consider the collision of two particles with $A, B \in G$, respectively, does it correspond to AB , BA or anything else? At present, we have no way to determine it. Amelino-Camelia et al. [66, 93] proposed to find the rule by experiments. Here, we introduce a phenomenological parameter a , which controls the form of conservation law as follows:

$$\begin{aligned} & a(E_1, p_1)(E_2, p_2) + (1 - a)(E_2, p_2)(E_1, p_1) \\ &= a(E_3, p_3)(E_4, p_4) + (1 - a)(E_4, p_4)(E_3, p_3). \end{aligned} \quad (7.28)$$

As regards plausible values for a , care must be taken. If we consider two particles of the same species, $a = 1/2$ would be physically reasonable value, since if they have same energy and move opposite direction each other, they have zero total momentum only for this choice. In fact, the parameter a may be a function of physical quantities of two particles such as mass, charge and/or spin for two different species. Here, we use the same value of a on the left and the right hand sides of (7.28) for convenience. Moreover, we restrict our attention to $0 \leq a \leq 1$ for clarity.

We also need to impose the condition that the resultant particles are at rest in the center-of-mass frame. To obtain a relation between momenta p_3 and p_4 , we use the boost transformation (7.9). For the same value of ξ , we obtain

$$\frac{p_3}{\tanh(\lambda m_3)} = \frac{p_4}{\tanh(\lambda m_4)}. \quad (7.29)$$

We can solve E_1 as a function of a , λ , m_1 , m_3 , m_4 and E_2 by using (7.26), (7.28) and (7.29). We apply this result to two astrophysical cases.

7.3.1 Threshold anomaly for TeV γ -rays

Here, we consider the process $\gamma + \gamma \rightarrow e^+ + e^-$, which may occur when a γ -ray travels in the IRBG. In this case, $m_1 = 0$ and $m_3 = m_4 = m_e$, where m_e is the electron mass. If we assume the existence of IRBG photons ($0.2 \lesssim E_2 \lesssim 5$ eV) then the threshold is $E_{th,0} \sim 1$ TeV in Minkowski spacetime. Then, the reported detection of ~ 20 TeV photons from Mk501 (~ 150 Mpc from the Earth) would be difficult to explain [44].

We summarize the equation for the threshold in κ -Minkowski spacetime which is derived from (7.26), (7.28) and (7.29) as

$$AB = yx(yx + 1)^2 \sinh^2 \frac{\lambda m_e}{2}, \quad (7.30)$$

where

$$A := (1 - a)y^4 - (1 - 2a)y^2 - a, \quad (7.31)$$

$$B := ax^4 + (1 - 2a)x^2 + a - 1, \quad (7.32)$$

and $x := e^{\lambda E_1/2}$ and $y := e^{\lambda E_2/2}$. Since we are considering the collision of two particles of the same species, $a = 1/2$ would be physically reasonable. Note that, though we have $E_{th,0} \approx p_{th,0}$ for high energy particles in the usual Minkowski spacetime, this is not the case in κ -Minkowski spacetime.

We should recall that, to estimate the energy of primary particles, we calculate the sum of energy of all secondary particles. Since energy is conserved in the usual sense even in κ -Minkowski spacetime, we do not need to take into account the effect of spacetime noncommutativity to estimate the energy of primary particles. Thus, the observation of ~ 20 TeV photons in usual Minkowski spacetime has the same meaning also in κ -Minkowski spacetime. On the other hand, the usual sum of momenta of all secondary particles does not coincide with the momentum of the primary particle in this spacetime. Therefore, if p_{th} could be evaluated independently of the observation of E_{th} , it might become important to extract information about spacetime noncommutativity through the detection of violation of the usual momentum conservation. We exhibit properties of both the energy and the momentum from this reason.

We first show the dependence of E_{th} and p_{th} on $\lambda > 0$ in Fig. 7.1. For simplicity, E_2 is chosen as $E_2 = 1$ eV for IRBG photons. For $a = 0$, E_{th} and p_{th} increase with λ , compared with the same quantities in Minkowski spacetime. In particular, E_{th} and p_{th} diverge for $\lambda := \lambda_c \sim 4$ TeV^{-1} . That is, the universe is entirely transparent for $\lambda > \lambda_c$. For $a = 1/2$ and 1, p_{th} increases with λ , though E_{th} decreases.

For all a , a first-order correction in λ arises for p_{th} . If we expand p_{th} as $p_{th} = \sum_{k=0}^{\infty} \frac{p_{th,k}}{k!} \lambda^k$, the first-order coefficient $p_{th,1}$ is written as

$$p_{th,1} = p_{th,0} \left[p_{th,0}(1 - a) + E_2 \left(a - \frac{1}{2} \right) \right]. \quad (7.33)$$

On the other hand, the first-order correction in λ for E_{th} , which we denote $E_{th,1}$, is written as

$$E_{th,1} = E_{th,0}(E_{th,0} - E_2) \left(\frac{1}{2} - a \right). \quad (7.34)$$

Thus, it disappears for $a = 1/2$.

The reason why E_{th} and p_{th} disappear for $a = 0$ above $\lambda_c \sim 4 \text{ TeV}^{-1}$ can be understood as follows. For $\lambda E_{th} \gg 1$, and $\lambda m_e, \lambda E_2 \ll 1$, we can approximate Eq. (7.30) as

$$(1 + \lambda E_2)x \approx \lambda E_2 - \frac{\lambda^2 m_e^2}{2} \quad \text{for } a = 0, \quad (7.35)$$

$$a E_2 x \approx \frac{\lambda m_e^2}{4} \quad \text{for } a \neq 0. \quad (7.36)$$

In this range of approximation, since $\lambda E_{th,0} = \lambda m_e^2 / E_2$ is expected to be larger than 1, Eq. (7.35) has no real solution E_{th} while a real solution E_{th} exists for $a \neq 0$. This means that λ_c for $a = 0$ is characterized by $1/E_{th,0} \sim 1 \text{ TeV}^{-1}$.

For $\lambda E_{th}, \lambda m_e, \lambda E_2 \gg 1$, we can summarize the results as follows. For $a = 0$, Eq. (7.30) is approximated as $y^4 x^2 \sim (yx)^3 e^{\lambda m_e} / 4$, which yields $E_1 = -2m_e + E_2 < 0$. This contradicts the first assumption. So a solution does not exist. In a similar way, we can show that E_1 approaches $2m_e + E_2$ and $2m_e - E_2$ for $a = 1$ and for $a \neq 0, 1$, respectively.

To investigate properties for $\lambda < 0$, we replace λ with $-\lambda$. In Eq. (7.30), this corresponds to the replacement $x \rightarrow 1/x$ and $y \rightarrow 1/y$. We find that Eq. (7.30) becomes invariant if a is also replaced by $(1 - a)$.

Thus, the case $a \ll 1$, $\lambda \gtrsim 4 \text{ TeV}^{-1}$, and the case $1 - a \ll 1$, $-\lambda \gtrsim 4 \text{ TeV}^{-1}$ remain as candidate solutions for $\sim 20 \text{ TeV}$ photons. On the other hand, we can exclude $a = O(1)$ and $\lambda \gtrsim 10 \text{ TeV}^{-1}$, or $(1 - a) = O(1)$ and $-\lambda \gtrsim 10 \text{ TeV}^{-1}$ from the present experimental data.

7.3.2 Threshold anomaly for GZK cutoff

Here, we consider the interaction of ultra high energy protons with CMB photons ($\sim 10^{-3} \text{ eV}$) which results in a pair production $p + \gamma \rightarrow p + \pi_0$. In this case, $m_1 = m_3 = m_p$ and $m_4 = m_\pi$, where m_p and m_π are the proton mass and the pion mass, respectively. Because of $E_{th,0} \sim 7 \times 10^{19} \text{ eV}$, it is difficult for EHECRs above $E_{th,0}$ to reach the Earth from cosmologically distant sources.

We solve (7.26), (7.28) and (7.29) numerically. We show the dependence of E_{th} and p_{th} for $\lambda > 0$, in Fig. 7.2. E_2 is chosen as $E_2 = 10^{-3} \text{ eV}$ for CMB photons. Compared with Fig. 7.1, we find that the qualitative features for small λ are quite similar, i.e., $E_{th}/E_{th,0} > 1$ for $a = 0$ and $E_{th}/E_{th,0} < 1$ for $a = 1$, while $p_{th}/p_{th,0} > 1$ for all cases.

However, we find qualitative differences from Fig. 7.1 for $\lambda \gtrsim 10^{-8} \text{ TeV}^{-1}$. The threshold disappears for $\lambda > \lambda_c \sim 2 \times 10^{-8} \text{ TeV}^{-1}$ in the $a = 0$ case, which can be explained as in the

γ -ray case since λ_c coincides approximately with $1/E_{th,0}$. For the case $a = 1/2$ and 1, $E_{th}/E_{th,0}$ increases with $\lambda (\gtrsim 3 \times 10^{-8} \text{ TeV}^{-1})$ and disappears for $\lambda \gtrsim 5 \times 10^{-8} \text{ TeV}^{-1}$, unlike the γ -ray case.

In this case, there is no simple symmetry about $\lambda \rightarrow -\lambda$, as found in the previous case. Thus, we also show the dependence of E_{th} and p_{th} for $\lambda < 0$, in Fig. 7.3. We have a crucial difference from the γ -ray case even for $\lambda > -10^{-9} \text{ TeV}^{-1}$. For $a = 1$, there is a value E_{th2} over which the reaction does *not* occur. We denote E_{th2} by a dot-dashed line. E_{th2} diverges as $\lambda \rightarrow -0$ and merges with E_{th} at $\lambda = \lambda_c \sim -7 \times 10^{-9} \text{ TeV}^{-1}$.

We find that the behavior for small $|\lambda|$ is that $E_{th}/E_{th,0} > 1$ for $a = 1$ and $E_{th}/E_{th,0} < 1$ for $a = 0$ as in the γ -ray case for $\lambda < 0$. For $a = 1/2$ and 1, E_{th} decreases with $\lambda (\lesssim -5 \times 10^{-8} \text{ TeV}^{-1})$.

Thus, the $a \ll 1$ case for $\lambda \gtrsim 2 \times 10^{-8} \text{ TeV}^{-1}$, the $a = O(1)$ case for $\lambda \gtrsim 5 \times 10^{-8} \text{ TeV}^{-1}$ and the $(1-a) \ll 1$ case for $\lambda \lesssim -7 \times 10^{-9} \text{ TeV}^{-1}$ remains as candidate explanations for detections of super GZK events. For $(1-a) = O(1)$, we can exclude $\lambda \lesssim -10^{-7} \text{ TeV}^{-1}$.

7.4 Summary and discussion

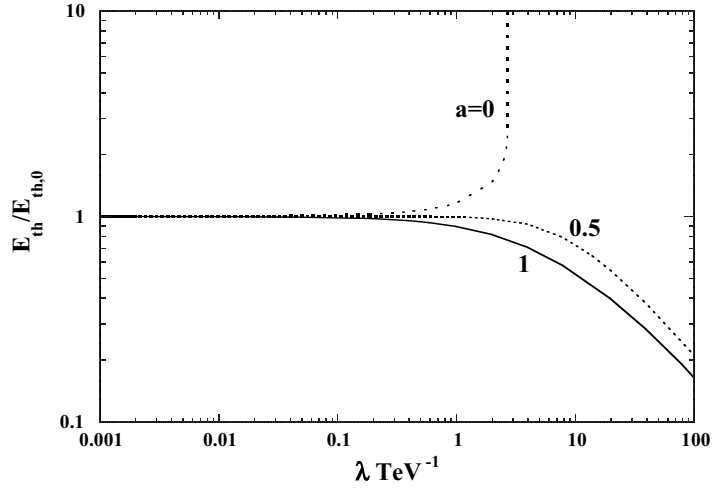
We have re-considered a velocity formula to describe the particle motion based on the motion of a wave packet in κ -Minkowski spacetime. In this formula, spacetime noncommutativity does not affect the motion of a massless particle. Thus, an arrival time analysis of γ -ray bursts in Refs. [65, 66, 93, 90] does not exclude spacetime noncommutativity in this model. Since this feature had not been discussed so far, it should be stressed and is one of our main conclusions here.

Based on this consideration, we have obtained threshold values for reactions $\gamma + \gamma \rightarrow e^+ + e^-$ and $p + \gamma \rightarrow p + \pi_0$ in κ -Minkowski spacetime and analyzed their relevance to the puzzling observations of $\sim 20 \text{ TeV}$ photons and EHECRs above the GZK cutoff, introducing a parameter a to take into account the ambiguity of the momentum conservation law.

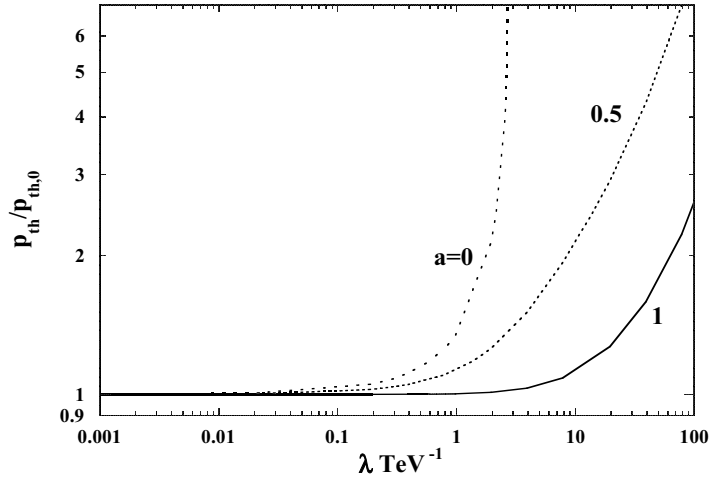
In the TeV γ -ray case, though $a = 1/2$ is favorable in the physical context, only $a \ll 1$ for $\lambda \gtrsim 4 \text{ TeV}^{-1}$, or $(1-a) \ll 1$ for $\lambda \lesssim -4 \text{ TeV}^{-1}$ appear able to explain the detections of γ -rays above $\sim 20 \text{ TeV}$. The possibilities $a = O(1)$ for $\lambda \gtrsim 10 \text{ TeV}^{-1}$, or $(1-a) = O(1)$ for $\lambda \lesssim -10 \text{ TeV}^{-1}$, are excluded.

In the EHECR case, we cannot assign definite values to a , because it may depend on, e.g., masses and/or charges of two particles. The possibilities $a \ll 1$ and $\lambda \gtrsim 2 \times 10^{-8} \text{ TeV}^{-1}$, or $a = O(1)$ and $\lambda \gtrsim 5 \times 10^{-8} \text{ TeV}^{-1}$ remain viable. We can exclude cases in which $(1-a) = O(1)$ and $\lambda \lesssim -10^{-7} \text{ TeV}^{-1}$.

Thus, $a \ll 1$ for $\lambda \gtrsim 4 \text{ TeV}^{-1}$ or $(1-a) \ll 1$ for $\lambda \lesssim -4 \text{ TeV}^{-1}$ appear able to explain both phenomena. Our results are important because they suggest that extremely high-energy particles might be expected in realistic models with spacetime noncommutativity. If this is the case, then we might have already detected symptoms of the spacetime noncommutativity.

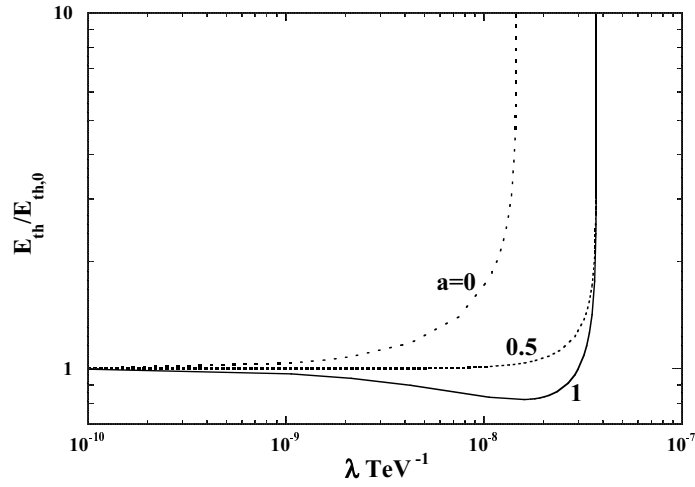


(a)

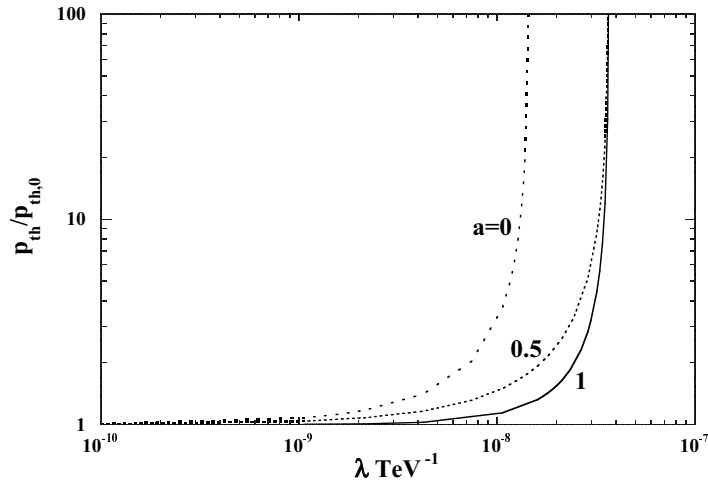


(b)

Figure 7.1: Threshold anomaly for TeV- γ rays for $\lambda > 0$. (a) λE_{th} , (b) λp_{th} are plotted for $E_2 = 1$ eV. For $a = 0.5$ and 1 , E_{th} decreases with λ increases for $\lambda > 1$ TeV $^{-1}$, while p_{th} monotonically increases. The $a \ll 0$ case is only desirable to explain ~ 20 TeV photons. It is noted that E_{th} is invariant under the transformation $\lambda \rightarrow -\lambda$ and $a \rightarrow (1 - a)$.

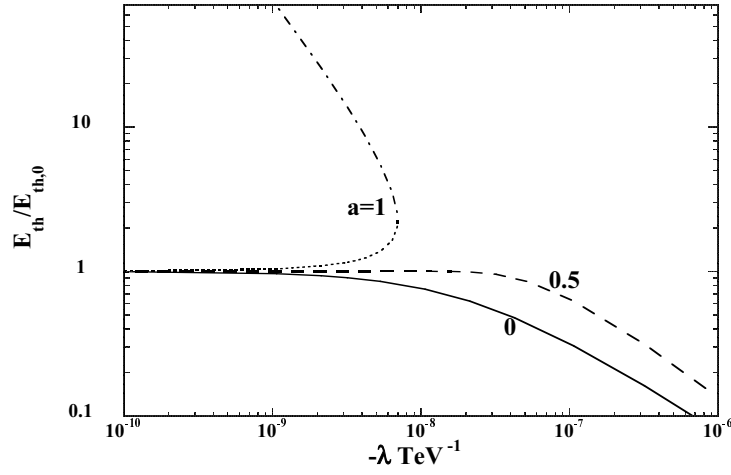


(a)

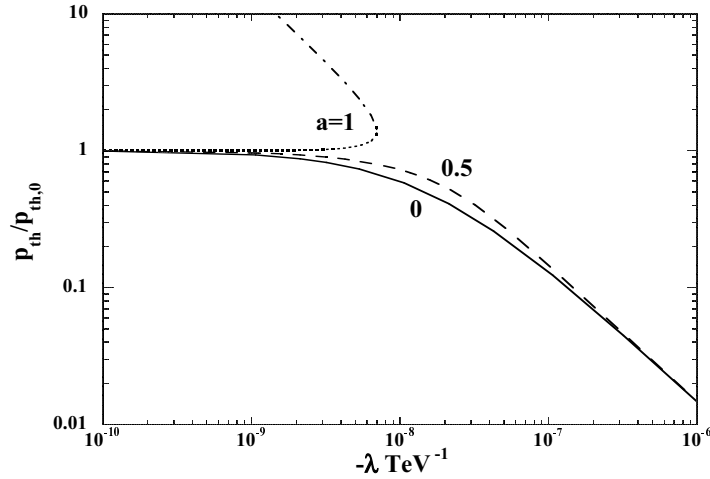


(b)

Figure 7.2: Threshold anomaly for GZK cutoff for $\lambda > 0$. (a) λE_{th} , (b) λp_{th} are plotted for $E_2 = 10^{-3}$ eV. Though qualitative features for small λ are similar to those of Fig. 1, they show drastic difference from Fig. 1 for $\lambda \gtrsim 3 \times 10^{-8}$ TeV $^{-1}$.



(a)



(b)

Figure 7.3: Threshold anomaly for GZK cutoff for $\lambda < 0$. (a) λE_{th} , (b) λp_{th} are plotted for $E_2 = 10^{-3}$ eV and $\lambda < 0$. Unlike the case $\lambda > 0$, the threshold vanishes only the $a = 1$ case for $\lambda \lesssim -7 \times 10^{-9}$ TeV $^{-1}$.

Chapter 8

Conclusion

8.1 Summary and conclusion

The naked singularities and the extremely high energy cosmic rays could carry the information of the microscopic nature of spacetime to us. In the first half of this thesis, we focus on the problem of the cosmic censorship hypothesis, which is related to the visibility of spacetime singularities, from the viewpoint of quantum field theory in curved spacetime. In the latter half of this thesis, we focus on the problem of the high energy cosmic rays, which could probe the microscopic nature of spacetime, from the viewpoint of the noncommutative geometry.

First, we have reviewed the general theory of particle creation during gravitational collapse in chapter 2. After that, we estimate the luminosity, energy, and redshift of particle creation during the NS formation in self-similar collapse in chapter 3. It is found that the power of particle creation is proportional to the inverse square of the remaining time to the appearance of the NS. Then, it is also shown that the proportional constant of the power can be arbitrarily large in the case that the event horizon and Cauchy horizon are very close. This result is striking because the Cauchy horizon would suffer from the instability due to the quantum field in spite of the cutoff expected by a quantum gravity. From the viewpoint of the self-similarity hypothesis, the self-similar spacetimes such as the general relativistic Larson-Penston solution, the quantum effect might cause an instability due to the backreaction. We find another interesting result in such a spacetime. The particle creation can remain finite at the Cauchy horizon. Such a result promotes us to investigate the relation between the curvature strength of naked singularities and the amount of quantum radiation.

Motivated from the result of chapter 3, we investigate the curvature strength and quantum effect of naked singularities in chapter 4. We estimate the amount of particle creation in the wide class of spherical dust collapse. It is shown that the quantum radiation during the strong naked singularity formation diverges as the Cauchy horizon is approached. On the other hand, the radiation from weaker naked singularities is finite. From the viewpoint of the cosmic censorship

hypothesis, the strong naked singularities would be subjected by the instability due to the quantum effect. On the other hand, weaker naked singularities would not.

The mathematical preparation is done to discuss the propagation of the high energy particle in noncommutative spacetimes in chapter 5. There, the κ -Poincaré algebra is introduced as an enveloping algebra of a Lie algebra. Then, the κ -Minkowski noncommutative spacetime appears as the dual Hopf algebra of the κ -Poincaré algebra. We see that in the κ -Poincaré algebra, the dispersion relation of a particle is deformed in high energy region. That is, the Lorentz invariance is violated in high energy region. In the Hopf algebra approach, the summation rule of energy and momenta is also modified.

In chapter 6, we derive the velocity formula by superposing wave packets, which have slightly different wave numbers. Then, we compare the formula with other velocity formula used in the literature. We have shown that the massless particle moves in a constant speed in κ -Minkowski spacetime. This shows that the arrival time analysis by γ -rays is not capable to constrain all kinds of Lorentz invariance. Therefore, we need to investigate specific models individually. The possibility that one can detect the spacetime noncommutativity by low-energy massive particles is discussed.

In chapter 7, we analyze the reaction process in κ -Minkowski spacetime which are related to the puzzling detection of extremely high energy cosmic rays above the Greisen-Zatsepin-Kuzmin cutoff and high energy γ -rays from Markarian 501. We take into account the ambiguity of the momentum conservation law in the theory. We find that the peculiar types of momentum conservation law with some length scale of noncommutativity can explain such puzzling detections. These results could imply that we have already detected astrophysical symptoms of the microscopic nature of spacetime, such as noncommutativity.

8.2 Future prospect

We have discussed the particle creation during the naked singularity formation in chapter 3 and 4. The analysis were based on some assumptions such as semiclassical and geometrical optics approximations. The validity of the latter approximation should be examined by estimating the spectrum of the radiation. Estimating the spectrum, however, confronts with a fundamental problem. The task is to calculate the Bogoliubov coefficient which needs the information of the null rays at \mathcal{I}^+ beyond the Cauchy horizon. In other words, the calculation needs the boundary condition at the naked singularity, which procedure does not have a leading principle. No one has succeeded the satisfactory derivation of the spectrum yet [18, 20, 23]. This point need further investigation. In addition, chapter 3, we had not completed the analysis of the semiclassical instability for the general relativistic Larson-Penston solution because the solution is a numerical one. Because the solution would be the most serious counterexample against the cosmic censorship hypothesis, the semiclassical instability/stability of the solution should be clarified by numerical calculation as well as the classical instability due to non-spherical

perturbations.

We have not obtained the necessary and sufficient condition of the curvature strength of a naked singularity for the quantum radiation to diverge or remain finite at the Cauchy horizon in chapter 4. We argue that the new definition of the curvature strength of singularity should be proposed from the viewpoint whether or not the Cauchy horizon suffers from the instability. From the field theoretical viewpoint, the point-mass particles, which are usually used to define the geodesic and hence to define the geometrical properties of spacetime, are just an approximation in which the quantum field have an extremely high frequency. As we can learn from the history of the physics, the quantum mechanics has resolved some singularities such as the divergent energy of a charged point particle. The wave function of a particle remains finite in spite that its classical self-energy is divergent. Such a investigation that classically singular spacetime is indeed singular quantum mechanically has been done in some literature. One of such works is to check the essentially self-adjointness of Hamiltonian of fundamental fields in classically singular spacetimes [83, 84, 85]. Essentially self-adjointness ensures the uniqueness of dynamics even if there are some singularities in the spacetime [86]. The classical naked singularities can be quantum mechanically either regular or singular, depending on the curvature potential around the singularity. Therefore, it will be interesting to show the relation between the curvature strength of naked singularities and their quantum mechanical regularity/singularity.

After the analysis in chapters. 6 and 7, much literature has appeared. The possibility of detecting the Lorentz invariance violation by the observation or the collider experiment is discussed. This region has been called the “quantum gravity phenomenology”. They also pursuits more fundamental justification of the noncommutative models. Especially, it seems interesting to investigate the Lorentz invariance violation in the loop quantum gravity [99].

Acknowledgements

I would like to thank my thesis adviser, Kei-ichi Maeda for invaluable suggestions and continuous encouragement. Thanks are due to T. Harada, H. Maeda, T. Tamaki, and T. Torii, who are collaborator of the present works, for stimulating discussion. I am also grateful to L.H. Ford, A. Ishibashi, A. Hosoya, K. Nakao, Kengo Maeda, D.A. Konkowski, T.P. Singh, E. Mitsuda, H. Yoshino, and T. Tanaka, as well as the colleagues at Waseda university, for helpful and enjoyable discussions. This work was partially supported by a Grant for The 21st Century COE Program (Holistic Research and Education Center for Physics Self-Organization Systems) at Waseda University. Finally, I would like to thank my parents and sister.

Appendix A

Cauchy horizon in self-similar collapse

¹ We shall prove the absence of an outgoing radial null geodesic which emanates from the origin $v = R = 0$ before the null geodesic $x = x^+$. Let (v, R) be a point on a radial null geodesic l in the region $0 < x = v/R < x^+$ which emanates from $v = R = 0$. Then, one can say that

$$\left. \frac{dx}{dv} \right|_l = \frac{x}{v} \left(1 - \frac{1}{f}\right) > 0. \quad (\text{A.1})$$

By the uniqueness of the solution of the null geodesic equation, l cannot cross $x = x^+$ at points other than $v = R = 0$. Therefore above inequality says that x decreases as $v \rightarrow +0$ but is bounded from below by 0. Hence the limit

$$\bar{x} \equiv \lim_{v \rightarrow +0} x(v) \Big|_l \quad (\text{A.2})$$

exists and satisfies $0 \leq \bar{x} < x^+$. In the case of $0 < \bar{x} < x^+$,

$$\bar{R} \equiv \lim_{v \rightarrow +0} R(v) \Big|_l \quad (\text{A.3})$$

$$= \lim_{v \rightarrow +0} \frac{v}{x(v)} \Big|_l \quad (\text{A.4})$$

$$= 0 \quad (\text{A.5})$$

holds, but

$$\bar{x} = \lim_{v \rightarrow +0} \frac{v}{R(v)} \Big|_l = \lim_{v \rightarrow +0} \frac{1}{R'(v)} \Big|_l = \lim_{v \rightarrow +0} x f(x) \Big|_l = \bar{x} f(\bar{x}), \quad (\text{A.6})$$

¹This appendix is for Sec. 3.1.

where the l'Hopital's rule is used in the second equality. This contradicts the assumption that x^+ is the smallest positive root of equation $f(x) = 1$. Next, we shall consider the case of $\bar{x} = 0$. The fact that the solution R converges to a finite nonzero constant as $x \rightarrow 0$ from the condition (3.7) contradicts the assumption that l is a geodesic which emanates from $v = R = 0$. Thus the case of $\bar{x} = 0$ is also excluded. Thus we see that $x = x^+$ is the first outgoing null ray which emanates from the singularity.

Appendix B

Local map and redshift in diagonal coordinates

¹ The line element of the class of spacetimes discussed in Sec. 3.1 in a diagonal coordinate system is written as

$$ds^2 = g_{tt}(z)dt^2 + g_{rr}(z)dr^2 + r^2 S^2(z)d\Omega^2, \quad (\text{B.1})$$

where $z \equiv t/r$ and S is a dimensionless metric function. The homothetic Killing vector field is of the form $\xi = t\partial_t + r\partial_r$. If one defines functions $w_{\pm}(z)$ as

$$w_{\pm}(z) \equiv \pm \frac{1}{z} \sqrt{-\frac{g_{rr}}{g_{tt}}}, \quad (\text{B.2})$$

the roots of the algebraic equation $w_{\pm}(z) = 1$ play important roles as do those of $f(x) = 1$ in Sec. 3.1. The existence of a positive (negative) root of $w_+(z) = 1$ ($w_-(z) = 1$) and the uniqueness of the root of $w_-(z) = 1$ are assumed. When the negative root and the smallest positive root are denoted by z^- and z^+ respectively, the curves $z = z^+$ and $z = z^-$ can be shown to be the CH and the ingoing null ray that terminates at the NS. In addition, it is assumed that $w'_{\mp}(z^{\mp}) \geq 0$.

The null geodesic equations are integrated to give

$$\frac{r}{r_0^{\pm}} = \exp \left[\int_{z_0^{\pm}}^z W_{\pm}(z') dz' \right] = \exp \left[\int_{z_0^{\pm}}^z W_{\pm}^*(z') dz' \right] \left(\frac{z^{\pm} - z}{z^{\pm} - z_0^{\pm}} \right)^{1/\delta_{\pm}}, \quad (\text{B.3})$$

¹This appendix is for chapter 3.

where

$$\begin{aligned} W_{\pm}(z) &\equiv \frac{1}{z(w_{\pm}(z) - 1)}, \\ \delta_{\pm} &\equiv z^{\pm} w'_{\pm}(z^{\pm}), \\ W_{\pm}^*(z) &\equiv W_{\pm}(z) - \frac{1}{\delta_{\pm}(z - z^{\pm})}, \end{aligned} \quad (\text{B.4})$$

and the signature $+$ ($-$) corresponds to outgoing (ingoing) null geodesic. The constants z_0^{\pm} and r_0^{\pm} are related as $r_0^+ = r(z = z_0^+)$ for an outgoing ray, while $r_0^- = r(z = z_0^-)$ for an ingoing one, where z_0^{\pm} is set as $z_0^{\pm} < z^{\pm}$ and $z_0^{\pm} \neq 0$. The constants r_0^{\pm} are related to $t_c \equiv t(r = 0)$ as

$$r_0^{\pm} = -\frac{t_c}{|z_0^{\pm}| J_{\pm}}, \quad J_{\pm} = \exp \left[\int_{z_0^{\pm}}^{-\infty} \frac{w_{\pm}(z') dz'}{z' (w_{\pm}(z') - 1)} \right]. \quad (\text{B.5})$$

Combination of Eqs. (B.3) and (B.5) yields

$$r = D_{\pm}(r, z) (t^{\pm}(r) - t)^{1/\delta_{\pm}} t_c, \quad (\text{B.6})$$

where

$$\begin{aligned} t^{\pm}(r) &\equiv z^{\pm} r, \\ D_{\pm}(r, z) &\equiv -|z_0^{\pm}|^{-1} J_{\pm}^{-1} [(z^{\pm} - z_0^{\pm})r]^{-1/\delta_{\pm}} \exp \left[\int_{z_0^{\pm}}^z W_{\pm}^*(z') dz' \right]. \end{aligned}$$

Now, let us consider a pair of ingoing and outgoing null rays such that the latter is the reflection of the former at the regular center ($r = 0, t < 0$). An observer who rests at $r = \varrho$ will encounter the null ray twice, so that we denote the time of first encounter by t_1 and that of the second by t_2 . By Eq. (B.6), the ingoing and outgoing null rays are matched at the center to give the local map as

$$t^-(\varrho) - t_1 = \left[\frac{D_+(\varrho, z_2)}{D_-(\varrho, z_1)} \right]^{\delta_-} (t^+(\varrho) - t_2)^{\alpha_2}, \quad (\text{B.7})$$

where

$$\begin{aligned} z_i &\equiv t_i / \varrho, \quad (i = 1, 2), \\ \alpha_2 &\equiv \delta_- / \delta_+. \end{aligned} \quad (\text{B.8})$$

The redshift of a radial null ray is obtained in similar way. The t -component of equation $k^{\mu} \nabla_{\mu} k^{\nu} = 0$ is integrated to give

$$\frac{k^t(z)}{k_0^{t, \pm}} = \exp \left[\int_{z_0^{\pm}}^z \tilde{W}_{\pm}(z') dz' \right] = \exp \left[\int_{z_0^{\pm}}^z \tilde{W}_{\pm}^*(z') dz' \right] \left(\frac{z^{\pm} - z}{z^{\pm} - z_0^{\pm}} \right)^{-(1+\delta_{\pm})/\delta_{\pm}}, \quad (\text{B.9})$$

where

$$\begin{aligned}\tilde{W}_\pm(z) &\equiv -\frac{1}{2(1-w_\pm^{-1})} \left\{ (1-2w_\pm^{-1}) \frac{1}{g_{tt}} \frac{dg_{tt}}{dz} + \frac{1}{g_{rr}} \frac{dg_{rr}}{dz} \right\}, \\ \tilde{W}_\pm^*(z) &\equiv \tilde{W}_\pm(z) + \frac{1+\delta_\pm}{\delta_\pm} \frac{1}{z-z^\pm}.\end{aligned}$$

The constants \tilde{z}_0^\pm and $k_0^{t,\pm}$ are related as $k_0^{t,+} = k^t(z_0^+)$ for an outgoing ray, while $k_0^{t,-} = k^t(z_0^-)$ for an ingoing one. The constants $k_0^{t,\pm}$ are related to $k_c^t \equiv k^t(r=0)$ as

$$k_0^{t,\pm} = \frac{k_c^t}{\tilde{J}_\pm}, \quad \tilde{J}_\pm \equiv \exp \left[\int_{\tilde{z}_0^\pm}^{-\infty} \tilde{W}_\pm(z') dz' \right]. \quad (\text{B.10})$$

Combination of Eqs. (B.9) and (B.10) yields

$$k^t(z) = \tilde{D}_\pm(r, z) (t^\pm(r) - t)^{-(1+\delta_\pm)/\delta_\pm} k_c^t, \quad (\text{B.11})$$

where

$$\tilde{D}_\pm(r, z) \equiv \tilde{J}_\pm^{-1} [(z^\pm - \tilde{z}_0^\pm)r]^{(1+\delta_\pm)/\delta_\pm} \exp \left[\int_{\tilde{z}_0^\pm}^z \tilde{W}_\pm^*(z') dz' \right].$$

Consider again the observer who rests at $r = \varrho$ and the pair of ingoing and outgoing null rays. The outgoing and ingoing null rays are matched at the center by Eqs. (B.7) and (B.11) to give

$$\frac{\hat{\omega}_2}{\hat{\omega}_1} = \sqrt{\left| \frac{g_{tt}(z^+)}{g_{tt}(z^-)} \right|} \frac{\tilde{D}_+(\varrho, z_2)}{\tilde{D}_-(\varrho, z_1)} \left[\frac{D_+(\varrho, z_2)}{D_-(\varrho, z_1)} \right]^{1+\delta_-} (t^+(\varrho) - t_2)^{\alpha_2-1}, \quad (\text{B.12})$$

where $\hat{\omega}_1 \equiv \lim_{z_1 \rightarrow z^-} \sqrt{|g_{tt}(z_1)|} k^t(z_1)$ and $\hat{\omega}_2 \equiv \lim_{z_2 \rightarrow z^+} \sqrt{|g_{tt}(z_2)|} k^t(z_2)$ are the observed frequencies.

There exists a plausible relation between the local map and redshift. From Eqs. (B.7) and (B.12), one obtains

$$\frac{d\tau_2}{d\tau_1} = \frac{\hat{\omega}_1}{\hat{\omega}_2},$$

where $d\tau_i \equiv \sqrt{|g_{tt}|} dt_i$ ($i = 1, 2$) is the proper time of the observers.

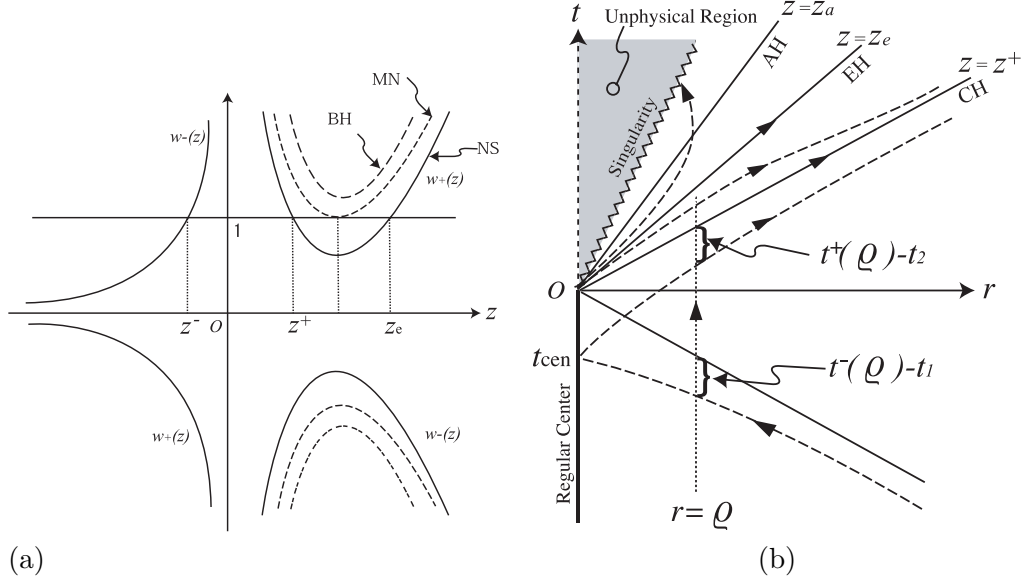


Figure B.1: (a) Schematic plots of $f(x)$ defined by Eq. (B.2) for typical collapsing spacetimes which end in a NS or a black hole. Depending on the number of roots of $w_{+}(x) = 1$, which we denote by j , the causal structure of spacetime changes. The cases of $j = 0, 1$, and 2 are depicted. (i) The case of $j = 2$: $w_{+}(x)$ ($x > 0$) is depicted by a solid line. The two roots are denoted by x^+ and z_e ($z^+ < z_e$). The geodesics $z = z^+$ and $z = z_e$ represent the CH and event horizon, respectively. This kind of spacetime admits a NS. (ii) The case of $j = 1$: $w_{+}(z)$ ($z > 0$) is depicted by a dashed line. In this case, $z^+ = z_e$ holds, i.e., the CH and event horizon coincide. This type of singularity is called marginally naked (MN). (iii) The case of $j = 0$: $w_{+}(z)$ ($z > 0$) is depicted by a dot-dashed line. In this case the collapse ends in a black hole (BH). (b) A typical spacetime diagram of a collapsing body which ends in a naked singularity in (t, r) coordinates. A null ray which is reflected at the regular center and characteristic null rays in respective regions divided by horizons are depicted. The time intervals $t^+(\varrho) - t_2$ and $t^-(\varrho) - t_1$ in Eq. (B.7) are depicted. The dotted line is the world line of an observer at $r = \varrho$.

Appendix C

Nakedness of the singularity in LTB spacetime

¹ In order to determine whether the singularity is naked or not, we investigate the future-directed outgoing null geodesics emanating from the singularity at $(t, r) = (0, 0)$. We find the asymptotic solutions that obey a power law near the center [100] as

$$t \simeq X_0 r^p, \tag{C.1}$$

where $X_0 > 0$ and $p \geq 1$ are constants. The latter condition is due to the fact that the orbit of the shell-focusing singularity is $t = t_s(r) = r$. After some straightforward calculations, one can find an asymptotic solution for $\mu > 0$ as

$$t \simeq \frac{\lambda}{\mu + 1} r^{\mu+1}. \tag{C.2}$$

With Eq. (C.2) and the fact that the apparent horizon, which is defined by $F = R$, behaves as $t = t_{ah}(r) = r - 2F(r)/3 \simeq r$ for $\mu > 0$ near the center, the singularity is at least locally naked. In the case of the self-similar case ($\mu = 0$), similar discussion is possible and the singularity is known to be naked for small values of λ [100]. We consider the situation in which the collapsing dust ball is attached to an outer vacuum region at a comoving radius $r = \text{constant}$, within which the null ray (C.2) is outside the apparent horizon. Then, the singularity is globally naked and the weak version of CCH is violated.

¹This appendix is for chapter 4.

Appendix D

Frequency of naked singularities

It will be helpful to compare the gauge of the LTB solution used in chapter 4 with one used in much literature. Such a comparison shows that ω_s defined in Sec. 4.3 coincides with the characteristic frequency of singularity introduced in [23] except for a numerical factor.

Let us denote the comoving coordinates by (\tilde{t}, \tilde{r}) , in which \tilde{r} is chosen to coincide with the physical radius R at the initial regular epoch of $\tilde{t} = 0$, i.e., $R(0, \tilde{r}) = \tilde{r}$. We assume that the mass function $F(\tilde{r})$ can be expanded near the regular center as

$$F(\tilde{r}) = F_1 \tilde{r}^a + F_2 \tilde{r}^b + \dots,$$

where a and b are constants satisfying $a < b$. Then the initial density profile is written as

$$\rho(0, \tilde{r}) = \frac{aF_1}{8\pi} R^{a-3} + \frac{bF_1}{8\pi} R^{b-3} + \dots. \quad (\text{D.1})$$

Comparing Eq. (D.1) with Eqs. (4.5) and (4.6), one obtains the powers and coefficients of $F(\tilde{r})$ as,

$$a = 3, \quad b = \frac{3(3\mu + 2)}{3\mu + 1},$$

$$F_1 = \frac{4}{9t_{in}^2}, \quad F_2 = -\frac{8(\mu + 1)^{3/(3\mu+1)}}{9\lambda^{3/(3\mu+1)}(-t_{in})^{(9\mu+5)/(3\mu+1)}}.$$

It is found that the power b is in the region of $3 < b \leq 6$ for $\mu \geq 0$. In Ref. [23], Harada *et al.* determined the characteristic frequency of the naked singularity in the analytic model ($\mu = 1/6$) through physical discussion. It is easy to repeat their discussion for the general value of $\mu > 0$. One possible quantity, which is composed only of F_1 and F_2 , independent of the choice of initial time slice, and has the dimension of frequency is

$$F_1^{(9\mu+5)/(6\mu)} (-F_2)^{-(3\mu+1)/(3\mu)} = (\mu + 1)^{-1/\mu} \left(\frac{2}{3}\right)^{(9\mu+5)/(3\mu)} \left(\frac{9}{8}\right)^{(3\mu+1)/(3\mu)} \omega_s, \quad (\text{D.2})$$

where we used Eq. (4.44). In terms of γ , the quantity of (D.2) is written as follows:

$$\Omega_\gamma(\lambda) \equiv F_1^{(2\gamma+9)/(2(3-\gamma))} (-F_2)^{-3/(3-\gamma)}.$$

In the case of the analytic LTB model ($\gamma = 2$),

$$\Omega_2(\lambda) = F_1^{13/2} (-F_2)^{-3},$$

which coincides with the frequency defined in [23] except for a numerical factor. This shows that it is valid to define $\omega_s \equiv \lambda^{1/\mu}$ as the frequency of singularity. In the self-similar LTB solution ($\mu = 0$), such a quantity does not exist because of the scale-invariant nature of self-similar spacetimes.

Bibliography

- [1] C.W. Misner, K.S. Thorn, and J.A. Wheeler, *Gravitation*, (Freeman, San Francisco, USA, 1973).
- [2] S. Weinberg, *Gravitation and Cosmology*, (Wiley, New York, 1972); P.J.E. Peebles, *Principles of Physical Cosmology*, (Princeton University Press, Princeton, 1993); E.W. Kolb and M.S. Turner, *The Early Universe*, (Addison-Wesley, Redwood City, California, 1990).
- [3] K.S. Thorn, in *Black Holes and Relativistic Stars*, edited by R.M. Wald, (The University of Chicago Press, Chicago, 1998); K.S. Thorn, in *Compact Stars in Binaries*, edited by J. van Paradijs, E.P.J. van den Heuvel and E. Kuulkers, (Kluwer Academic Publishers, Dordrecht, Netherlands, 1994).
- [4] S.W. Hawking and G.F.R. Ellis, *The large scale structure of spacetime*, (Cambridge University Press, Cambridge, England, 1973).
- [5] C. Rovelli, *Quantum Gravity*, (Cambridge University Press, Cambridge, England, 2004), Living Review in Relativity, **1**, 1 (1998), <http://relativity.livingreviews.org/Articles/lrr-1998-1/>; T. Thiemann, gr-qc/0110034; A. Ashtekar and J. Lewandowski, Class. Quantum Grav. **21**, R53 (2004).
- [6] M.B. Green, J.H. Schwarz, and E. Witten, *Superstring theory*, (Cambridge University Press, Cambridge, England, 1987); J. Polchinski, *String Theory*, (Cambridge University Press, Cambridge, England, 1998).
- [7] S.W. Hawking and R. Penrose, Proc. R. Soc. Lond. A **314**, 529 (1970).
- [8] N.D. Birrell and P.C.W. Davies, *Quantum Fields in Curved Space*, (Cambridge University Press, Cambridge, England, 1982).
- [9] B.S. DeWitte, Phys. Rep. **10**, 295 (1975).
- [10] U. Miyamoto and T. Harada, Phys. Rev. D **69**, 104005 (2004).
- [11] U. Miyamoto, H. Maeda, and T. Harada, Prog. Theor. Phys. (in press), gr-qc/0411100.

- [12] T. Tamaki, T. Harada, U. Miyamoto, and T. Torii, *Phys. Rev. D* **65**, 083003 (2002).
- [13] T. Tamaki, T. Harada, U. Miyamoto, and T. Torii, *Phys. Rev. D* **66**, 105003 (2002).
- [14] R. Penrose, *Riv. Nuovo Cim.* **1**, 252 (1969), reprinted in *Gen. Relat. Grav.* **34**, 1141 (2002); in *General Relativity, An Einstein Century Survey*, edited by S.W. Hawking and W. Israel (Cambridge University Press, Cambridge, England, 1979), p. 581.
- [15] P.S. Joshi, *Global Aspects in Gravitation and Cosmology* (Oxford University Press, New York, 1993).
- [16] T. Harada, *Pramana* **63(4)** (2004), 741, *Proceedings of the 5th International Conference on Gravitation and Cosmology*, edited by B.R. Iyer, V. Kuriakose, and C.V. Vishveshwara, gr-qc/0407109.
- [17] L.H. Ford and L. Parker, *Phys. Rev. D* **17**, 1485 (1978).
- [18] W.A. Hiscock, L.G. Williams, and D.M. Eardley, *Phys. Rev. D* **26**, 751 (1982).
- [19] S. Barve, T.P. Singh, C. Vaz, and L. Witten, *Nucl. Phys. B* **532**, 361 (1998); *Phys. Rev. D* **58**, 104018 (1998).
- [20] C. Vaz and L. Witten, *Phys. Lett. B* **442**, 90 (1998) .
- [21] H. Iguchi and T. Harada, *Class. Quantum Grav.* **18**, 3681 (2001).
- [22] T. P. Singh and C. Vaz, *Phys. Lett. B* **481**, 74 (2000).
- [23] T. Harada, H. Iguchi, K. Nakao, *Phys. Rev. D* **61**, 101502 (2000); *ibid.* **62**, 084037 (2000).
- [24] P.S. Joshi, N. Dadhich, and R. Maartens, *Mod. Phys. Lett. A* **15**, 991 (2000).
- [25] B. Waugh and K. Lake, *Phys. Rev. D* **40**, 2137 (1989).
- [26] K. Lake and T. Zannias, *Phys. Rev. D* **41**, 3866 (1990).
- [27] A. Ori and T. Piran, *Phys. Rev. D* **42**, 1068 (1990).
- [28] A. Ori and T. Piran, *Phys. Rev. Lett.* **59**, 2137 (1987); *Gen. Relat. Grav.* **20**, 7 (1988).
- [29] T. Harada and H. Maeda, *Phys. Rev. D* **63**, 084022 (2001).
- [30] B.J. Carr, in *Proceedings of the Ninth Workshop on General Relativity and Gravitation*, 1999, edited by Y. Eriguchi *et al.* (Hiroshima, Japan), p. 425, gr-qc/0003009.
- [31] B.J. Carr and A.A. Coley, *Class. Quantum. Grav.* **16**, R31 (1999).

- [32] C. Gundlach, Phys. Rep. **376**, 339 (2003); J.M. Martin-Garcia and C. Gundlach, Phys. Rev. D **68**, 024011 (2003).
- [33] T. Tanaka and T.P. Singh, Phys. Rev. **63**, 124021 (2001).
- [34] B.C. Nolan and T. Waters, Phys. Rev. D **66**, 104012 (2002).
- [35] M.D. Roberts, Gen. Relativ. Grav. **21**, 907 (1989).
- [36] F.J. Tipler, Phys. Rev. Lett. A **64**, 8 (1977).
- [37] A. Królak, J. Math. Phys. **28**, 138 (1987).
- [38] C.J.S. Clarke and K. Królak, J. Geom. Phys. **2**, 127 (1985).
- [39] S.S. Deshingkar, P.S. Joshi, and I.H. Dwivedi, Phys. Rev. D **59** (1999), 044018.
- [40] T. Harada, K. Nakao, and H. Iguchi, Class. Quantum Grav. **16**, 2785 (1999).
- [41] D.J. Bird *et al.*, Astrophys. J. **441**, 144 (1995).
- [42] M. Takeda *et al.*, Phys. Rev. Lett. **81**, 1163 (1998).
- [43] K. Greisen, Phys. Rev. Lett. **16**, 748 (1966); G.T. Zatsepin and V.A. Kuzmin, Sov. Phys. JETP Lett. **4**, 78 (1966).
- [44] F.A. Aharonian *et al.*, Astron. Astrophys. **349**, 11A (1999).
- [45] A.N. Nikishov, Sov. Phys. JETP **14**, 393 (1962); J. Gould, G. Schreder, Phys. Rev. D **155**, 1404 (1967); F.W. Stecker, O.C. De Jager and M.H. Salmon, Astro. Phys. J. **390**, L49 (1992).
- [46] P.S. Coppi and F.A. Aharonian, Astropart. Phys. **11**, 35 (1999).
- [47] A.V. Olinto, Phys. Rep. **333-334**, 329 (2000).
- [48] S. Coleman and S.L. Glashow, Phys. Rev. D **59**, 116008 (1999).
- [49] R. Jackiw and V. A. Kostelecky, Phys. Rev. Lett. **82**, 3572 (1999).
- [50] O. Bertolami and C.S. Calvalho, Phys. Rev. D **61**, 103002 (2000).
- [51] R. Aloisio, P. Blasi, P.L. Ghia and A.F. Grillo, Phys. Rev. D **62**, 053010 (2000).
- [52] H. Sato and T. Tati, Prog. Theor. Phys. **47**, 1788 (1972); H. Sato, *Proc. of the International Workshop: Space Factory on JEM/ISS* (1999), astro-ph/0005218.

- [53] T. Kifune, *Astrophys. J. Lett.* **518**, L21 (1999).
- [54] W. Kluzniak, *Proc. of the 8th International Workshop on "Neutrino Telescopes"*, (Milla Baldo Ceolin ed., 1999), astro-ph/9905308.
- [55] R. J. Protheroe and H. Meyer, *Phys. Lett. B* **493**, 1 (2000).
- [56] G. Amelino-Camelia and T. Piran, *Phys. Rev. D* **64**, 036005 (2001).
- [57] M.R. Douglas and C. Hull, *JHEP* **02**, 8 (1998).
- [58] A. Connes, M.R. Douglas, and A. Schwarz, *JHEP* **02**, 3 (1998).
- [59] C.S. Chu and P.M. Ho, *Nucl. Phys. B* **550**, 151 (1999).
- [60] V. Schomerus, *JHEP* **06**, 030 (1999).
- [61] N. Seiberg and E. Witten, **09**, 032 (1999).
- [62] A. Hashimoto and N. Itzhaki, *Phys. Lett. B* **465**, 142 (1999).
- [63] T. Yoneya, *Wandering in the Fields*, p. 419, (World Scientific, 1987); *ibid.*, *Quantum String Theory*, p. 23, (Springer, 1988); *ibid.*, *Prog. Theor. Phys.* **103**, 1081 (2000).
- [64] M. Jimbo, *Lett. Math. Phys.* **10**, 63 (1985).
- [65] G. Amelino-Camelia *et al.*, *Nature* **393**, 763 (1998).
- [66] G. Amelino-Camelia, J. Lukierski and A. Nowicki, *Int. J. Mod. Phys. A* **14**, 4575 (1999).
- [67] G. Amelino-Camelia and T. Piran, *Phys. Lett. B* **497**, 265 (2001).
- [68] G. Amelino-Camelia, J. Lukierski, and A. Nowicki, *Czech. J. Phys.* **51**, 1247 (2001).
- [69] R. Oeckl, *J. Math. Phys.* **40**, 3588 (1999).
- [70] S. Majid and R. Oeckl, *Commun. Math. Phys.* **205**, 617 (1999).
- [71] J. Lukierski, A. Nowicki, H. Ruegg, and V. N. Tolstoy, *Phys. Lett. B* **264**, 331 (1991).
- [72] S. Majid and H. Ruegg, *Phys. Lett. B* **334**, 348 (1994).
- [73] J. Lukierski and A. Nowicki, *Acta Phys. Polon. B* **33**, 2537 (2002).
- [74] S.M. Carroll *et al.*, *Phys. Rev. Lett.* **87**, 141601 (2001).
- [75] T. Harada, H. Iguchi, K. Nakao, T. Tanaka, T.P. Singh and C. Vaz, *Phys. Rev. D* **64**, 041501 (2001).

- [76] S.W. Hawking, *Commun. Math. Phys.* **43**,199 (1975).
- [77] P.C. Vaidya, *Current Science* **13**, 183 (1943); *Phys. Rev.* **47**, 10 (1951); *Proc. Indian Acad. Sci. A* **33**, 264 (1951).
- [78] G. Lemaître, *Ann. Soc. Sci. Bruxelles I A* **53**, 51 (1933); R.C. Tolman, *Proc. Nat. Acad. Sci.* **20**, 169 (1934); H. Bondi, *Mon. Not. R. Astron. Soc.* **107**, 410 (1947).
- [79] D. Christodoulou, *Commun. Math. Phys.* **93**, 171 (1984).
- [80] L. H. Ford, *Phys. Rev. D*, **15** 2955 (1987).
- [81] T. Harada, H. Iguchi, and K. Nakao, *Phys. Rev. D* **58**, 041502 (1998); H. Kudoh, T. Harada, and H. Iguchi, *Phys. Rev. D* **62**, 104016 (2000).
- [82] T. Harko and K.S. Chang, *Phys. Lett. A* **266**, 259 (2000).
- [83] G.T. Horowitz and D. Marolf, *Phys. Rev. D* **52**, 5670 (1995).
- [84] A. Ishibashi and A. Hosoya, *Phys. Rev. D* **60**, 104028 (1999).
- [85] D.A. Konkowski and T.M. Helliwell, *Gen. Relativ. Gravit.* **33**, 1131 (2001).
- [86] R.M. Wald, *J. Math. Phys.* **21**, 2802 (1980); A. Ishibashi and R.M. Wald, *Class. Quantum Grav.* **20**, 3815 (2003).
- [87] S. Majid, *Foundation of quantum group theory*, (Cambridge University Press, Cambridge, 1995); M. Jimbo, *Quantum Group and Yang-Baxter Equations* (in Japanese), (Springer-Verlag, Tokyo, 1990).
- [88] S. Coleman and S.L. Glashow, *Phys. Rev. D* **59**, 116008 (1999).
- [89] G. Amelino-Camelia, J. Ellis, N.E. Mavromatos and D.V. Nanopoulos, *Int. J. Mod. Phys. A* **12**, 607 (1997).
- [90] Biller *et al.*, *Phys. Rev. Lett.* **83**, 2108 (1999).
- [91] L.J. Garay, *Phys. Rev. Lett.* **80**, 2508 (1998); R. Gambini and J. Pullin, *Phys. Rev. D* **59**, 124021 (1999).
- [92] P. Kosiński, J. Lukierski, P. Maślanka, and A. Sitarz, *Czech. Journal of Phys.* **48**, 1407 (1998); P. Kosiński, J. Lukierski and P. Maślanka, *Proc. of XXII Int. Colloquium on Group-Theor. Methods in Physics*, p.423 (International Press, Boston, 1999); P. Kosiński, J. Lukierski and P. Maślanka, *Phys. Rev. D* **62**, 025004 (2000).
- [93] G. Amelino-Camelia and S. Majid, *Int. J. Mod. Phys. A* **15**, 4301 (2000).

- [94] E. Waxman and J. Bahcall, Phys. Rev. Lett. **78**, 2292 (1997).
- [95] D. Dubbers, Prog. in Part. and Nucl. Phys. A **26**, 173 (1991).
- [96] D.R. Rich *et al.*, physics/9908050.
- [97] N.R. Bruno, G. Amelino-Camelia, and J. Kowalski-Glikman, Phys. Lett. B **522**, 133 (2001).
- [98] J. Kowalski-Glikman, Mod. Phys. Lett. A **17**, 1 (2002).
- [99] R. Gambini and J. Pullin, Phys. Rev. D **59**, 124021 (1999); J. Alfro, H.A. Morales-Técolt, and L.F. Urrutia, Phys. Rev. Lett. **84**, 2318 (2000); Phys. Rev. D **65** 103509 (2002); J. Alfro, M. Reyes, H.A. Morales-Técolt, and L.F. Urrutia, Phys. Rev. D **70**, 084002 (2004); J. Phys. A **36**, 12097 (2003); M. Bojowald, H.A. Morales-Técolt, gr-qc/0411101.
- [100] P.S. Joshi and I.H. Dwivedi, Phys. Rev. D **47**, 5357 (1993).